Rising temperatures drive lower summer minimum flows across hydrologically diverse catchments in British Columbia

S. W. Ruzzante[1] and T. Gleeson[1]

[1]University of Victoria, Victoria, BC, Canada

Corresponding author: Sacha W. Ruzzante (sruzzante@uvic.ca)

Key Points:

- Summer low flows are highly sensitive to summer temperature and precipitation, with winter storage historically playing a secondary role
- Regression models outperform process-based hydrologic models for minimum summer flow prediction and enable valuable process understanding
- Precipitation variability historically drove low flows but rising temperatures are responsible for recent declines in warmer catchments

Abstract

Excessively low stream flows harm ecosystems and societies, so two key goals of low-flow hydrology are to understand their drivers and to predict their severity and frequency. We show that linear regressions can accomplish both goals across diverse catchments. We analyse 230 unregulated moderate to high relief catchments across rainfall-dominated, hybrid, snowmelt-dominated, and glacial regimes in British Columbia, Canada, with drainage areas spanning 5 orders of magnitude from 0.5 to 55,000 km^2. Summer low flows are decreasing in rainfall-dominated and hybrid catchments but have been stable in catchments that remain snowmelt or glacial-dominated. However, we find that since 1950 approximately one third of snowmelt-dominated catchments have transitioned to a hybrid rain-snow regime. The declines in rainfall-dominated and hybrid catchments are dominantly driven by summer precipitation and temperature, and only weakly influenced by winter storage. We apply this understanding to create regression models that predict the minimum summer flow using monthly temperature and precipitation data. These models outperform distributed process-based models for every common goodness-of-fit metric; the performance improvement is mostly a result of abandoning the requirement to simulate all parts of the annual hydrograph. Using these regression models we reconstruct streamflow droughts and low flow anomalies from 1901-2022. We reproduce recent drying trends in rainfall-dominated and hybrid catchments, but also show that present conditions are comparable to those seen one hundred years ago. However, anomalously low flows last century were caused by large precipitation deficits while current declines are driven by rising summer temperatures despite near-normal precipitation.

Plain Language Summary

Late-summer streamflow in British Columbia, Canada, is essential for ecosystems and for water resources. We used statistical techniques to analyse and model the annual minimum summer flow in free-flowing streams across the province. We found that summer minimum flows across the province have decreased (become drier) since mid-20th century, particularly in warmer and coastal watersheds where precipitation mainly falls as rain. Summer streamflow drought in warmer watersheds is now more common and more severe than at any point since the early 20th century. Summer minimum flows are mainly controlled by precipitation but also by high summer temperatures, which increase evaporation and reduce water storage. Although there were dry periods during the 20th century, these were primarily caused by below-average rainfall, while recent declines in summer minimum flows in warmer watersheds are primarily a result of hotter summer temperatures. Summer flows in colder watersheds (where more precipitation falls as snow) have been relatively stable since mid-century but these snow-dominated watersheds are becoming less common.

1 Introduction

1.1 Environmental flows and streamflow drought

Preserving environmental flows, and especially low flows, is critical to maintaining healthy riverine ecosystems and the societies that depend on them (Arthington et al., 2018; Bradford & Heinonen, 2008). Living things, including humans, can be harmed when rivers have less water

than normal: low flows that are significantly below the natural envelope of variability have been shown to disrupt lifecycles of aquatic species and reduce biodiversity (Poff & Zimmerman, 2010), cause economic losses (Folkens et al., 2023), and disrupt cultural practices (Morgan, 2012; Tipa & Nelson, 2012). The more evocative term "streamflow drought" has also been coined, presumably to attribute some gravity to a concept that is defined drily as a "sustained period" of "below-normal river discharge" (Van Loon, 2015).

Climate change and human activity increasingly threaten environmental flows globally, resulting in severe and probably irreparable harm to riverine ecosystems (Porkka et al., 2022; Richardson et al., 2023; Virkki et al., 2022). Streamflow drought is driven by precipitation (P) and temperature (T) anomalies: in a process called drought propagation, these anomalies cause below-normal storage of groundwater, snow, and soil moisture, resulting in below-normal discharge (Van Loon, 2015). Land use and water abstraction can also affect low flow occurrence and severity (de Graaf et al., 2019; Guzha et al., 2018; Wada et al., 2016). Effective water management requires an understanding of the relative importance of human and climate drivers because land and water use can be managed at local scales, while climate change is a global challenge. Within the category of climate drivers, it is important to distinguish precipitation and temperature effects because climate model projections of temperature are considered highly reliable, while projections of precipitation are less robust (Ukkola et al., 2020).

The province of British Columbia (BC) in so-called Canada is a microcosm of the water resource challenges posed by low flows and the hydrologic uncertainties regarding their driving mechanisms. The ecosystems and communities of BC have acutely felt the impacts of streamflow drought. In the late summer and early fall, photographs of drying rivers and dead salmon regularly make national and international news (Cecco, 2022; Hernandez, 2023), and increasingly severe droughts are threatening Indigenous nations' ways of life that have existed for millennia (First Nations Fisheries Council of British Columbia, 2020).

British Columbia is the colonial name for the westernmost province of Canada. In this manuscript we use this name to refer to the extent of the study area (although the spatial unit of analysis is watersheds). We acknowledge that colonial boundaries and names do not reflect the traditional territories of the (at least) 194 distinct First Nations located within our study area (British Columbia Assembly of First Nations, 2024), whose inherent rights to the land are unceded and unsurrendered. Many Indigenous governments continue to assert and exercise their jurisdiction over land and resource decisions within their traditional territories. Indigenous communities throughout BC are acutely impacted by drought and other water-related disasters, and are at the forefront of many environmental restoration and adaptation efforts (Cruickshank, 2023; First Nations Fisheries Council of British Columbia, 2020; Page, 2007; Teegee, 2023; The Columbia River Salmon Reintroduction Initiative, 2023; Wood, 2021).

The public perception that summer low flows are getting lower in British Columbia is supported by empirical evidence. Around the year 2000 various authors analysed streamflow data from the Reference Hydrometric Basin Network and found that September, October, and annual minimum flows had decreased in southern BC (Burn & Hag Elnur, 2002; YUE et al., 2003; X. Zhang et al., 2001). Ehsanzadeh et al. (2011) conducted another Canada-wide study and found that low flows

in southern BC continued to decrease to 2008. However, these national studies provide little insight into the behavior of different hydrologic regimes within BC. Hernández-Henríquez et al. (2017) found persistent decreases in summer runoff to the year 2015 for catchments on the western side of the Coast Mountains. Stahl & Moore (2006) found that mean August flows were decreasing in most glacierized basins in BC, particularly between 1976-1996, but trends were inconsistent in non-glacierized basins, a pattern they attributed to glacial retreat. Other authors have found mixed trends in regional studies with smaller samples of catchments (Anderson, 2016; Najafi et al., 2017; Rayne & Forest, 2011, 2012). There is a need for an updated provincial-scale analysis of low flow trends that allows disaggregation by region and hydrologic regime.

The provincial government enacted, in 2016, legislation declaring their authority to prohibit water use for irrigation when streamflow falls below a critical threshold. This authority has been exercised nine times from 2016 to 2023, alleviating ecosystem stress at the cost of economic hardship for many farmers. Thus, debates about the drivers of low flows are politically charged: is human water use really to blame, or are climate drivers more consequential? If climate is responsible, are increasingly severe low flows primarily driven by rising temperatures (which will almost certainly continue to rise) or changing precipitation patterns (which may continue, or reverse, or stabilize)?

Unfortunately, in BC as in many parts of the world, there is a shortage of scientific evidence to answer these questions. Assessments of low flow drivers have usually been limited to a small number of catchments and, as we find in Section 3.2, may have placed outsized importance on the role of winter snow storage. Thus, there is a need to investigate the widely-held view that streamflow drought is becoming more common across the province, and if so, why.

1.2 Limitations of hydrologic models

Hydrologic models often produce unsatisfactory low flow simulations and forecasts (Newman, 2014; Kim et al, 2021; Nicolle et al., 2014; Collins, 2020). One reason for these inaccuracies is that models are usually calibrated to all parts of the annual hydrograph. Low-flow generating mechanisms can differ from those that generate high and medium flows (Smakhtin, 2001), so parameters that are calibrated to reproduce high and medium flows may not accurately reflect hydrologic conditions nor accurately reproduce low flows (Cenobio-Cruz et al, 2023). In addition, since low flows are usually less variable than medium and high flows, low flows exert less influence on model calibration.

Various flow transforms can be used to force models to prioritize low flow estimation, but estimation of yearly minimum flows, or zero-flow days, remains challenging. For example, Aryal et al (2020) achieved a median modified Kling-Gupta Efficiency of 0.5 and a median Nash-Sutcliffe Efficiency of about 0.35 for the prediction of zero-flow days in 595 Australian catchments. Using 9 hydrologic models in 10 major river basins worldwide, Huang *et al.*, (2017) found percent bias values from -675% to 98% (median absolute value of 48%) for the flow duration curve low-segment volume and -83% to 1067% (median absolute value of 38%) for the 10 and 30-year low flow levels.

Studies in the Pacific Northwest region show the same limitations. Whitfield et al., (2003) modelled six watersheds around the Salish Sea (southwestern BC), and found that models produced biased 7-day low flow estimates for pluvial (rain-dominated) catchments. Various authors have used a distributed hydrological model (Variable Infiltration Capacity, or VIC) to model climate impacts in the Fraser River Basin, but found that simulated low flows were systematically lower than measured flows (Islam et al., 2017; Kang et al., 2016; Shrestha et al., 2012). We will return to these VIC simulations in Section 3.3. No comprehensive analysis of summer low flows across BC has been published.

1.3 Low flow drivers

We consider six climatic mechanisms that may influence summer low flows in BC, derived from previous work on low flows and streamflow drought (Smakhtin, 2001; Van Loon, 2015). We group these six mechanisms into three categories of driver: a) below-normal winter storage, which includes groundwater and snowmelt drought b) accelerated summer hydrograph recession, which includes rainfall deficits and storage depletion driven by evapotranspiration (ET), and c) short-term anomalies caused by temperature fluctuation, which include transmission losses and glacier melt drought. These mechanisms are listed in Table 1.

Which mechanisms are most important? In 2005, Barnett et al. published a widely-cited article showing that warming temperatures would induce snowmelt drought and decrease summer water availability across much of the northern hemisphere. It was thought that potential effects of warming on ET were small because actual evapotranspiration (related to temperature) is often much less than potential evapotranspiration in catchments that become water-limited in the summer. Much research over the last two decades has been focused on the effects of declining snowpack (Adam et al., 2009; Diffenbaugh et al., 2015; Godsey et al., 2014) and in the Pacific Northwest region (Ban et al., 2023; Chang et al., 2012; Clifton et al., 2018; J. R. Dierauer et al., 2018, 2021; Hale et al., 2023; Safeeq et al., 2014).

More recently, however, researchers have identified that, in some regions, summer ET may also be driving streamflow droughts. Teuling et al. (2013) showed that summer ET was amplifying European droughts; Woodhouse et al. (2016) and Udall and Overpeck (2017), working independently and using different methods, showed that air temperature is increasingly a driver of drought in the Colorado River basin. Floriancic *et al.* (2020) found that summer ET and precipitation controlled drought occurrence, and that winter snow storage had only minor effects on warm-season low flows in Switzerland. Then Brunner et al. (2021) and Floriancic et al. (2021) analysed catchments across the United States and Europe and both found that the importance of temperature as a driver of low flows was increasing or likely to increase in many places. However, Brunner et al. found that the effect of summer temperature was increasing in the Pacific Northwest, while Floriancic et al. argued that summer temperature was not a driver in this region. Boeing et al. (2024) found that increasing evapotranspiration has contributed to water storage deficits in Germany over recent decades.

Regional studies focused on the Pacific Northwest do not resolve this inconsistency. Kormos et al. (2016) found that low flows in the Pacific Northwest were more sensitive to precipitation than to temperature. Cooper et al. (2018) found the opposite: that low flows in the western US are

more sensitive to ET than to precipitation, but that sensitivity to both climate variables decreases towards the northern end of their study range. Georgiadis and Baker (2023) argued that both temperature and precipitation exert important controls on low flows in the Puget Sound.

In addition to climatic drivers, water and land use can alter low flows. In some watersheds, surface and groundwater use substantially reduces low flow discharge. The main land use and land cover disturbance throughout most of British Columbia is forest harvesting, which has been observed to both increase and decrease warm-season low flows (R. D. (Dan) Moore et al., 2020). Coble et al. (2020) reviewed 25 small catchment studies in the Pacific Northwest and found that there tends to be an increase in low flows following harvesting, sometimes followed by low flows similar to pre-harvest conditions, and then low flows below pre-harvest conditions. However, they also reviewed 19 large-catchment studies from around the world and found that long-term reductions in low flows were observed at large scales. Hou et al. (2024) analysed 20 catchments in British Columbia and did not find consistent increases or decreases in summer flows.

With this study we aim to improve the understanding and prediction of low flows in a well-gauged but understudied region, and in so doing develop novel approaches that can be applied in other regions. Our first objective is to quantify the drivers of low flows in diverse hydroclimatic regimes and whether these drivers are changing over time (Section 3.2). This will contribute to the debate about the importance of winter storage, summer ET, and summer precipitation as drivers of low flows. Second, we aim to extend the statistical analysis of drivers to create predictive regression models, enabling the reconstruction of low flows since 1901 (Sections 3.3 and 3.4). This modeling strategy will be of interest to the hydrologic modelling community, as it demonstrates a data-driven approach that improves the simulation of low flows by avoiding many of the challenges posed by traditional process-based hydrologic models, while also providing valuable process understanding by attributing low-flow trends to climate drivers. Our final objective is to apply these methods to produce locally-relevant information about low flow trends and drivers for British Columbia. These results will be of interest to a local audience as well as researchers focused on similar hydrologic environments.

2 Data and methods

2.1 Study Location

British Columbia occupies an area of almost 1 million km^2 on the western coast of Canada between 48.3º and 60º latitude. The province is endowed with a rich climatic diversity, ranging from Mediterranean climates in the southwest of the province (southern Vancouver Island) to polar climates at high elevations, with cold arid steppe climates in parts of the Interior (Beck et al., 2018). The geography is dominated by mountains, which rise up to 4653 metres above the Pacific.

We focus on the part of the province west of the continental divide (approximately 663,000 km^2, roughly the size of Myanmar, or 20% larger than metropolitan France). This excludes the northeast of the province, where most precipitation falls in the summer months, leading to high

flows in the summer. Also, since one of the chief concerns regarding low flows in British Columbia is the threat to Pacific salmon spawning habitat, it makes sense to focus on the Pacific drainage basin.

2.2 Catchments

We examine records from 230 hydrometric stations in British Columbia, maintained by the Water Survey of Canada. Of the 2235 operational and discontinued stations in British Columbia that measure Pacific-draining streams, 1477 measure unregulated flows. We filter these records for data completeness and recency criteria: at least 20 years of data (from August to October), at least 1 year of continuous year-round operation, and a data record not ending before January 1, 2000. 240 stations met the completeness and recency criteria. We then removed 8 intermittent streams, which recorded a zero flow in more than one year, and 2 streams for which urban land use accounted for more than 20% of the catchment area.

We designed an algorithm to classify the catchments as rainfall-dominated, snowmelt-dominated, hybrid, or glacial regimes based on average annual hydrographs for the years 1991-2020. Rainfall regimes are those with a single low flow period in late summer, snowmelt regimes are those with a single low flow period in late winter, while hybrid regimes show two distinct low flow periods (Fleming et al., 2007; Wade et al., 2001). The algorithm to identify flow minima is described in Appendix A. Glacial regimes are those where glaciers occupied more than 5% of the catchment area, which is a threshold used by previous researchers to identify basins most affected by glacial processes (Brighenti et al., 2023; R. D. Moore et al., 2020; Stahl & Moore, 2006).

Figure 1, panel A shows the catchment classification based on data from 1991-2020. Example annual hydrographs for each regime are shown in panel B. There are 28 rainfall, 79 hybrid, 89 snowmelt, and 34 glacial catchments.

Although the classification used throughout this paper is static in time, we found that many formerly snowmelt-dominated catchments have transitioned to a hybrid regime. We ran our classification algorithm on data from 30-year intervals between 1951 to 2022 (see Appendix A for details). 112 stations had enough data in each interval to run the algorithm (at least 10 years or glacial cover >5%). Of 56 stations classified as snowmelt-dominated in 1951, 18 transitioned to a hybrid regime by 2022, more than doubling membership in the hybrid regime. Four formerly glacial catchments lost enough glacial cover to be reclassified as snowmelt-dominated. Overall the combined membership in the snowmelt-dominated and glacial regimes fell from 82% to 66% of the 112 catchments. Appendix A provides more detail on the regime classifications through time.

Throughout the rest of the paper, the regimes correspond the period 1991-2020 (Figure 1 panel A).

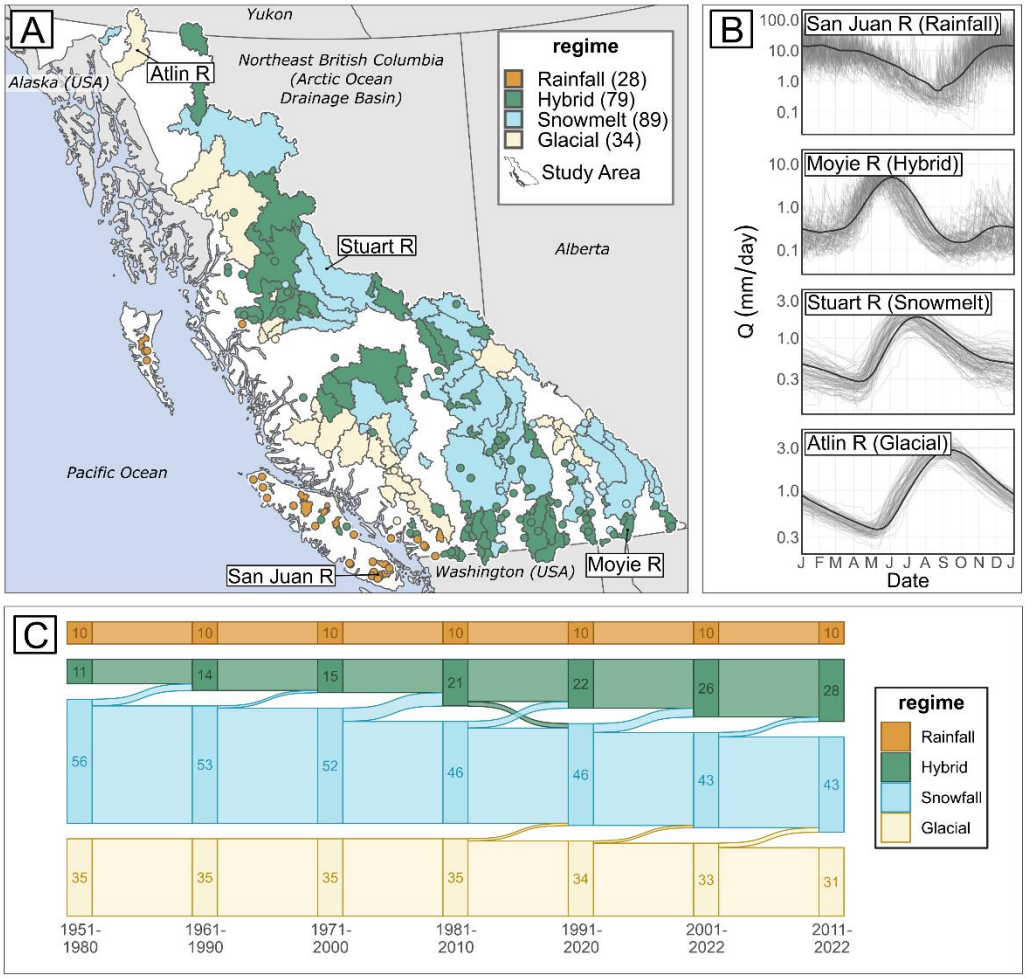

*Figure 1: **A**: Regime classification for catchments in our sample, for 1991-2020. Circles represent catchments of less than 200 km². **B**: Example hydrographs are shown for four catchments. San Juan River Near Port Renfrew (rainfall-dominated, gauge ID 08HA010), Moyie River at Eastport (hybrid, gauge ID 08NH006), Stuart River near Fort St James (snowmelt-dominated, gauge ID 08JE001) and Atlin River Near Atlin (glacial, gauge ID 09AA006). The thick black line in each graph is the 30-day mean flow, averaged across all years. Areas outside of study are shown in grey. **C:** The evolution of catchment classification since 1951, for 112 catchments with enough data to classify the regime in each interval.*

2.3 Definitions

We define the warm season as the snow-free season, based on the monthly average snow-water-equivalent (SWE) for the period 1991-2020, using data from the ERA-5 Reanalysis (Muñoz Sabater, 2019). We include months with a catchment-average SWE of less than 1 mm. For catchments with perennial snow or ice cover we defined the warm season as months for which SWE is within the bottom 10% of the annual range.

We define the *low-flow month* based on the timing of the minimum warm-season flow on the average annual hydrograph of 30-day mean discharge. This minimum is also constrained to occur after the spring freshet. We define the *low-flow season* as the low-flow month plus the month before and the month after, if the neighboring months are within the previously defined warm season.

The 7-day flow, Q7 is the 7-day running mean of discharge. The 7-day low flow, $Q7_{min}$, is the minimum value of Q7, and can be defined for each month or for the entire low-flow season (the 'overall' low flow).

2.4 Historical Trends

First, we analyze historical trends in low flows. We analyze overall low flows as well as low flows for July, August, September and October separately. We use Sen's slope on the log-transformed values, $\log(Q7_{min})$, from 1950-2022. Using the logarithm allows the estimated trend coefficient b to be interpreted as a percentage change per decade:

$$\%\Delta_{10} = (\exp(10 \dot{\times} b) - 1) \times 100\% \quad (1)$$

We assess significance at $p<0.05$ using the modified Mann-Kendall trend test for autocorrelated data (Hamed & Ramachandra Rao, 1998), implemented in R by Patakamuri and O'Brien (2021).

2.5 Climate and Anthropogenic Drivers

We assess stream sensitivity to the mechanisms discussed in Section 1.3 using several ancillary datasets. For each catchment, we create a linear regression model with $\log(Q7_{min})$ as the dependent variable (Equation 2). All variables are standardized to mean 0 and unit variance.

$$\log(Q7_{min}) \sim \beta_1 SWE_{max} + \beta_2 BF_{winter} + \beta_3 P_{summer} + \beta_4 T_{summer} + \beta_5 T_7 + \beta_6 Abstraction + \beta_7 ECA_I + \beta_8 ECA_{III} \quad (2)$$

β_i are the standardized regression coefficients and the independent variables are defined in Table 1. For gridded datasets (SWE, P, T, ECA_I, and ECA_{III}) we took the arithmetic average of all grid cells within each catchment. For Abstraction data we took the sum of values for all points of use within each catchment. The regression models are fit using all years with streamflow data from 1950-2020, which is the common subperiod for which all the ancillary datasets (Table 1) are available.

Since the objective here is to test a theory, we fit the regression models using forced simultaneous entry of the predictor variables (we enter all eight variables at once rather than using stepwise regression or any other data-driven variable selection techniques). We refer to these models as *explanatory* regressions.

The log transformation is used here to increase the influence of the lowest annual low flows and because $\log(Q7_{min})$ meets Shapiro-Wilk and Anderson-Darling tests for normality much more frequently than the untransformed values.

Large β coefficients indicate that the mechanism is responsible for a large portion of historical interannual variability in $\log(Q7_{min})$. This contrasts with the elasticities reported by Cooper et al. (2018), which express the % change in y related with % change in x. Low flows are more variable from year to year in warmer catchments than in colder catchments, so elasticities will tend to be greater in rainfall-dominated and hybrid catchments. However, we think sensitivities are better understood in the context of historical variability than in absolute terms, so we prefer to use the correlation coefficient.

Table 1: Data used to assess sensitivity to climate and anthropogenic drivers

Driver	Mechanism/ drought type	Variable	Description	Dataset	Dates
Below-normal winter storage	Snowmelt drought	SWE_{max}	Maximum Snow Water Equivalent	ERA5 Land Hourly (Muñoz Sabater, 2019)	1950-present
	Groundwater drought	BF_{winter}	Average baseflow for 30 days prior to SWE_{max}	Eckhardt baseflow separation of discharge time series	Same as discharge
Accelerated summer recession	Rainfall deficit	P_{summer}	Total Precipitation from May to the low-flow month	North American gridded monthly historical climate (~2 km resolution) (MacDonald et al., 2020)	1900-2022
	ET-driven storage depletion	T_{summer}	Average Temperature from May the low-flow month		
Short-term anomalies	ET-driven transmission losses	T_7	7-day mean temperature, concurrent with $Q7_{min}$	Canadian gridded daily historical climate (~10 km resolution) (Hutchinson et al., 2009)	1949-2020
	Glacier melt drought				
Direct Human Interventions	Water Abstraction	$Abstraction$	Estimated annual water use	Estimated based on water licenses, well construction records, and land use data. See Appendix B.	1863-2023
	Forest Harvesting	ECA_I	Fraction of watershed harvested or burned within 9 years	Calculated from BC Consolidated Cutblocks (Province of BC, 2024b) and Fire Perimeters (Province of BC, 2024a)	1900-2023
		ECA_{III}	Fraction of watershed harvested or burned between 24 and 80 years ago		1900-2023

We assess below-normal winter snow storage using ERA5-Land reanalysis snow water equivalent (SWE) data (Muñoz Sabater, 2019). Shao et al. (2022) found that these data performed better than other published gridded snow data products, and we also found that this dataset provided a much better match to snow survey data (Vionnet et al., 2021), than a Canadian data product (Environment and Climate Change Canada, 2021). SWE_{max} is the maximum catchment-averaged SWE for each year. We tested two alternatives: an alternative variable

definition SWE_{fixed}, which is the average SWE for the median peak accumulation month, and the snow disappearance date calculated from daily ERA5-Land SWE.

We estimate groundwater drought based on spring baseflow (BF_{winter}). British Columbia's monitoring well network is very sparse (Curran et al., 2023), precluding an analysis based on groundwater levels. We estimate baseflow using an Eckhardt filter, implemented in R in the FlowScreen package with parameters $\alpha = 0.97$ and $\mathrm{BFI_{max}} = 0.8$ (J. Dierauer & Whitfield, 2019). These parameters are considered typical for perennial streams with porous aquifers (Eckhardt, 2012). We also test the Eckhardt filter with parameters suitable for hard rock aquifers and 5 other baseflow filtering algorithms. BF_{winter} is the average estimated baseflow for 30 days prior to SWE_{max}, and we also test using a fixed timing (the same timing as SWE_{fixed}).

To estimate the impact of accelerated summer recession, we use the average summer temperature T_{summer} and the total summer precipitation P_{summer}. The summer season is defined as May-August, May-September, or May-October, depending on the low flow month. We use the interpolated, gridded, monthly data produced using the ANUSPLIN algorithm by MacDonald et al. (2020).

We investigate ET-driven transmission losses and glacier melt drought using T_7, 7-day mean temperature for the same 7 days used to calculate $Q7_{min}$. We cannot, unfortunately, separate the drying effects of ET-driven transmission losses from the wetting effects of increased meltflow. However, we may expect that glacial catchments will exhibit more positive (or less negative) streamflow-temperature correlations (Stahl & Moore, 2006). We use the interpolated, gridded, daily data produced using the ANUSPLIN algorithm by Hutchinson et al. (2009).

The ANUSPLIN monthly and daily data are derived from unadjusted precipitation records (Hutchinson et al., 2009; MacDonald et al., 2020), so changes to operating procedures, instrumentation, and station locations over time may introduce non-stationarity to the precipitation data (MacDonald et al., 2021; Werner & Cannon, 2016). We compared the ANUSPLIN data to Adjusted and Homogenized Canadian Climate Data (AHCCD: see Mekis & Vincent, 2011; Vincent et al., 2020) from climate stations within our study region (Appendix G). Surprisingly, we found that the ANUSPLIN dataset was as temporally consistent (the bias did not change over time) as two datasets developed using adjusted precipitation data and homogenized temperature data: ANUSPLIN-adjusted (MacDonald et al., 2021) and PNWNAmet (Werner et al., 2019). We also found that ANUSPLIN was more temporally consistent than ERA5-Land reanalysis data (Muñoz Sabater, 2019). We chose the ANUSPLIN dataset for the main analyses in this study because it offers the longest temporal coverage and finest resolution of available datasets for the region. We also repeat our sensitivity analyses using the PNWNAmet gridded dataset, which is available from 1945-2012 and the ERA5-Land reanalysis, which is available from 1950-present.

Water abstraction is estimated following the strategy in Barroso and Wainwright (2020). For licensed water use, we converted yearly and daily allocations to m^3/s. Although surface water licensing is thorough in BC, most groundwater use is unlicensed. We spatially joined well construction records to BC Assessment parcels and determined the most likely well use based on the intended well use from the well record (where available) and the property description from

the BC Assessment. For most well uses we assigned a representative water use value, but for irrigation wells we estimated water demand based on the size of the property. More details are provided in Appendix B. $Abstraction$ is only included for catchments in which the estimated mean annual water use is greater than 10% of the low-flow discharge in any individual year.

We include two variables related to forest disturbance: ECA_I and ECA_{III}. These correspond to hydrological periods I and III as described by Coble et al. (2020). Hydrologic period I is expected to be a period of increased low flow discharge, lasting between up to 40 years after the disturbance; the median length in the studies reviewed by Coble *et al.* was 9 years. ECA_I is defined here as the fraction of the catchment with a stand age of 9 years or less. Hydrologic period III is expected to be a period of reduced low flow discharge, beginning some years after the disturbance. The onset of period III has been found to be highly variable, with a median onset timing of 24 years following the disturbance. We defined ECA_{III} as the fraction of the catchment with stand age between 24 and 80 years old. These variables are only included if more than 10% of the catchment area has ever been logged and if less than 10% of the catchment area is privately held (where logging records are not public).

2.5.1 Nonlinearity in temperature effects

A common argument is that temperature (or potential evapotranspiration) does not drive droughts because actual evapotranspiration becomes water limited, not energy-limited as the landscape dries (Barnett et al., 2005). As temperature increases, there may be thresholds above which no water is available for evaporation, or when plants close their stomata to regulate transpiration. Thus, we may expect a nonlinear relationship between temperature and $Q7_{min}$.

Our linear regression models assume that the effect of temperature on $Q7_{min}$ is loglinear. This means that a unit increase in temperature will produce a fractional reduction in $Q7_{min}$, which is consistent with the expectation that the ratio of actual evapotranspiration to potential evapotranspiration decreases as water availability decreases. This is a reasonable assumption, but the real relationship could be either concave up or down on a loglinear plot, and we can statistically test the assumption in two ways.

First, we add a squared term in the linear regressions, $\beta_9(T_{summer})^2$. If the effect of temperature is diminished at high temperatures, we expect that β_9 will be positive. For each regime we use a binomial test to compare the number of positive coefficients to a binomial distribution with probability=0.5 as a test for field significance, which is the extent to which the distribution of results for several catchments differs from a random distribution (Burn and Hag Elnur, 2002). We also test whether the number of positive or negative significant coefficients exceeds the number expected by chance, by using binomial test with probability=0.05.

Second, we can substitute space for time and test whether temperature is a weaker driver in warmer catchments. For each regime, we evaluate the correlation between β_4 (the T_{summer} coefficient) and the mean summer temperature.

2.5.2 Stationarity

The trends that will be shown in Figure 2 are evidence of non-stationary time series, which could be due to non-stationary drivers and/or non-stationarity in low-flow generating mechanisms. The latter, which we term 'mechanistic non-stationarity' has been variably described as parameter instability, model non-stationarity, rainfall-runoff non-stationarity, and non-stationarity in catchment characteristics (Beven, 2016; Niel et al., 2003; Westra et al., 2014). If part of the trend in low flows is related to mechanistic non-stationarity, then inferences drawn from analysing historical data will be less useful for making predictions about the future or simulating years before the calibration period.

We can evaluate whether low-flow generating mechanisms have been stationary in the past by repeating the sensitivity analysis over early and late (recent) time frames. For this analysis we choose 153 catchments that have at least 20 years of data up to 1997 and at least 20 years from 1998 onwards (this split maximizes the number of catchments meeting the criterion). We fit the explanatory regression models (Equation 2) to the early (up to 1997) and late (1998 onwards) datasets.

If there is mechanistic non-stationarity, β_{early} and β_{late} will differ. We tested agreement between the two sets of coefficients for each catchment by comparing the test statistic, $\Delta\beta = \beta_{late} - \beta_{early}$, to an empirical distribution generated by a Monte Carlo permutation test with 10,000 random assignments of the data to the early and late periods. For this analysis we exclude the $Abstraction$, ECA_I, and ECA_{III} variables because a) they are less consistently measured through time, which could lead to erroneous findings of non-stationarity, b) this would also reduce the statistical power to correctly detect non-stationarity in the climate variables, and c) these variables are strongly autocorrelated by construction, which violates the independence assumption necessary for the Monte Carlo permutation test.

We assess field significance for this test statistic in with three tests: Test 1 is a binomial test with an expected probability of 0.5 to evaluate if the proportion of catchments with $\Delta\beta > 0$ is more or less than expected. Test 2 is a binomial test with an expected probability of 0.05 to test whether the proportion of catchments with individually significant positive differences is greater than expected. Test 3 is the same as Test 2 but for negative significant differences. Each binomial test is applied 20 times (4 regimes and 5 variables), so we assess significance using the Holm-Bonferroni method to control the family-wise error rate (Holm, 1979).

2.6 Predictive Regression Models

We build on the analysis of low flow drivers to create ordinary least squares regression models that predict the yearly minimum flow, $Q7_{min}$ for each catchment.

Despite its simplicity, regression is an appropriate model to simulate summer low flows. In the 20th century multiple regression models were often used for streamflow simulation and forecasting (eg. US Soil Conservation Service, 1972; Cayan et al., 1993; Garen, 1992; Vogel et al, 1999). Process-based computer models, though first proposed in the 1960's (Freeze and Harlan, 1969), became more popular in the late 1990s and 2000s with improvements in computer

technology (McMahon, 1992; Todini, 2007). More recently, data-driven approaches have made a comeback in the form of machine learning models, with some authors showing that data-driven approaches can outperform process-based models in a wide variety of settings (Kim et al, 2021; Arsenault et al, 2023). Regression is a simple form of machine learning, and its use is thus neither particularly new nor out of step with current practices.

We ruled out more complex machine learning models because of limitations in the size of the dataset. We have chosen to predict only the minimum yearly summer/fall low flow, in contrast to many previous low-flow and hydrologic drought studies that analyse flow percentiles or spell durations. The minimum flow has relevance for fish survival, passage, and spawning, has regulatory implications for British Columbia, and is also commonly the portion of the hydrograph that is most poorly predicted by process-based hydrologic models. By abandoning the requirement to simulate all parts of the annual hydrograph, we can more accurately represent the flow-generating mechanisms that are most relevant to low flows. However, we also reduce the size of our calibration data to one observation per year, so a high-order machine learning model would likely be overfit. Regression works well with small datasets and produces models that are straightforward to interpret, whose properties have been studied over more than a century.

We choose to make bespoke models for each catchment, rather than to create one model for the region with catchment characteristics as covariates, because the one-model approach did not perform well in our preliminary tests (results not shown). Our approach allows us to accurately simulate the unique response of each catchment to climate variability and change. We are then able to analyse how these responses across the four hydrologic regimes.

2.6.1 Model Selection

For each catchment we develop three regression models to predict $\log(Q7_{min})$: one for each of the three months comprising the low-flow season. We use all available years of streamflow data up to 2022 to build these regression models. In our sample of 230 catchments the longest record begins in 1903.

For each catchment-month combination, we construct the best model using 5-fold cross-validation, which is repeated 10 times with random partitions of the data into folds. We evaluate the models using the Kling-Gupta Efficiency (KGE), evaluated jointly on the predicted $Q7_{min}$ of the five folds. Due to the known problems with using the KGE on log-transformed flow values (Santos et al., 2018), we use the square root of $Q7_{min}$.

We start with 15 physically plausible variables and train models for all subsets of variables (2^{13}= 32,768 models). The model with the highest average KGE for each catchment-month is selected. We then evaluate the models using 10 new random partitions of the data into folds.

The 15 candidate variables are chosen to represent climate variables and water abstraction (Equation 3). We only use precipitation (P) and temperature (T) as predictor variables because they are uniformly available in the historical climate data from 1900-2022. We chose to include mean T and total P variables over seven averaging times (1, 2, 3, 4, 6, 8, and 12 months prior to

the month being predicted). This allows the cross-validation routine to select the most appropriate lag times, or combinations thereof, for each catchment. Using overlapping averaging times ensures that the model will include more recent months, which prevents the construction of physically implausible models.

For month k the full model with all 15 variables is:

$$\begin{aligned}\log(Q7_{min})_k \sim & b_1 T_{[k-11,k]} + b_2 T_{[k-7,k]} + b_3 T_{[k-5,k]} + b_4 T_{[k-3,k]} + b_5 T_{[k-2,k]} + b_6 T_{[k-1,k]} \\ & + b_7 T_{[k]} + b_8 P_{[k-11,k]} + b_9 P_{[k-7,k]} + b_{10} P_{[k-5,k]} + b_{11} P_{[k-3,k]} \\ & + b_{12} P_{[k-2,k]} + b_{13} P_{[k-1,k]} + b_{14} P_{[k]} + Abstraction\end{aligned} \quad (3)$$

b_i are the regression coefficients and the subscripts $[k-m, k]$ indicates the period ending on month k and beginning m months before. For each year, the predicted minimum summer low flow is the lowest prediction of the three months comprising the low-flow season.

We construct our models based on ANUSPLIN data. For comparison, we also construct predictive regression models using the same process with PNWNAmet and ERA5-Land data.

We can compare the model fits to published models for some of the catchments. The Pacific Climate Impacts Consortium (2020) has created distributed, physically-based hydrologic models for 56 of the 230 catchments studied here, using a Variable Infiltration Capacity model with a glacier model (VIC-GL). These 56 models include 21 hybrid, 26 snowmelt, and 9 glacial regimes. No rainfall-dominated catchments are included. To enable comparison of low-flow predictions between the VIC-GL models and the regression models developed in this study, we fit the regression models to the same time period (1945-2012) using the same gridded meteorological data (PNWNAmet , Werner et al., 2019). Only the final calibrated model data are available for the VIC-GL models, so we compare the performance to our final regression models, trained and evaluated on all years of data. These performance statistics are referred to as 'in-sample' statistics, in contrast to the 'out of sample' statistics derived from cross-validation. One catchment had less than 20 years of data between 1945-2012 so we compare the remaining 55.

We evaluate our models for residual autocorrelation and stationarity. We used the Breusch-Godfrey test for lag-1 autocorrelation (Breusch, 1978; Godfrey, 1978), and evaluated the critical value of the test statistic using Monte Carlo randomization of the lagged residuals with 10,000 draws. We evaluated residual stationarity by subjecting the residuals to the same trend analysis as described in Section 2.4. We applied the same binomial tests for field significance as described in Section 2.5.1.

2.7 Environmental Flow Thresholds

We compare the predicted low flows with two flow thresholds. The BC government has the authority to set a Critical Environmental Flow Threshold (CEFT) for any stream, which is defined as the discharge "below which significant or irreversible harm to the stream's aquatic ecosystem is likely to occur" (Water Sustainability Act, 2016). The presumptive CEFT is often set using a modified Tennant method, at 5% of the long-term mean annual discharge (McCleary & Ptolemy, 2017). However, for rainfall-dominated catchments, flows are frequently less than 5% long-term mean annual discharge. As such, the interim CEFT for the Xwulqw'selu

(Koksilah) Watershed (a typical rainfall-dominated catchment) was set close to 2% long-term mean annual discharge. We follow this strategy and set the presumptive CEFT at 2% long-term mean annual discharge for rainfall regimes and 5% for other catchments.

British Columbia has a separate drought classification framework, which is based on flow percentiles calculated for each day of the year. The most severe drought level (5) corresponds to flows below the 2nd percentile (a 1-in-50-year event), while level 4 corresponds to flows below the 5th percentile, and Level 3 to the 10th percentile. At level 5 "adverse impacts to socio-economic or ecosystem values are almost certain", regulatory action to limit water use is "highly likely", and the province prepares for "emergency response where risk of failure or loss of [water] supply exists" (BC Ministry of Water, Land and Resource Stewardship, 2023). The North American Drought Monitor classifies events below the 10th, 5th and 2nd percentiles as "Severe", "Extreme", and "Exceptional" droughts.

We calculate the 10th, 5th, and 2nd percentiles of $Q7_{min}$, based on available data from 1950 to present. Compared to British Columbia's drought monitoring this is somewhat conservative (less likely to classify events as drought), since the province calculates percentiles for each day of the year.

2.8 Historical Reconstruction

We reconstruct low flows from 1901 to 2022 using the optimized regression models (Section 2.6) and the historical monthly temperature and precipitation data. We compare the simulated low flows to the thresholds described in Section 2.7.

We also assess what has driven decadal changes in low flows over the last century. To answer this question, we estimate the yearly anomaly in $Q7_{min}$ for each catchment, relative to the average simulated $Q7_{min}$ from 1950-1999 (in the absence of any effect of water abstraction). This 'total anomaly' is composed of anomalies driven by winter and summer temperature and precipitation, as well as water abstraction.

We estimate the $Q7_{min}$ anomalies and their components using the regression model for the low-flow month for each catchment. First, we find the temperature and precipitation anomaly for each month, year, and catchment. We construct the predictor matrix for each regression model using these anomalies, considering temperature and precipitation separately and winter (November-April) and Summer (May – October) separately and setting all other values to 0. We run these predictor matrices through each regression model; the predicted values, minus the model intercept, are the anomalies in $\log(Q7_{min})$ associated with each driver.

3 Results

3.1 Dissecting past trends in low flows

Figure 2 shows the trends in summer to fall low flows, from 1950 to 2022. Overall low flows have decreased in 174 of 230 (76%) watersheds. There has been a significant ($p<.05$) decrease in 50 watersheds, and only five watersheds have seen a significant increase.

Rainfall and hybrid regimes have seen strong drying trends. Low flows in 27 of 28 rainfall-dominated catchments have decreased, with 16 statistically significant trends. 74 of 79 hybrid catchments have seen declines, with 22 significant drying trends.

Snowfall and glacial regimes show weaker evidence of regional trends. 61 of 89 snowfall-dominated catchments show drying trends, with 11 significant drying trends and three significant wetting trends. Over half of glacial catchments (22 of 34) have seen increases in summer low flows, with only one significant increase and one significant decrease.

Only two catchments have seen statistically significant increases of more than 10% per decade. Further inspection revealed that these are small (<100 km^2) catchments located very near to the two largest open-pit copper mines in Canada, which were operating since before hydrometric monitoring began. Although a detailed investigation of these sites is beyond the scope of this study, we hypothesize that historical mining operations (water use and/or mine dewatering) have induced a non-natural streamflow response.

July, August, September, and October trends are shown individually in the Appendix C. Drying trends are strongest in August (210/230 drying, 104 significantly), and weakest in October (121/228 drying, 21 significantly). Glacial regimes have seen more increases than decreases in September and October but across the three other regimes drying trends are more common in all months.

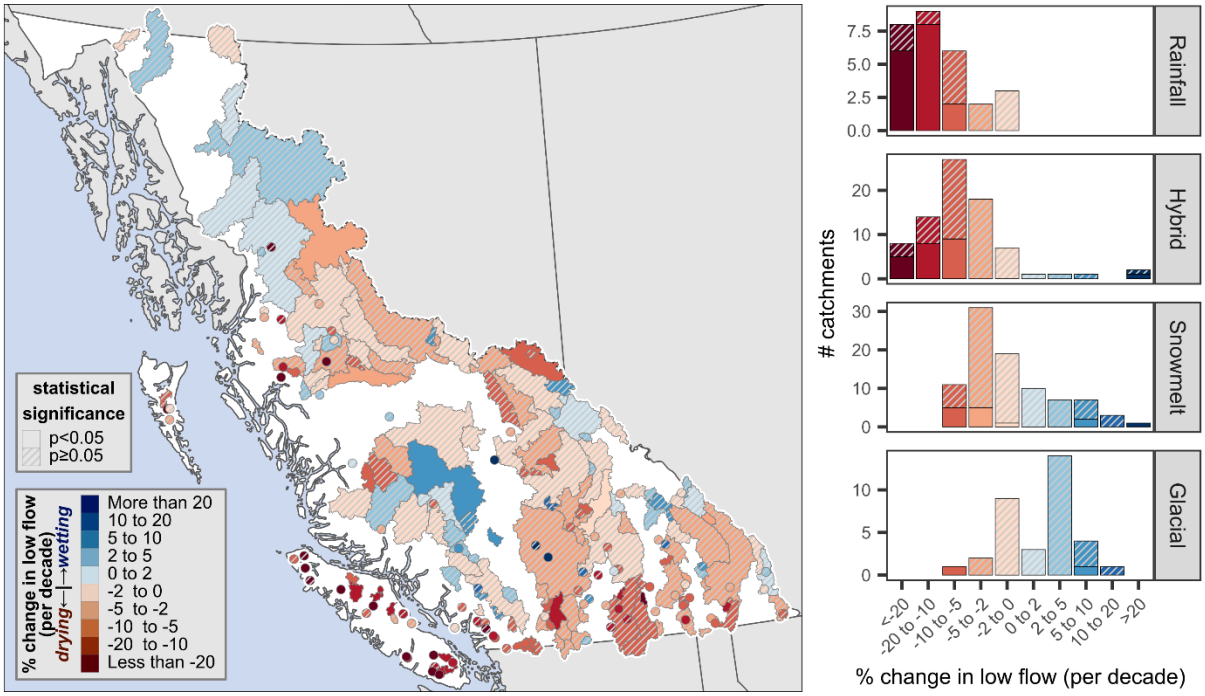

Figure 2: Trends for the overall (August – October) low flow in the 230 study catchments, using available data from 1950 to 2022. Hatched polygons denote non-significant trends. Red denotes drying trends and blue denotes wetting trends. 174 of 230 catchments are drying, and 50 of these decreases are statistically significant. Rainfall-dominated and hybrid catchments are drying much more than snowmelt-dominated and glacial catchments. Only five catchments show statistically significant increases (wetting trends).

3.2 Examining sensitivity to key climate variables

Figure 3 shows the standardized regression coefficients for regression models with each the variables listed in Table 1. Figure D1 shows bivariate (Pearson) correlation coefficients for each of the variables for comparison.

Below-normal winter storage has historically had a minor influence on summer low flows. For winter snow storage, the median coefficient is less than 0.2 across all regimes, with one third being significant. We found no meaningful differences in the strength of the correlations when using a fixed timing for the SWE variable (Figure D2). The snow disappearance date was a slightly stronger predictor than SWE_{max}, probably because the snow disappearance date includes information about both winter snow accumulation and summer melting rates. The bivariate correlation coefficients (Figure D1) were only slightly larger than the standardized coefficients in Figure 3 (median of 0.249 with 43% being significant).

Winter snow accumulation also does not necessarily prevent severe low flows. Across the 230 catchments, 35% of the catchment-years in the bottom decile (10^{th} percentile) of $Q7_{min}$ had above-median winter snow accumulation; 210 of 230 catchments had at least one year with above-median snow accumulation and $Q7_{min}$ in the bottom decile, and 52 catchments had at least one year with exceptionally high snow accumulation (top decile) that nevertheless had $Q7_{min}$ in the bottom decile, including 6 rainfall-dominated, 17 hybrid, 21 snowmelt-dominated, and 8 glacial catchments.

Correlations with end-of winter baseflow (BF_{winter}) are small in all hydroclimatic regimes. The median coefficient is 0.08. Only 12% are significant and positive, which is slightly more than the 5% that would be expected by chance. The bivariate correlation coefficients (Figure C1) were similar to the standardized coefficients in Figure 3 (median of 0.11 with 14% being significant). We tested six other baseflow filtering algorithms (Figure D3). Although the baseflow time series were considerably different, we did not find meaningful differences in the correlations with $\log(Q7_{min})$. We also tried holding the timing constant and calculating the average baseflow over the same month for each year (the median peak SWE accumulation month) and found even weaker correlations.

As another robustness check on our conclusions about the importance of winter storage, we tried including winter (November to April) T and P in place of SWE_{max} and BF_{winter} (Figure D4). The coefficients of T_{winter} and P_{winter} were similar in magnitude to the correlations with SWE_{max}, indicating that these variables serve as reasonable proxies for snow accumulation.

Summer precipitation, P_{summer}, shows large positive correlations for most catchments across all regimes (median of 0.48), and 79% of these correlations are statistically significant. Summer temperature, T_{summer}, shows negative coefficients for most rainfall-dominated and hybrid catchments, with median coefficients of -0.26 for both regimes, and 36% and 39% significant, respectively. In snowmelt-dominated catchments the median coefficient for T_{summer} is close to zero and in glacial catchments it is positive.

We note that bivariate correlation coefficients (Figure D1) for T_{summer} are considerably more negative than the coefficient from the multiple linear regression. For rainfall-dominated and hybrid catchments, the median bivariate correlations for T_{summer} are -0.54 and -0.55, respectively, which are approximately equal and opposite to the correlations for P_{summer}. The discrepancy between the bivariate correlations and the coefficients of the multiple linear regression occurs because T_{summer} tends to be correlated with many of the other predictor variables, especially P_{summer}, T_7, Abstraction, ECA_I and ECA_{III}.

The results are similar when we specify an alternate regression model with potential evapotranspiration and precipitation from the ERA5-Land model instead of T_{summer} and P_{summer} from the observational ANUSPLIN data (Figure D5). However, the correlations with potential evapotranspiration are slightly stronger (more negative) than those with temperature, probably because the potential evapotranspiration data accounts for the effects of humidity, wind speed and radiation, and the nonlinear shape of the saturation vapour pressure curve. The correlations with precipitation are slightly weaker, probably because the ERA5-Land precipitation data are less accurate than the ANUSPLIN data and because there is some collinearity between precipitation and potential evapotranspiration.

There are both positive and negative coefficients with T_7, but most of these relationships are weak. The coefficients are more likely to be negative in rainfall and hybrid catchments, which is similar to the pattern for T_{summer}.

Abstraction tends to reduce low flows, as expected. However, the magnitude of the effect varies widely, probably because the magnitude of water use varies. Most catchments in our sample had very little water use.

The two forest harvesting variables, ECA_I and ECA_{III}, do not show the expected behaviour of low flow increases in period I and decreases in period III. Both positive and negative coefficients are common for ECA_I and ECA_{III} and the median is near zero in all regimes.

We replicated Figure 3 using PNWNAmet data (Werner et al., 2019) for T_{summer}, P_{summer}, and T_7. We found that results were very similar to those using ANUSPLIN (Figure D6).

We also performed a more detailed analysis of the effect of forest disturbances on low flows (Appendix E), using four different Equivalent Clearcut Area functions and the pre-whitening strategy applied by Zhang and Wei (2012) and various other authors. This analysis also showed mixed and mostly non-significant results for most regimes. We found that pre-whitening resulted in extremely low statistical power to detect even large effects, so we also conducted an analysis without pre-whitening. There was some evidence that forest disturbance lowers low flows in snowmelt-dominated and glacial catchments, but we were unable to detect effects in rainfall or hybrid regimes.

We note that the standardized regression coefficients, β, measure the effect of each explanatory variable as a fraction of the standard deviation of $\log(Q7_{min})$. However, this variance tends to be smaller in cold catchments: the average coefficient of variation of $Q7_{min}$ is 0.53 in rainfall, 0.49 in hybrid, 0.34 in snowmelt and 0.30 in glacial regimes. This means that, all else being equal, the

same β indicates a greater effect on the magnitude of the low flow in rainfall-dominated catchments than in colder catchments.

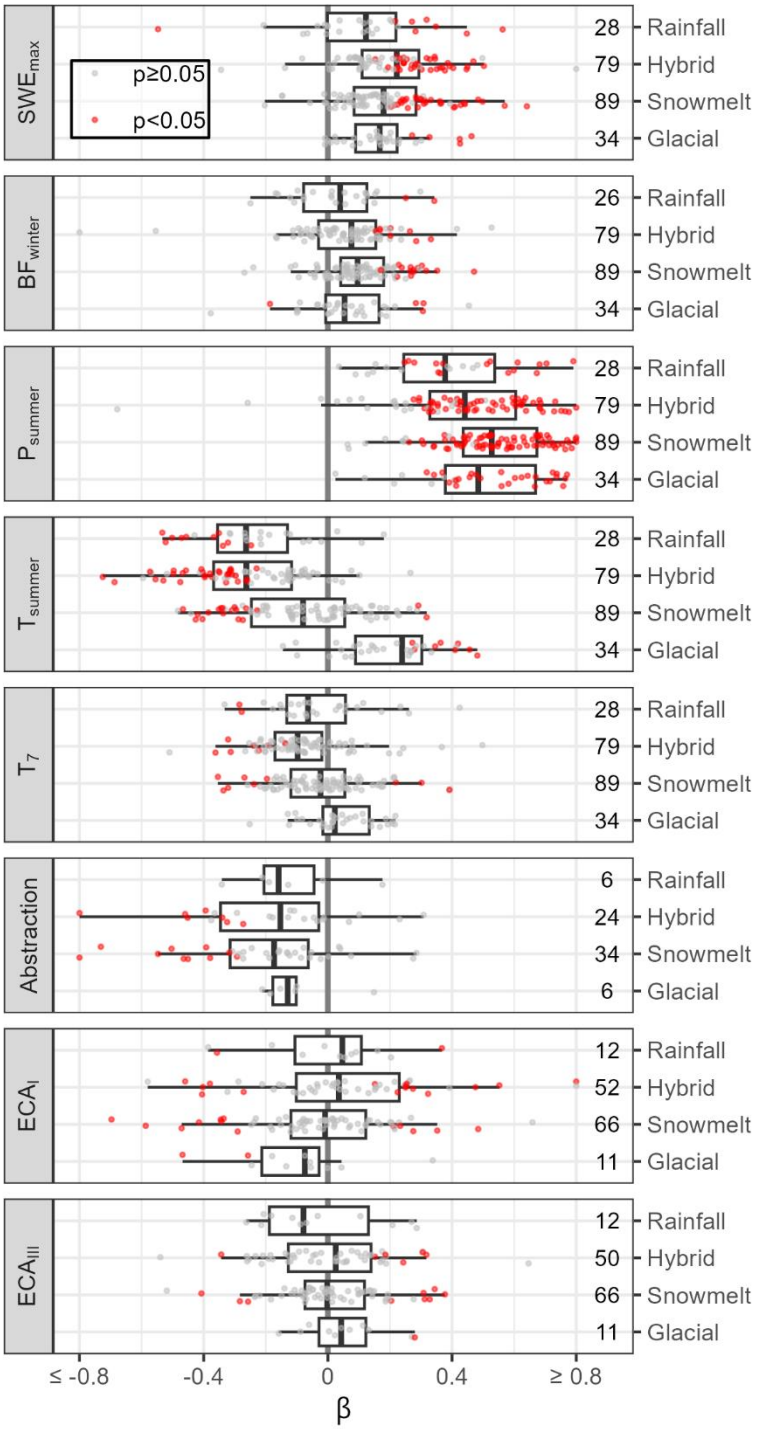

Figure 3: Standardized regression coefficients for log-transformed summer low flows with 8 explanatory variables. Analogous graphs with bivariate Pearson correlation coefficients are shown in Figure D1. The numbers indicate the number of catchments.

3.2.1 Nonlinearity of temperature effects

The first test for non-linearity in the effect of temperature was to include $(T_{summer})^2$ in our explanatory regression models. The coefficient for $(T_{summer})^2$ is positive in 57%, 77%, 74%,

and 65% of rainfall, hybrid, snowmelt, and glacial catchments; these rates are field-significant (greater than would be expected by chance) for hybrid and snowmelt, catchments and not significant for rainfall-dominated and glacial catchments. The rate of positive *significant* coefficients is significant only for the hybrid regime. These results suggest that the effect of temperature on $\log(Q7_{min})$ may be slightly nonlinear, and that the effect of temperature diminishes at high temperatures for hybrid and snowmelt-dominated catchments.

The second test for nonlinearity was to examine whether the effect of temperature was weaker in warmer catchments. We found the opposite: for all regimes, the coefficient for T_{summer} was larger (more negative) in warmer catchments; this relationship was statistically significant for the snowmelt-dominated regime, not significant for the rainfall-dominated regime, and marginally significant ($p<0.1$) in hybrid and glacial catchments.

3.2.2 Testing stationarity

We did not find evidence of significant non-stationarity in most of the correlations. Tests 2 and 3 (the number of positive and negative significant differences) were non-significant for all variables and regimes, even before applying the Holm-Bonferroni method.

Test 1 (the ratio of positive to negative differences) was significant for T_{summer} in hybrid and snowmelt-dominated regimes (for most catchments the coefficients were less negative in the late period), indicating that the influence of summer temperature may be decreasing. However, the influence of T_7 appears to be increasing in snowmelt-dominated regimes (most catchments had more negative coefficients in the later period), although this was non-significant after applying the Holm-Bonferroni method. Test 1 was also significant for SWE_{max} in hybrid and snowmelt-dominated regimes, indicating that the influence of winter snow accumulation may be decreasing. P_{summer} and BF_{winter} were not significantly non-stationary in this analysis.

We tested the robustness of our analysis by splitting the data at years 1995, 1996, and 1998. All results are included in Appendix D.

3.3: Parsimonious predictive regression models

Figure 4 shows the modelled response (change in low flow as a percentage) to temperature and precipitation anomalies, based on the predictive regression models (Section 2.6). The x-axis indicates the lag time between the anomaly and the low-flow month. The top row shows the response to 10 mm of additional precipitation, and the bottom row shows the response to a 1ºC increase in temperature over a single month.

All regimes show increases in $Q7_{min}$ related to precipitation events over a period of about 4 months. The lag-0 effect is smaller for some catchments because low-flow events can occur early in the month, before large precipitation events. Some hybrid and snowmelt-dominated catchments have longer lag times (up to 11 months) which is probably related to winter snow accumulation that persists into the summer.

The response to temperature for the low-flow month (lag 0) is strongly negative in rainfall regimes and variable in hybrid regimes. For snowmelt and glacial regimes, increased temperature leads to higher flows over the short term (up to a lag of 1 month) probably because of increased

meltflow, but lower flows over the longer term (3-6 months) because of storage depletion. The short term increase could also be partly related to catchments where low-flow month precipitation falls as snow in particularly cold years.

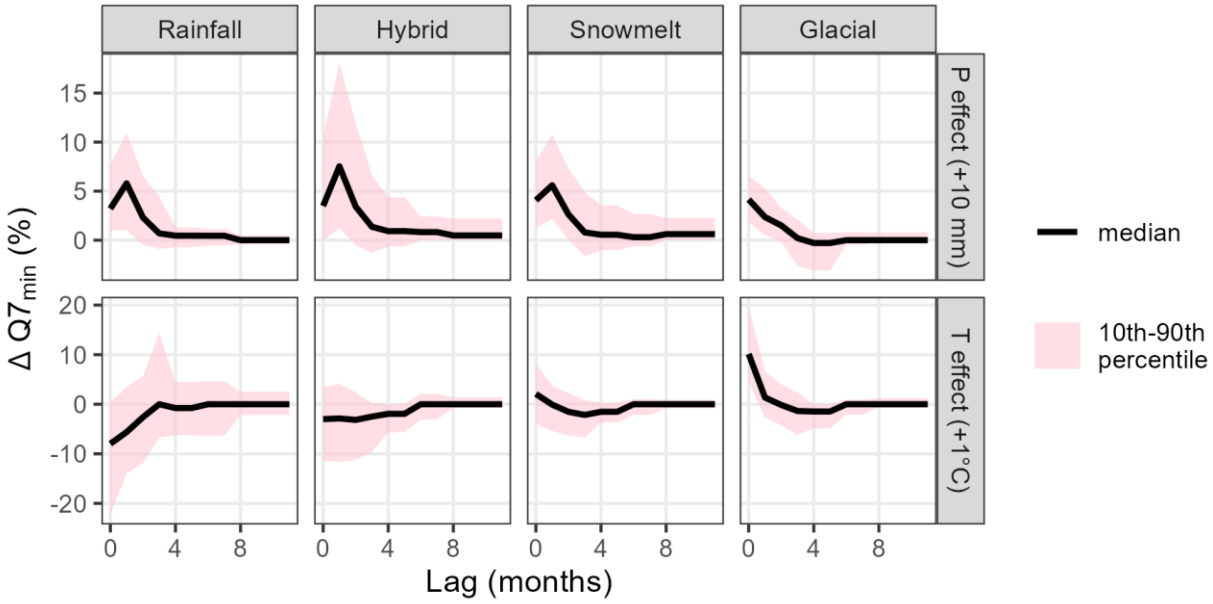

Figure 4: The modelled response to precipitation and temperature anomalies occurring 0 to 11 months before the month for which the low flow is predicted. The top row shows responses to 10 mm of additional precipitation and the bottom row shows responses to a 1ºC increase in temperature over a single month.

Table 2 shows the KGE, NSE, and R^2 statistics for the predictive regression models, derived from 10 repeated 5-fold cross-validations. The median KGE for the overall low-flow prediction is 0.64, with a range from 0.18 to 0.92. All the models perform significantly better than the benchmark KGE of -0.41 (Knoben et al., 2019). Three models have negative NSEs. We also tested the modelling framework using three other datasets: ANUSPLIN-adjusted (MacDonald et al., 2021), ERA5-Land (Muñoz Sabater, 2019) and PNWNAmet (Werner et al., 2019); we found that performance was very similar across ANUSPLIN, ERA5-Land, and PNWNAmet, but the ANUSPLIN-adjusted models performed slightly worse (see Appendix H).

Based on the R^2 values, the models explain a median of 48% of the historical variance. The residual error may be due to unobserved variables (eg. land use change) and measurement errors in streamflow, climate, and water use variables. Some of the error can also be attributed to variability in the timing of precipitation events during the month of interest.

Table 2: Median goodness of fit statistics for best regression models selected for the 230 catchments. Minimum and maximum values are provided in brackets.

	Rainfall	**Hybrid**	**Snowfall**	**Glacial**
N	28	79	89	34
KGE($Q7_{min}^{1/2}$)	0.68 (0.28, 0.77)	0.72 (0.28, 0.91)	0.66 (0.12, 0.88)	0.57 (0.26, 0.77)
NSE($\log(Q7_{min})$)	0.47 (-0.07, 0.6)	0.55 (-0.19, 0.8)	0.46 (-0.08, 0.8)	0.36 (-0.07, 0.63)
R^2($Q7_{min}$)	0.49 (0.08, 0.74)	0.54 (-1.8, 0.86)	0.47 (-0.15, 0.78)	0.39 (-0.04, 0.63)

PBIAS($Q7_{min}$)	-4.14 (-24.15, 3.78)	-1.04 (-19.38, 8.22)	-0.37 (-18.08, 7.27)	-0.69 (-5.17, 6.51)

In terms of predicting the overall summer low flow, the regression models presented here generally outperform the VIC-GL models (Pacific Climate Impacts Consortium, 2020). KGE($Q7_{min}$) and NSE($Q7_{min}$) for the regression models are better in 96% and 98% of the catchments, respectively. Evaluated on transformed flow values, KGE($Q7_{min}^{1/2}$) and NSE(log($Q7_{min}$)) are better in 95% and 98% of the catchments. Table 3 shows the median and range of NSE and KGE for the regression and VIC-GL models. Strikingly, NSE(log($Q7_{min}$)) is negative for 40 of 55 of the VIC-GL models but none of the regression models.

Table 3: Median Nash-Sutcliffe and Kling-Gupta Efficiencies for regression and VIC-GL models. Minimum and maximum statistics are provided in brackets.

	Regression	**VIC-GL**	**Regression outperforms VIC-GL**
KGE($Q7_{min}$)	0.80 (0.42, 0.93)	0.43 (-1.71, 0.86)	53/55 catchments
KGE($Q7_{min}^{1/2}$)	0.80 (0.46, 0.92)	0.45 (-0.48, 0.88)	52/55 catchments
NSE($Q7_{min}$)	0.71 (0.29, 0.91)	-0.22 (-70.6, 0.75)	54/55 catchments
NSE(log($Q7_{min}$))	0.71 (0.38, 0.88)	-0.56 (-44.74, 0.7)	54/55 catchments
PBIAS($Q7_{min}$)	-0.3 (-3.2, 5.8)	-12.8 (-88, 129.1)	52/55 catchments

We also evaluated 27 common goodness-of-fit statistics included in the hydroGOF R package (Zambrano-Bigiarini, 2024) under square-root, log, and identity transformations (81 statistics total). The regression models outperformed the VIC-GL models for every one of these statistics; on average for the 81 statistics, the regression models outperformed VIC-GL in 52 of 55 catchments.

The efficiency statistics in Table 3 are evaluated using in-sample statistics to ensure a like-with-like comparison. However, the regression models outperform the VIC-GL models even if we give the regressions an artificial disadvantage by using their cross-validated efficiency statistics (Table 2). The cross-validated regression KGE($Q^{1/2}$) scores are better than the in-sample scores for VIC-GL in 43 of 55 (78%) catchments, and the cross-validated Regression NSE(log(Q)) are better than the in-sample VIC-GL scores of 53 of 55 (96%) catchments.

The VIC-GL models are not poorly calibrated overall. When calculated on daily flows for the entire time series, the median NSE(log(Q)) and KGE($Q^{1/2}$) for these models are 0.76 and 0.84. Only one VIC-GL model has a negative KGE($Q^{1/2}$), and only five have a negative NSE(log(Q)). However, the models clearly perform poorly for low-flow prediction. The VIC-GL models were not calibrated with the sole purpose of predicting low flows, so general conclusions about the relative suitability of regression vs process-based models for predicting low flows may not be appropriate. It is possible that process-based models calibrated to optimize low-flow prediction could outperform the regression models presented here, but a rigorous benchmarking of different models and calibration techniques is out of the scope of the current work.

We found little evidence of residual autocorrelation. Overall, the Breusch-Godfrey test was significant for 8% of the catchments. Hybrid regimes were most likely to be autocorrelated

(13%), followed by rainfall and snowmelt-dominated catchments (7% each), glacial catchments (0%). Based on binomial tests, these rates of significant results are field-significant (greater than expected by chance) for the hybrid regime but not field-significant for the other regimes. Despite the finding of field-significance for the hybrid regime, the proportion catchments with significant autocorrelation is low. This indicates that ignoring interannual catchment storage in the models is a reasonable choice.

We also found little evidence of non-stationarity in the model residuals. We found individually significant trends in 13% of the catchments (18% of rainfall catchments, 14% of hybrid catchments, 10% of snowmelt catchments and 15% of glacial catchments). Approximately half (48%) of all catchments had positive trends in the residuals. Based on binomial tests, none of the regimes had an abnormal number of positive/negative trends nor an abnormal number of significant positive/negative trends.

3.4: Hindcasted low-flow conditions

We use the regression models to simulate past low flows from 1901-2022 and compare low flows to the Critical Environmental Flow Threshold (CEFT) and drought thresholds. Figure 5 shows the percentage of catchments within each regime that transgress these thresholds smoothed using a running mean of 10 years.

Rainfall-dominated catchments are, in general, more likely to transgress the CEFT than hybrid catchments, even though the CEFT for these catchments is set at 2% of long-term mean annual discharge for rainfall-dominated catchments and 5% for hybrid catchments. This is because low flows in these catchments are more variable from year to year than low flows in colder catchments, as was noted in Section 3.2. This larger envelope of variability means that low flows transgress the CEFT more frequently.

Warm-season low flows in snowmelt-dominated and glacial catchments almost never fall below the CEFT because these catchments tend to see their lowest flows in the winter months. However, drought thresholds were defined on a seasonal basis, and these catchments do experience warm-season droughts.

Drought and CEFT transgressions in rainfall-dominated catchments have risen erratically but persistently since the 1980s. There has also been a recent increase in transgressions for hybrid regimes over the same period, although it has been less dramatic than the trend in rainfall regimes. These simulated trends are consistent with the declining trends in measured $Q7_{min}$ observed in Figure 2.

Another remarkable detail in Figure 5 is that, for hybrid, snowmelt, and glacial regimes, streamflow drought was more common 100 years ago than it is currently. Although CEFT transgressions are rising in hybrid regimes, they are currently no more common than they were throughout the warm and dry 1920’s and 1930’s.

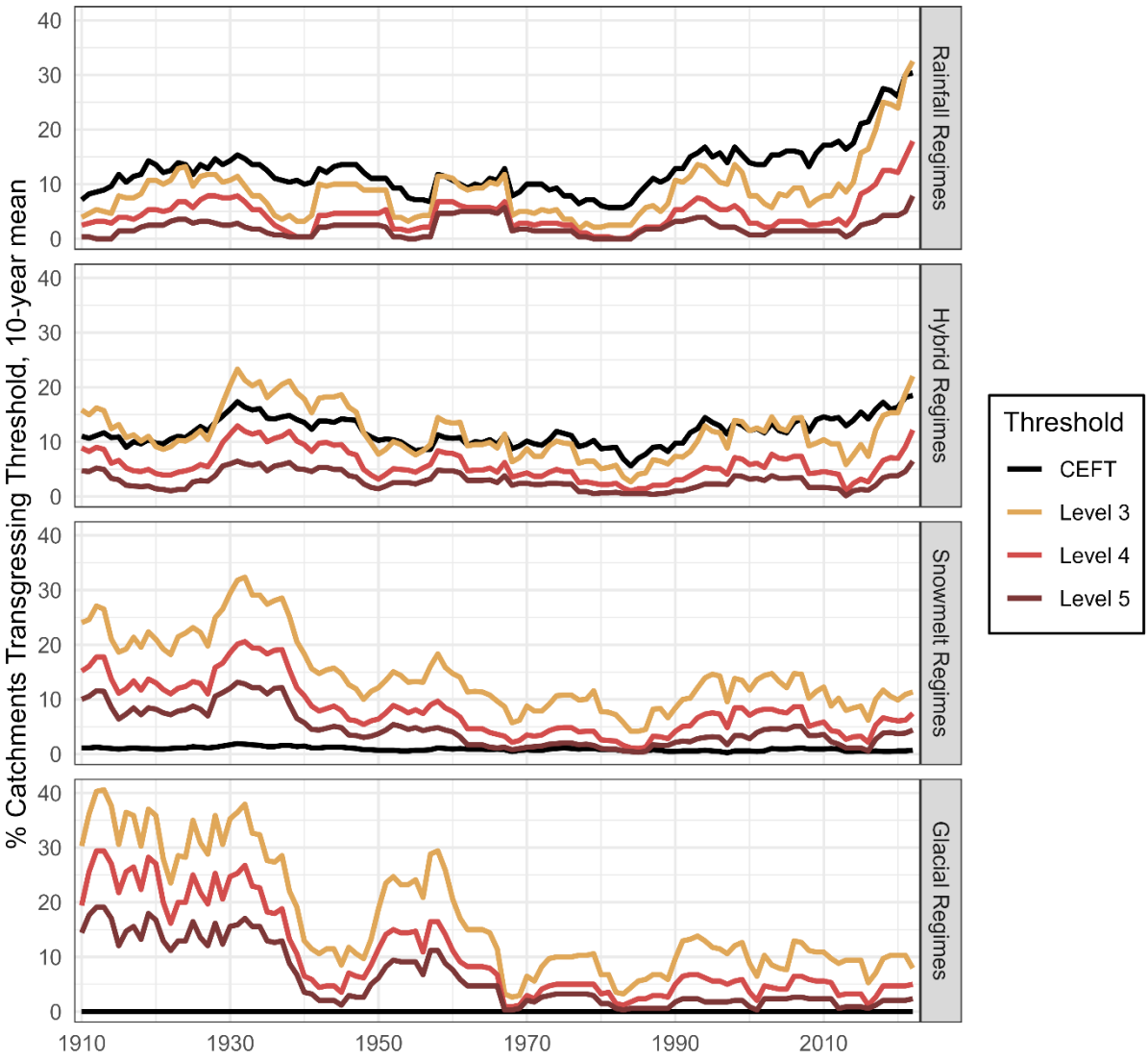

Figure 5: The simulated percentage of catchments transgressing the Critical Environmental Flow Threshold (CEFT) as well as Drought Levels 3, 4, and 5. A 10-year rolling mean (beginning in 1900) is used to smooth the data.

Figure 6 shows the total anomaly in $Q7_{min}$ (black line) and the components of this anomaly that can be attributed to winter and summer temperature and precipitation. Low flows in the early 20th century were considerably below-average in hybrid, snowmelt, and glacial regimes, and this was mostly related to a long-term precipitation deficit. Variability in precipitation drove most of the overall low-flow variability throughout the 20th century.

In recent years temperature has begun to play a much larger role. Since 1990, warm summer temperatures have led to large negative low-flow anomalies associated with temperature in rainfall-dominated and hybrid regimes (dark brown in Figure 6). This, in combination with slightly below-average precipitation, has led to large negative anomalies which continue to trend downwards. Hotter summers are continuing to increase the size of the negative anomaly driven temperature.

Increasing water abstraction began in earnest around 1950 and the effect on low flows has grown ever since. On average, in 2022 abstraction is estimated to have reduced flows by 7%, 13%, and 1% in rainfall, hybrid, and snowmelt-dominated catchments. Note that this is an average across all studied catchments, many of which have little or no water use; the effect on some catchments is much larger.

We created similar plots of $Q7_{min}$ anomalies using models trained and applied to the ANUSPLIN-adjusted, ERA5-Land, and PNWNAmet datasets, and found similar patterns (Appendix H). All datasets show a large and growing deficit associated with summer temperatures in rainfall and hybrid catchments, and all datasets show similar patterns precipitation-dominated variability in the 20th century. The ANUSPLIN-adjusted dataset depicts much drier conditions for the first half of the 20th century, so models created using this dataset show larger negative anomalies prior to 1950. However, the ANUSPLIN-adjusted dataset produces annual runoff ratios much greater than one between 1900 and 1950, particularly in coastal, rainfall-dominated catchments, so we believe that these data underestimate precipitation prior to 1950 (Appendix G). The hindcasts created using the unadjusted ANUSPLIN data are probably more reliable.

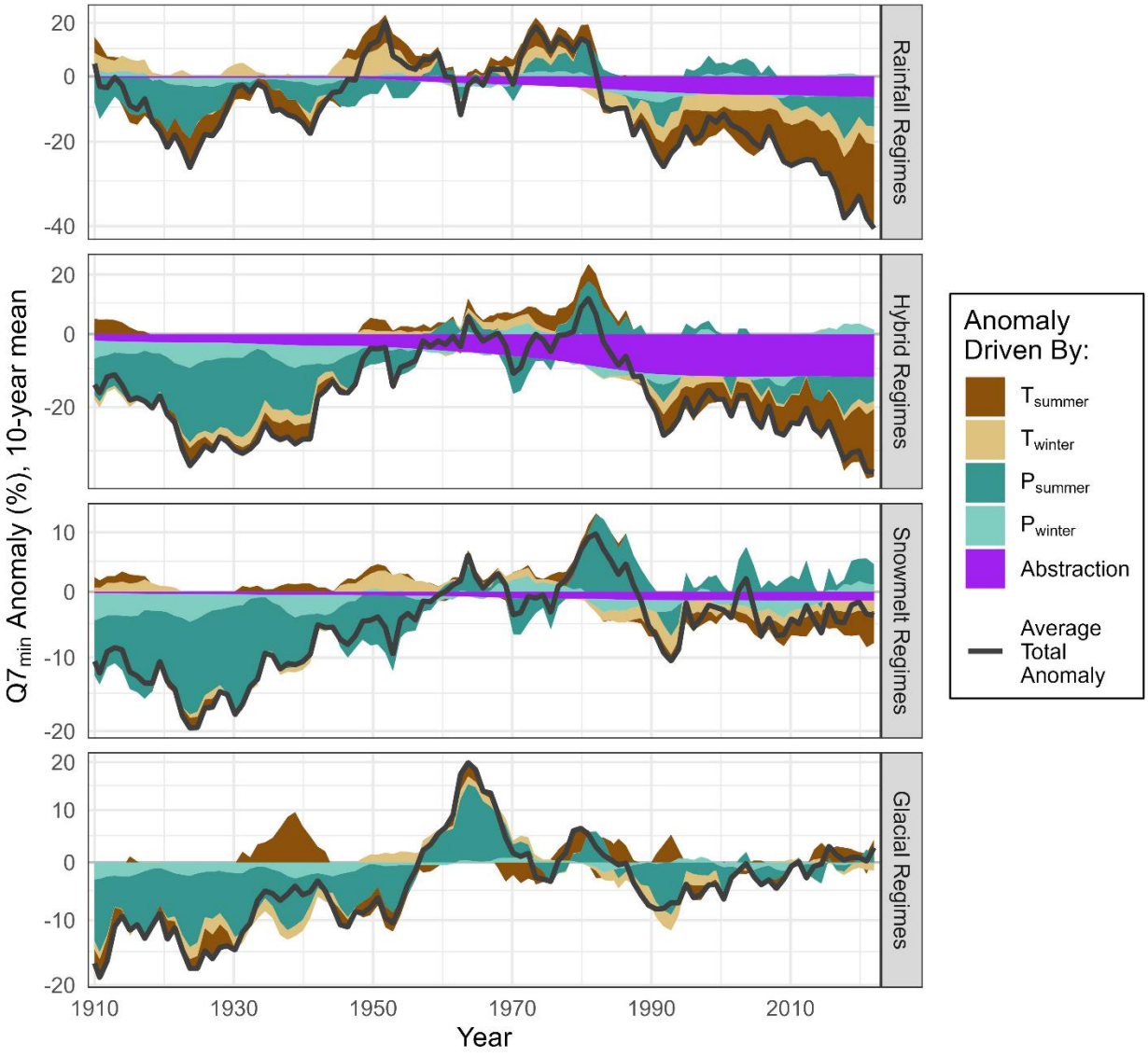

Figure 6: The average total anomaly in $Q7_{min}$ (relative to the period 1950-1999, with no water abstraction) is shown as a black for each catchment. The total anomaly is composed of anomalies driven by winter and summer temperature and precipitation, as well as abstraction. The y-axis is log-scaled so the width of the coloured ribbons can be directly compared.

4 Discussion

In the introduction we acknowledged that the extent of our study area was determined by colonial boundaries, which do not reflect the traditional territories or jurisdictions of the many First Nations located within this region. We start this discussion by acknowledging that in the future it could be useful to reframe the methods and results to explicitly consider Indigenous rights, jurisdictions, and priorities, if this would be of interest to Indigenous governing bodies. This could include considering the colonial roots of climate change, taking an environmental

justice lens to consider disproportionate impacts on Indigenous and other marginalized communities, or remapping and synthesizing results for specific Indigenous territories.

Regarding our first objective, we found that low flows in rainfall-dominated catchments are currently lower than at any point during the 20th century, and there are strong drying trends over the last few decades. There are similar drying trends in hybrid catchments, but drought was probably as common during the 1920's and 1930's as it is now. We did not find strong trends in snowmelt or glacial catchments since 1950, but our hindcasts indicate that summer flows in the early 20th century were probably substantially lower than they are now. However, these hindcasts should be interpreted with caution as the ANUSPLIN data are less accurate prior to 1950.

Our second objective was to analyse the drivers of low flows, with particular attention to the impact of changing winter snow accumulation (Barnett et al., 2005) and recent work indicating that the impact of evapotranspiration and summer temperature may be increasing (Boeing et al., 2024; Brunner et al., 2021).

We found low flows have not been very sensitive to winter storage of snow and groundwater. In section 3.2 we found small correlations between winter maximum snow water equivalent and near-zero correlations with end-of-winter baseflow. We also found some evidence that the effect of snowpack has been non-stationary (the correlations have shrunk in recent years) in hybrid and snowmelt-dominated catchments. Low flows below the 10th percentile occur regularly in years with above-average snowpack and have even been observed in years with snowpack above the 90th percentile. In Section 3.4 we found that winter precipitation and temperature anomalies have not contributed substantially to decadal variability in $Q7_{min}$. These findings are consistent with some past sensitivity analyses, including Cooper et al. (2018) who found low sensitivities to snow in the northwestern United States, and Floriancic et al. (2020) who found similar results in Switzerland.

However, sensitivity analyses rely on historical data, and the magnitude of future declines in snow accumulation may be much larger than the variability in the historical record. A very large decline multiplied by a small sensitivity could still result in a large impact to low flows, as predicted by Barnett et al. (2005) and Dierauer et al.(2021). We also found that sensitivities to groundwater storage were usually smaller than sensitivities to snow storage, suggesting that groundwater will not adequately buffer against the effects of declining snowpack. We propose that studies that investigate low flow drivers should consider both historical sensitivities and the magnitude of projected changes in each driver.

Across all regimes, accelerated summer recession has been the most important driver of summer low flows. In section 3.2 we found that on average, a 1 standard deviation-increase summer precipitation leads to half a standard deviation increase in $\log(Q7_{min})$. The opposite is probably true for T_{summer} in hybrid and rainfall regimes, although this relationship is obscured by collinearity with several other predictors. The correlations with T_{summer} are weaker in snowmelt-dominated catchments, probably because these regimes are more water-limited than energy-limited: the average mean annual precipitation in snowmelt-dominated catchments is only 840 mm, compared to 2191 mm in rainfall-dominated, 1145 mm in hybrid, and 1163 mm in glacial

861 catchments. In glacial catchments correlations with T_{summer} are often positive, probably because
862 increasing meltflow contributions at higher temperatures offset losses due to increased ET.

863 Our predictive regression models tell a similar story. These models predict that low flows are
864 most influenced by temperature and precipitation over a period of about 4 months (Figure 4).
865 Temperature generally exerts a negative influence on low flows, except for short-term
866 temperature (up to 1 month) in snowmelt-dominated and glacial catchments, where it tends to
867 increase flows.

868 We hindcasted anomalies in $Q7_{min}$ from 1901-2022 and found that these anomalies were
869 primarily driven by precipitation variability except in rainfall-dominated catchments where
870 temperature has also played a dominant role. Warmer temperatures over the last 30 years have
871 also exerted negative pressures on $Q7_{min}$ in hybrid and snowmelt-dominated catchments (Figure
872 6). This finding is robust across four climate datasets (Appendix H).

873 These results align with those of Brunner et al. (2021) and Kormos et al. (2016), who studied the
874 US portion of the Pacific Northwest. However, our finding that summer temperature is an
875 important driver of low flows stands in contrast to the conclusion of Floriancic *et al.* (2021) who
876 argued that summer ET was not a driver of low flows in this region. Their argument relied on the
877 fact that low flow timing in this region (late August – October) is not coincident with the timing
878 of maximum ET (July or August). However, their analysis did not consider that precipitation
879 often remains low across the region until mid-Autumn, so the water balance typically remains in
880 deficit even though ET is not at a maximum in September and October. We have shown here that
881 temperature over a period of about 4 months (not just the 30-day windows used by Floriancic
882 and colleagues) strongly influences the severity of low flows in the late summer and early
883 autumn.

884 The effect of temperature on low flows may be changing, but the evidence is mixed. By
885 including $(T_{summer})^2$ in our explanatory regressions, we found some evidence of nonlinearity (that
886 the effect of summer temperature dissipates at high temperatures) in colder catchments. This is
887 corroborated by the finding that the effect of summer temperature in hybrid and snowmelt-
888 dominated catchments has been nonstationary, and has decreased in more recent (warmer) years.
889 These findings are physically plausible if evapotranspiration in these catchments is becoming
890 more water-limited, rather than energy-limited (Barnett et al., 2005). On the other hand, when
891 substituting space for time, we found that the effect of temperature tends to be stronger in
892 warmer catchments within each regime: this is opposite to the expected behaviour if the warmest
893 catchments are the most water limited. We also did not find evidence of non-stationarity in the
894 residuals of the predictive regression models, so we conclude that any mechanistic non-
895 stationarity has probably had minor effects on overall low-flow behaviour.

896 Importantly, in rainfall-dominated catchments, which have seen the most severe declines in low
897 flows, and where rising summer temperatures have had the largest effect, the effect of
898 temperature does not appear to dissipate at high temperatures and has remained robust in recent
899 years.

Transmission losses appear to play a secondary role in controlling low flows. We found mostly negative but small correlations of T_7 with $\log(Q7_{min})$, particularly occur in rainfall and hybrid catchments. These represent transmission losses: when temperatures are high, ET from open water and from riparian zones increases. This leads to a temporary reduction in streamflow that may rebound once temperatures decrease. On the other hand, in snowmelt-dominated and glacial regimes temporary increases in temperature can lead to increased meltflow (Stahl & Moore, 2006).

We note that our catchment classification was defined using data from 1991-2020, but many catchments are transitioning from snowmelt-dominated to hybrid regimes. From 1951 to 2022 approximately one third of snowmelt-dominated catchments transitioned to the hybrid regime and the hybrid regime more than doubled in size. Due to glacial retreat, some catchments also transitioned from the glacial regime to a snowmelt-dominated regime. With further warming these shifts are likely to continue, and many currently snowmelt-dominated catchments may behave more like hybrid catchments. They may begin to see more negative trends in low flows, and may become more sensitive to summer temperature.

Beginning in earnest around 1950, surface and groundwater abstraction has reduced summer low flows in many parts of the province. We estimate that total water use has exceeded 10% of low flow discharge in 30% of the catchments studied. Although the regime-average anomalies in $Q7_{min}$ associated with abstraction are estimated to be small (0% in glacial catchments, up to 13% in hybrid catchments), many individual catchments have seen much larger reductions.

We were unable to find strong evidence of the impact of harvesting on low flows, although several of our analyses did point towards reduced low flows for 5-20 years post-harvest in snowmelt-dominated catchments. This is the opposite of the typical response reported in the literature, but several reviews have shown that responses are highly heterogeneous and difficult to predict (Coble et al., 2020; Goeking & Tarboton, 2020; R. D. (Dan) Moore et al., 2020). Moore et al. (2020) point out that longitudinal analyses of streamflow in disturbed catchments (as presented here) are less robust and statistically powerful than paired catchment studies. The issues they raised are compounded here by the gradual nature and low levels of disturbance in most of the studied catchments as well as the uncertain quality and completeness of historical forestry and fire data.

Our third objective was to build regression models to predict and hindcast low flows from 1901-2022. Our predictive regression models predict low flows much more accurately than models currently being used for climate change impact assessment (Pacific Climate Impacts Consortium, 2020). We found that the regression models had low levels of residual autocorrelation and non-stationarity. Some caveats do apply to our historical reconstructions. Land use changes over the past century may have led to other forms of mechanistic non-stationarity. Our analysis of stationarity was based on a before/after analysis split at 1997; we do not have enough data to evaluate stationarity at the time scale of a century. The climate data on which the models are based are less accurate for the early 20th century because meteorological stations were more sparsely distributed (MacDonald et al., 2020), and we found that there may be temporal inconsistencies in the ANUSPLIN data. Nevertheless, streamflow records from the few

941 hydrometric stations with continuous records throughout the 1920's and 1930's largely confirm
942 very low flows in these decades. Long-term records for some select stations are shown in
943 Appendix F. See, for example Figure F14 (South Thompson River, a tributary of the Fraser), or
944 Figure F20 (the Columbia River).

945 We can also look to anecdotal evidence to confirm historical droughts. In our reconstruction,
946 1929 was the year with the highest number of hybrid catchments experiencing Level 5 drought.
947 Newspaper records show that the region was so dry in 1929 that Vancouver and Seattle's
948 hydroelectric reservoirs almost ran out of water[1], water was rationed[2], wells ran dry, and Catholic
949 clergy appealed for divine intervention[3]. In those years newspapers also regularly ran headlines
950 with dire warnings that salmon stocks were disappearing[4]. Most Canadian articles from the time
951 blamed dwindling salmon stocks on overfishing, American traps, seals, and dam construction,
952 but in 1929 the Washington State Supervisor of Fisheries, Charles Pollock, identified that
953 "Drought is imperiling the fish industry of the Pacific northwest"[5]. 1929 drought levels were
954 equaled in 2022.

955 For rainfall-dominated catchments, the most drought-stricken year in our reconstruction was
956 1958 which, according to tree-ring data from Vancouver Island, may have been the driest year for
957 350 years (Coulthard et al., 2016). In snowmelt-dominated and glacial catchments 1928 and
958 1919 take the top spots; 1928 was the start of a 5-year drought in the Quesnel Basin (Brice et al.,
959 2021) but 1919 does not stand out in paleohydrological studies. In snowmelt and glacial
960 catchments 1904 and 1905 each take 2nd place in our reconstruction; 1905 took 4th place in the
961 reconstruction presented by Coulthard et al. (2016), 1904 took 6th place since 1789 in the Stikine
962 River (Welsh et al., 2019), and 1904-1905 was the second worst drought in a separate 300-year
963 tree-ring reconstruction of snow droughts in Southwestern BC (Mood et al., 2020).

964 **5 Conclusions**

965 We have shown that linear regression provides a simple, highly interpretable, and surprisingly
966 accurate way of analysing and predicting low flows across a diverse range of hydrologic
967 regimes. First, we assessed low-flow sensitivities to various climate and anthropogenic drivers
968 and examined whether these sensitivities were changing. We then developed predictive
969 regression models that outperformed process-based models on every standard goodness-of-fit
970 metric. These regression models require just monthly temperature, precipitation, and water
971 abstraction data, so we were able to hindcast droughts, environmental flow transgressions, and
972 low flow anomalies to 1901. Due to the additive nature of the models, we were able to
973 disaggregate these anomalies by driving mechanism, and so corroborate our sensitivity analysis.

[1] Capilano Flow Hits New Low (1929, December 3). *The Vancouver Daily Province*, p. 5.
[2] Plan to Curtail Street Lighting As Power Economy (1929, November 27). *The Vancouver Sun*, p. 1.
[3] Prayers for Rain Ordered by Archbishop (1929, November 29). *The Vancouver Daily Province*, p. 1.
[4] See, for example: B.C. Salmon Run Tends to Decline (1933, August 11). *The Vancouver Daily Province*, p. 1.; Malloy, M. (1921, October 9). What is a Poor Fish to do? Government Conservation Tactics Fail to Protect the Fraser River's Former Wealth; Sockeye Salmon, under Conservation, are Disappearing. *The Vancouver Sun,* p. 30; Y, E. M. (1920, February 15). Preservation of Salmon Problem for Authorities. *The Vancouver Sun,* p. 7; Says Salmon Runs Facing Destruction (1922, September 22). *The Vancouver Sun,* p. 1;
[5] Associated Press: Fish Affected (1929, December 6). *The Vancouver Sun,* p.14.

We propose that these regression techniques could be useful for explaining and predicting low flows and droughts in other regions.

Rainfall-dominated and hybrid catchments have seen large and statistically significant decreasing trends in the annual summer minimum flow. Rainfall-dominated catchments are now experiencing streamflow drought and environmental flow transgressions more often than at any point over the past 122 years. Hybrid catchments, on the other hand, are experiencing conditions about as dry as the 1930's. However, negative low flow anomalies through the Great Depression were caused by lack of precipitation while present-day low flows are being driven by warming temperatures, despite above-average precipitation.

Summer low flows in snowmelt-dominated and glacial catchments have not shown strong trends since the 1950s but seem to be substantially higher than flows during the early 20th century. We found that these catchments are primarily sensitive to summer rainfall. Sensitivity to temperature is low, probably because high temperatures induce melting which offsets increased evaporative losses in glacial catchments and because snowmelt-dominated catchments tend to more water-limited than energy-limited. However, we note that our catchment classification indicated that about one third of previously snowmelt-dominated catchments have become hybrid. If this shift continues then many catchments currently classified as snowmelt-dominated may become more sensitive to temperature and summer low flows may begin to decline.

We found that winter conditions and annual snow accumulation have historically only weakly driven variability in low flows. However, climate-change-induced reductions in snowpack and glacial extent will probably be large compared to historical variability, and this large change combined with a weak sensitivity could still result in large reductions in low flow (J. R. Dierauer et al., 2021; Schnorbus et al., 2014).

Acknowledgments

We have no conflicts of interest to disclose. SR is funded by a NSERC CGS –D award but there is no specific project funding.

We wish to thank Drs. Dan Moore, Thorsten Wagener, Sandra Walde and Daniel Ruzzante for their feedback, which improved the manuscript.

Open Research

All code developed for this project is available at https://github.com/sruzzante/low-flows-BC

References

Adam, J. C., Hamlet, A. F., & Lettenmaier, D. P. (2009). Implications of global climate change for snowmelt hydrology in the twenty-first century. *Hydrological Processes*, *23*(7), 962–972. https://doi.org/10.1002/hyp.7201

Anderson, K. S. (2016). *Hydro-climatological Trend Analysis and Influences on the Discharge in the Elk River Watershed, Southeast British Columbia* [Text, University of Northern British Columbia]. https://doi.org/10.24124/2016/1218

Arthington, A. H., Bhaduri, A., Bunn, S. E., Jackson, S. E., Tharme, R. E., Tickner, D., Young, B., Acreman, M., Baker, N., Capon, S., Horne, A. C., Kendy, E., McClain, M. E., Poff, N. L., Richter, B. D., & Ward, S. (2018). The Brisbane Declaration and Global Action Agenda on Environmental Flows (2018). *Frontiers in Environmental Science*, *6*. https://www.frontiersin.org/articles/10.3389/fenvs.2018.00045

Ban, Z., Li, D., & Lettenmaier, D. P. (2023). The Increasing Role of Seasonal Rainfall in Western U.S. Summer Streamflow. *Geophysical Research Letters*, *50*(9), e2023GL102892. https://doi.org/10.1029/2023GL102892

Barnett, T. P., Adam, J. C., & Lettenmaier, D. P. (2005). Potential impacts of a warming climate on water availability in snow-dominated regions. *Nature*, *438*(7066), Article 7066. https://doi.org/10.1038/nature04141

Barroso, S., & Wainwright, M. (2020). *Water Use and Management Options in the Koksilah River Watershed: Preliminary analysis and recommendations for future work* (WSS2020-02; Water Science Series). https://a100.gov.bc.ca/pub/acat/documents/r59126/Koksilah_wateruse_1620692372737_E9980F7DAE.pdf

BC Ministry of Water, Land and Resource Stewardship. (2023). *British Columbia Drought and Water Scarcity Response Plan* (pp. 1–54). Government of British Columbia.

https://www2.gov.bc.ca/assets/gov/environment/air-land-water/water/drought-info/drought_response_plan_final.pdf

Beck, H. E., Zimmermann, N. E., McVicar, T. R., Vergopolan, N., Berg, A., & Wood, E. F. (2018). Present and future Köppen-Geiger climate classification maps at 1-km resolution. *Scientific Data*, *5*(1), Article 1. https://doi.org/10.1038/sdata.2018.214

Beven, K. (2016). Facets of uncertainty: Epistemic uncertainty, non-stationarity, likelihood, hypothesis testing, and communication. *Hydrological Sciences Journal*, *61*(9), 1652–1665. https://doi.org/10.1080/02626667.2015.1031761

Boeing, F., Wagener, T., Marx, A., Rakovec, O., Kumar, R., Samaniego, L., & Attinger, S. (2024). Increasing influence of evapotranspiration on prolonged water storage recovery in Germany. *Environmental Research Letters*, *19*(2), 024047. https://doi.org/10.1088/1748-9326/ad24ce

Bradford, M. J., & Heinonen, J. S. (2008). Low Flows, Instream Flow Needs and Fish Ecology in Small Streams. *Canadian Water Resources Journal / Revue Canadienne Des Ressources Hydriques*, *33*(2), 165–180. https://doi.org/10.4296/cwrj3302165

Breusch, T. S. (1978). Testing for Autocorrelation in Dynamic Linear Models*. *Australian Economic Papers*, *17*(31), 334–355. https://doi.org/10.1111/j.1467-8454.1978.tb00635.x

Brice, B. L., Coulthard, B. L., Homfeld, I. K., Dye, L. A., & Anchukaitis, K. J. (2021). Paleohydrological context for recent floods and droughts in the Fraser River Basin, British Columbia, Canada. *Environmental Research Letters*, *16*(12), 124074. https://doi.org/10.1088/1748-9326/ac3daf

Brighenti, S., Engel, M., Dinale, R., Tirler, W., Voto, G., & Comiti, F. (2023). Isotopic and chemical signatures of high mountain rivers in catchments with contrasting glacier and rock glacier cover. *Journal of Hydrology*, *623*, 129779. https://doi.org/10.1016/j.jhydrol.2023.129779

British Columbia Assembly of First Nations. (2024). *First Nations in BC*. https://www.bcafn.ca/first-nations-bc

1053 Brunner, M. I., Swain, D. L., Gilleland, E., & Wood, A. W. (2021). Increasing importance of temperature
1054 as a contributor to the spatial extent of streamflow drought. *Environmental Research Letters*,
1055 *16*(2), 024038. https://doi.org/10.1088/1748-9326/abd2f0
1056 Burn, D. H., & Hag Elnur, M. A. (2002). Detection of hydrologic trends and variability. *Journal of*
1057 *Hydrology*, *255*(1), 107–122. https://doi.org/10.1016/S0022-1694(01)00514-5
1058 Cecco, L. (2022, October 5). Thousands of salmon found dead as Canada drought dries out river. *The*
1059 *Guardian*. https://www.theguardian.com/environment/2022/oct/05/canada-dead-salmon-drought-
1060 british-columbia
1061 Chang, H., Jung, I.-W., Steele, M., & Gannett, M. (2012). Spatial Patterns of March and September
1062 Streamflow Trends in Pacific Northwest Streams, 1958–2008. *Geographical Analysis*, *44*(3),
1063 177–201. https://doi.org/10.1111/j.1538-4632.2012.00847.x
1064 Clifton, C. F., Day, K. T., Luce, C. H., Grant, G. E., Safeeq, M., Halofsky, J. E., & Staab, B. P. (2018).
1065 Effects of climate change on hydrology and water resources in the Blue Mountains, Oregon,
1066 USA. *Climate Services*, *10*, 9–19. https://doi.org/10.1016/j.cliser.2018.03.001
1067 Coble, A. A., Barnard, H., Du, E., Johnson, S., Jones, J., Keppeler, E., Kwon, H., Link, T. E., Penaluna, B.
1068 E., Reiter, M., River, M., Puettmann, K., & Wagenbrenner, J. (2020). Long-term hydrological
1069 response to forest harvest during seasonal low flow: Potential implications for current forest
1070 practices. *Science of The Total Environment*, *730*, 138926.
1071 https://doi.org/10.1016/j.scitotenv.2020.138926
1072 Cooper, M. G., Schaperow, J. R., Cooley, S. W., Alam, S., Smith, L. C., & Lettenmaier, D. P. (2018).
1073 Climate Elasticity of Low Flows in the Maritime Western U.S. Mountains. *Water Resources*
1074 *Research*, *54*(8), 5602–5619. https://doi.org/10.1029/2018WR022816
1075 Coulthard, B., Smith, D. J., & Meko, D. M. (2016). Is worst-case scenario streamflow drought
1076 underestimated in British Columbia? A multi-century perspective for the south coast, derived
1077 from tree-rings. *Journal of Hydrology*, *534*, 205–218.
1078 https://doi.org/10.1016/j.jhydrol.2015.12.030

1079 Cruickshank, A. (2023, September 21). Restoring the flow: Tsleil-Waututh's race to save salmon habitat in
1080 drought stricken southwest B.C. *The Narwhal*. https://thenarwhal.ca/tsleil-waututh-nation-
1081 salmon-restoration/
1082 Curran, D., Gleeson, T., & Huggins, X. (2023). Applying a science-forward approach to groundwater
1083 regulatory design. *Hydrogeology Journal*, *31*(4), 853–871. https://doi.org/10.1007/s10040-023-
1084 02625-6
1085 de Graaf, I. E. M., Gleeson, T., van Beekl, L. P. H. (Rens), Sutanudjaja, E. H., & Bierkens, M. F. P.
1086 (2019). Environmental flow limits to global groundwater pumping. *Nature*, *574*, 90–94.
1087 https://doi.org/10.1038/s41586-019-1594-4
1088 Dierauer, J. R., Allen, D. M., & Whitfield, P. H. (2021). Climate change impacts on snow and streamflow
1089 drought regimes in four ecoregions of British Columbia. *Canadian Water Resources Journal /*
1090 *Revue Canadienne Des Ressources Hydriques*, *46*(4), 168–193.
1091 https://doi.org/10.1080/07011784.2021.1960894
1092 Dierauer, J. R., Whitfield, P. H., & Allen, D. M. (2018). Climate Controls on Runoff and Low Flows in
1093 Mountain Catchments of Western North America. *Water Resources Research*, *54*(10), 7495–7510.
1094 https://doi.org/10.1029/2018WR023087
1095 Dierauer, J., & Whitfield, P. (2019). *FlowScreen: Daily Streamflow Trend and Change Point Screening*
1096 (Version 1.2.6) [Computer software]. https://cran.r-
1097 project.org/web/packages/FlowScreen/index.html
1098 Diffenbaugh, N. S., Swain, D. L., & Touma, D. (2015). Anthropogenic warming has increased drought
1099 risk in California. *Proceedings of the National Academy of Sciences*, *112*(13), 3931–3936.
1100 https://doi.org/10.1073/pnas.1422385112
1101 Eckhardt, K. (2012). Technical Note: Analytical sensitivity analysis of a two parameter recursive digital
1102 baseflow separation filter. *Hydrology and Earth System Sciences*, *16*(2), 451–455.
1103 https://doi.org/10.5194/hess-16-451-2012

1104 Ehsanzadeh, E., Ouarda, T. B. M. J., & Saley, H. M. (2011). A simultaneous analysis of gradual and
1105 abrupt changes in Canadian low streamflows. *Hydrological Processes*, *25*(5), 727–739.
1106 https://doi.org/10.1002/hyp.7861
1107 Environment and Climate Change Canada. (2021). *Historical gridded snow water equivalent and snow*
1108 *cover fraction over Canada from remote sensing and land surface models* [Dataset].
1109 https://climate-scenarios.canada.ca/?page=blended-snow-data
1110 First Nations Fisheries Council of British Columbia. (2020). *Environmental Flow Needs—A Primer for*
1111 *First Nations* (pp. 1–11). https://www.fnfisheriescouncil.ca/wp-content/uploads/2022/01/WFF-
1112 ENVIRONMENTAL-FLOW-NEEDS-2020.pdf
1113 Fleming, S. W., Whitfield, P. H., Moore, R. D., & Quilty, E. J. (2007). Regime-dependent streamflow
1114 sensitivities to Pacific climate modes cross the Georgia–Puget transboundary ecoregion.
1115 *Hydrological Processes*, *21*(24), 3264–3287. https://doi.org/10.1002/hyp.6544
1116 Floriancic, M. G., Berghuijs, W. R., Jonas, T., Kirchner, J. W., & Molnar, P. (2020). Effects of climate
1117 anomalies on warm-season low flows in Switzerland. *Hydrology and Earth System Sciences*,
1118 *24*(11), 5423–5438. https://doi.org/10.5194/hess-24-5423-2020
1119 Floriancic, M. G., Berghuijs, W. R., Molnar, P., & Kirchner, J. W. (2021). Seasonality and Drivers of Low
1120 Flows Across Europe and the United States. *Water Resources Research*, *57*(9), e2019WR026928.
1121 https://doi.org/10.1029/2019WR026928
1122 Folkens, L., Bachmann, D., & Schneider, P. (2023). Driving Forces and Socio-Economic Impacts of Low-
1123 Flow Events in Central Europe: A Literature Review Using DPSIR Criteria. *Sustainability*,
1124 *15*(13), Article 13. https://doi.org/10.3390/su151310692
1125 Georgiadis, N. J., & Baker, J. E. (2023). A multidecadal oscillation in precipitation and temperature series
1126 is pronounced in low flow series from Puget Sound streams. *JAWRA Journal of the American*
1127 *Water Resources Association*, *59*(5), 970–983. https://doi.org/10.1111/1752-1688.13129

1128 Godfrey, L. G. (1978). Testing Against General Autoregressive and Moving Average Error Models when
1129 the Regressors Include Lagged Dependent Variables. *Econometrica*, *46*(6), 1293–1301.
1130 https://doi.org/10.2307/1913829
1131 Godsey, S. E., Kirchner, J. W., & Tague, C. L. (2014). Effects of changes in winter snowpacks on summer
1132 low flows: Case studies in the Sierra Nevada, California, USA. *Hydrological Processes*, *28*(19),
1133 5048–5064. https://doi.org/10.1002/hyp.9943
1134 Goeking, S. A., & Tarboton, D. G. (2020). Forests and Water Yield: A Synthesis of Disturbance Effects on
1135 Streamflow and Snowpack in Western Coniferous Forests. *Journal of Forestry*, *118*(2), 172–192.
1136 https://doi.org/10.1093/jofore/fvz069
1137 Guzha, A. C., Rufino, M. C., Okoth, S., Jacobs, S., & Nóbrega, R. L. B. (2018). Impacts of land use and
1138 land cover change on surface runoff, discharge and low flows: Evidence from East Africa.
1139 *Journal of Hydrology: Regional Studies*, *15*, 49–67. https://doi.org/10.1016/j.ejrh.2017.11.005
1140 Hale, K. E., Jennings, K. S., Musselman, K. N., Livneh, B., & Molotch, N. P. (2023). Recent decreases in
1141 snow water storage in western North America. *Communications Earth & Environment*, *4*(1),
1142 Article 1. https://doi.org/10.1038/s43247-023-00751-3
1143 Hamed, K. H., & Ramachandra Rao, A. (1998). A modified Mann-Kendall trend test for autocorrelated
1144 data. *Journal of Hydrology*, *204*(1), 182–196. https://doi.org/10.1016/S0022-1694(97)00125-X
1145 Hernandez, J. (2023, July 21). Drought conditions threatening B.C. salmon as river levels drop | CBC
1146 News. *CBC*. https://www.cbc.ca/news/canada/british-columbia/drought-hurting-b-c-salmon-
1147 1.6912670
1148 Hernández-Henríquez, M. A., Sharma, A. R., & Déry, S. J. (2017). Variability and trends in runoff in the
1149 rivers of British Columbia's Coast and Insular Mountains. *Hydrological Processes*, *31*(18), 3269–
1150 3282. https://doi.org/10.1002/hyp.11257
1151 Holm, S. (1979). A Simple Sequentially Rejective Multiple Test Procedure. *Scandinavian Journal of*
1152 *Statistics*, *6*(2), 65–70.

1153 Hou, Y., Wei, X., Hui, J., Xu, Z., Qiu, M., Zhang, M., Li, Q., & Chen, Q. (2024). Forest disturbance
1154 thresholds on summer low flows in the interior of British Columbia, Canada. *CATENA*, *243*,
1155 108173. https://doi.org/10.1016/j.catena.2024.108173
1156 Huang, S., Kumar, R., Flörke, M., Yang, T., Hundecha, Y., Kraft, P., Gao, C., Gelfan, A., Liersch, S.,
1157 Lobanova, A., Strauch, M., van Ogtrop, F., Reinhardt, J., Haberlandt, U., & Krysanova, V. (2017).
1158 Evaluation of an ensemble of regional hydrological models in 12 large-scale river basins
1159 worldwide. *Climatic Change*, *141*(3), 381–397. https://doi.org/10.1007/s10584-016-1841-8
1160 Hutchinson, M. F., McKenney, D. W., Lawrence, K., Pedlar, J. H., Hopkinson, R. F., Milewska, E., &
1161 Papadopol, P. (2009). Development and Testing of Canada-Wide Interpolated Spatial Models of
1162 Daily Minimum–Maximum Temperature and Precipitation for 1961–2003. *Journal of Applied*
1163 *Meteorology and Climatology*, *48*(4), 725–741. https://doi.org/10.1175/2008JAMC1979.1
1164 Islam, S. ul, Déry, S. J., & Werner, A. T. (2017). Future Climate Change Impacts on Snow and Water
1165 Resources of the Fraser River Basin, British Columbia. *Journal of Hydrometeorology*, *18*(2),
1166 473–496. https://doi.org/10.1175/JHM-D-16-0012.1
1167 Kang, D. H., Gao, H., Shi, X., Islam, S. ul, & Déry, S. J. (2016). Impacts of a Rapidly Declining
1168 Mountain Snowpack on Streamflow Timing in Canada's Fraser River Basin. *Scientific Reports*,
1169 *6*(1), Article 1. https://doi.org/10.1038/srep19299
1170 Knoben, W. J. M., Freer, J. E., & Woods, R. A. (2019). *Technical note: Inherent benchmark or not?*
1171 *Comparing Nash-Sutcliffe and Kling-Gupta efficiency scores* [Preprint]. Catchment
1172 hydrology/Modelling approaches. https://doi.org/10.5194/hess-2019-327
1173 Kormos, P. R., Luce, C. H., Wenger, S. J., & Berghuijs, W. R. (2016). Trends and sensitivities of low
1174 streamflow extremes to discharge timing and magnitude in Pacific Northwest mountain streams.
1175 *Water Resources Research*, *52*(7), 4990–5007. https://doi.org/10.1002/2015WR018125
1176 MacDonald, H., McKenney, D. W., Papadopol, P., Lawrence, K., Pedlar, J., & Hutchinson, M. F. (2020).
1177 North American historical monthly spatial climate dataset, 1901–2016. *Scientific Data*, *7*(1),
1178 Article 1. https://doi.org/10.1038/s41597-020-00737-2

MacDonald, H., McKenney, D. W., Wang, X. L., Pedlar, J., Papadopol, P., Lawrence, K., Feng, Y., & Hutchinson, M. F. (2021). Spatial Models of Adjusted Precipitation for Canada at Varying Time Scales. *Journal of Applied Meteorology and Climatology*, *60*(3), 291–304. https://doi.org/10.1175/JAMC-D-20-0041.1

McCleary, R., & Ptolemy, R. (2017). *Setting Critical Environmental Flow Thresholds for Drought Response: Coldwater River Case Study* (FNR-2017-72956; p. 23). http://docs.openinfo.gov.bc.ca/Response_Package_FNR-2017-72956.pdf

Mekis, É., & Vincent, L. A. (2011). An Overview of the Second Generation Adjusted Daily Precipitation Dataset for Trend Analysis in Canada. *Atmosphere-Ocean*, *49*(2), 163–177. https://doi.org/10.1080/07055900.2011.583910

Mood, B. J., Coulthard, B., & Smith, D. J. (2020). Three hundred years of snowpack variability in southwestern British Columbia reconstructed from tree-rings. *Hydrological Processes*, *34*(25), 5123–5133. https://doi.org/10.1002/hyp.13933

Moore, R. D. (Dan), Gronsdahl, S., & McCleary, R. (2020). Effects of Forest Harvesting on Warm-Season Low Flows in the Pacific Northwest: A Review: *Confluence: Journal of Watershed Science and Management*, *4*(1), Article 1. https://doi.org/10.22230/jwsm.2020v4n1a35

Moore, R. D., Pelto, B., Menounos, B., & Hutchinson, D. (2020). Detecting the Effects of Sustained Glacier Wastage on Streamflow in Variably Glacierized Catchments. *Frontiers in Earth Science*, *8*. https://doi.org/10.3389/feart.2020.00136

Morgan, M. (2012). Cultural Flows: Asserting Indigenous Rights and Interests in the Waters of the Murray-Darling River System, Australia. In B. R. Johnston, L. Hiwasaki, I. J. Klaver, A. Ramos Castillo, & V. Strang (Eds.), *Water, Cultural Diversity, and Global Environmental Change: Emerging Trends, Sustainable Futures?* (pp. 453–466). Springer Netherlands. https://doi.org/10.1007/978-94-007-1774-9_31

Muñoz Sabater, J. (2019). *ERA5-Land monthly averaged data from 1950 to present* [Dataset]. Copernicus Climate Change Service (C3S) Climate Data Store (CDS). https://doi.org/10.24381/cds.68d2bb30

1205 Najafi, M. R., Zwiers, F. W., & Gillett, N. P. (2017). Attribution of Observed Streamflow Changes in Key
1206 British Columbia Drainage Basins. *Geophysical Research Letters*, *44*(21), 11,012-11,020.
1207 https://doi.org/10.1002/2017GL075016
1208 Niel, H., Paturel, J.-E., & Servat, E. (2003). Study of parameter stability of a lumped hydrologic model in
1209 a context of climatic variability. *Journal of Hydrology*, *278*(1), 213–230.
1210 https://doi.org/10.1016/S0022-1694(03)00158-6
1211 Pacific Climate Impacts Consortium. (2020). *VIC-GL BCCAQ CMIP5 RVIC: Station Hydrologic Model*
1212 *Output.* [Dataset]. University of Victoria. https://www.pacificclimate.org/data/station-hydrologic-
1213 model-output
1214 Page, J. (2007). Salmon Farming in First Nations' Territories: A Case of Environmental Injustice on
1215 Canada's West Coast. *Local Environment*, *12*(6), 613–626.
1216 https://doi.org/10.1080/13549830701657349
1217 Patakamuri, S. K., & O'Brien, N. (2021). *modifiedmk: Modified Versions of Mann Kendall and*
1218 *Spearman's Rho Trend Tests* (Version 1.6) [Computer software]. https://cran.r-
1219 project.org/web/packages/modifiedmk/
1220 Poff, N. L., & Zimmerman, J. K. H. (2010). Ecological responses to altered flow regimes: A literature
1221 review to inform the science and management of environmental flows. *Freshwater Biology*,
1222 *55*(1), 194–205. https://doi.org/10.1111/j.1365-2427.2009.02272.x
1223 Porkka, M., Virkki, V., Wang-Erlandsson, L., Gerten, D., Gleeson, T., Mohan, C., Fetzer, I., Jaramillo, F.,
1224 Staal, A., Wierik, S. te, Tobian, A., Ent, R. van der, Döll, P., Flörke, M., Gosling, S., Hanasaki, N.,
1225 Satoh, Y., Schmied, H. M., Wanders, N., … Kummu, M. (2022). *Global water cycle shifts far*
1226 *beyond pre-industrial conditions – planetary boundary for freshwater change transgressed*.
1227 https://eartharxiv.org/repository/view/3438/
1228 Province of BC. (2024a). *Fire Perimeters—Historical* [Dataset].
1229 https://catalogue.data.gov.bc.ca/dataset/22c7cb44-1463-48f7-8e47-88857f207702

1230 Province of BC. (2024b). *Harvested Areas of BC (Consolidated Cutblocks)* [Dataset].
1231 https://catalogue.data.gov.bc.ca/dataset/harvested-areas-of-bc-consolidated-cutblocks-
1232 Rayne, S., & Forest, K. (2011). Historical temporal trends in monthly, seasonal, and annual mean,
1233 minimum, and maximum streamflows from the Okanagan River watershed in south-central
1234 British Columbia, Canada. *Nature Precedings*, 1–1. https://doi.org/10.1038/npre.2011.6662.1
1235 Rayne, S., & Forest, K. (2012). Hydrologic and climate trends for the Coldwater River watershed in
1236 south-central British Columbia, Canada. *Nature Precedings*, 1–1.
1237 https://doi.org/10.1038/npre.2012.6785.1
1238 Richardson, K., Steffen, W., Lucht, W., Bendtsen, J., Cornell, S. E., Donges, J. F., Drüke, M., Fetzer, I.,
1239 Bala, G., von Bloh, W., Feulner, G., Fiedler, S., Gerten, D., Gleeson, T., Hofmann, M., Huiskamp,
1240 W., Kummu, M., Mohan, C., Nogués-Bravo, D., … Rockström, J. (2023). Earth beyond six of
1241 nine planetary boundaries. *Science Advances*, *9*(37), eadh2458.
1242 https://doi.org/10.1126/sciadv.adh2458
1243 Safeeq, M., Grant, G. E., Lewis, S. L., Kramer, M. G., & Staab, B. (2014). A hydrogeologic framework
1244 for characterizing summer streamflow sensitivity to climate warming in the Pacific Northwest,
1245 USA. *Hydrology and Earth System Sciences*, *18*(9), 3693–3710. https://doi.org/10.5194/hess-18-
1246 3693-2014
1247 Santos, L., Thirel, G., & Perrin, C. (2018). Technical note: Pitfalls in using log-transformed flows within
1248 the KGE criterion. *Hydrology and Earth System Sciences*, *22*(8), 4583–4591.
1249 https://doi.org/10.5194/hess-22-4583-2018
1250 Schnorbus, M., Werner, A., & Bennett, K. (2014). Impacts of climate change in three hydrologic regimes
1251 in British Columbia, Canada. *Hydrological Processes*, *28*(3), 1170–1189.
1252 https://doi.org/10.1002/hyp.9661
1253 Shao, D., Li, H., Wang, J., Hao, X., Che, T., & Ji, W. (2022). Reconstruction of a daily gridded snow
1254 water equivalent product for the land region above 45° N based on a ridge regression

machine learning approach. *Earth System Science Data*, *14*(2), 795–809. https://doi.org/10.5194/essd-14-795-2022

Shrestha, R. R., Schnorbus, M. A., Werner, A. T., & Berland, A. J. (2012). Modelling spatial and temporal variability of hydrologic impacts of climate change in the Fraser River basin, British Columbia, Canada. *Hydrological Processes*, *26*(12), 1840–1860. https://doi.org/10.1002/hyp.9283

Smakhtin, V. U. (2001). Low flow hydrology: A review. *Journal of Hydrology*, *240*(3), 147–186. https://doi.org/10.1016/S0022-1694(00)00340-1

Stahl, K., & Moore, R. D. (2006). Influence of watershed glacier coverage on summer streamflow in British Columbia, Canada. *Water Resources Research*, *42*(6). https://doi.org/10.1029/2006WR005022

Teegee, T. (2023, September 25). *Why First Nations Bear the Brunt of BC's Drought*. The Tyee. https://thetyee.ca/Opinion/2023/09/25/First-Nations-Bear-Brunt-BC-Drought/

Teuling, A. J., Van Loon, A. F., Seneviratne, S. I., Lehner, I., Aubinet, M., Heinesch, B., Bernhofer, C., Grünwald, T., Prasse, H., & Spank, U. (2013). Evapotranspiration amplifies European summer drought. *Geophysical Research Letters*, *40*(10), 2071–2075. https://doi.org/10.1002/grl.50495

The Columbia River Salmon Reintroduction Initiative (Director). (2023). *Bringing the Salmon Home* [Video recording]. https://vimeo.com/822794112?share=copy

Tipa, G., & Nelson, K. (2012). Identifying Cultural Flow Preferences: Kakaunui River Case Study. *Journal of Water Resources Planning and Management*, *138*(6), 660–670. https://doi.org/10.1061/(ASCE)WR.1943-5452.0000211

Udall, B., & Overpeck, J. (2017). The twenty-first century Colorado River hot drought and implications for the future. *Water Resources Research*, *53*(3), 2404–2418. https://doi.org/10.1002/2016WR019638z

Ukkola, A. M., De Kauwe, M. G., Roderick, M. L., Abramowitz, G., & Pitman, A. J. (2020). Robust Future Changes in Meteorological Drought in CMIP6 Projections Despite Uncertainty in

1280 Precipitation. *Geophysical Research Letters*, *47*(11), e2020GL087820.
1281 https://doi.org/10.1029/2020GL087820
1282 Van Loon, A. F. (2015). Hydrological drought explained. *WIREs Water*, *2*(4), 359–392.
1283 https://doi.org/10.1002/wat2.1085
1284 Vincent, L. A., Hartwell, M. M., & Wang, X. L. (2020). A Third Generation of Homogenized Temperature
1285 for Trend Analysis and Monitoring Changes in Canada's Climate. *Atmosphere-Ocean*, *58*(3),
1286 173–191. https://doi.org/10.1080/07055900.2020.1765728
1287 Vionnet, V., Mortimer, C., Brady, M., Arnal, L., & Brown, R. (2021). Canadian historical Snow Water
1288 Equivalent dataset (CanSWE, 1928–2020). *Earth System Science Data*, *13*(9), 4603–4619.
1289 https://doi.org/10.5194/essd-13-4603-2021
1290 Virkki, V., Alanärä, E., Porkka, M., Ahopelto, L., Gleeson, T., Mohan, C., Wang-Erlandsson, L., Flörke,
1291 M., Gerten, D., Gosling, S. N., Hanasaki, N., Müller Schmied, H., Wanders, N., & Kummu, M.
1292 (2022). Globally widespread and increasing violations of environmental flow envelopes.
1293 *Hydrology and Earth System Sciences*, *26*(12), 3315–3336. https://doi.org/10.5194/hess-26-3315-
1294 2022
1295 Wada, Y., Flörke, M., Hanasaki, N., Eisner, S., Fischer, G., Tramberend, S., Satoh, Y., van Vliet, M. T. H.,
1296 Yillia, P., Ringler, C., Burek, P., & Wiberg, D. (2016). Modeling global water use for the 21st
1297 century: The Water Futures and Solutions (WFaS) initiative and its approaches. *Geoscientific*
1298 *Model Development*, *9*(1), 175–222. https://doi.org/10.5194/gmd-9-175-2016
1299 Wade, N. L., Martin, J., & Whitfield, P. H. (2001). Hydrologic and Climatic Zonation of Georgia Basin,
1300 British Columbia. *Canadian Water Resources Journal / Revue Canadienne Des Ressources*
1301 *Hydriques*, *26*(1), 43–70. https://doi.org/10.4296/cwrj2601043
1302 Water Sustainability Act, [SBC 2014] CHAPTER 15 § 87 (2016).
1303 https://www.bclaws.gov.bc.ca/civix/document/id/complete/statreg/14015

1304 Welsh, C., Smith, D. J., & Coulthard, B. (2019). Tree-ring records unveil long-term influence of the
1305 Pacific Decadal Oscillation on snowpack dynamics in the Stikine River basin, northern British
1306 Columbia. *Hydrological Processes*, *33*(5), 720–736. https://doi.org/10.1002/hyp.13357
1307 Werner, A. T., & Cannon, A. J. (2016). Hydrologic extremes – an intercomparison of multiple gridded
1308 statistical downscaling methods. *Hydrology and Earth System Sciences*, *20*(4), 1483–1508.
1309 https://doi.org/10.5194/hess-20-1483-2016
1310 Werner, A. T., Schnorbus, M. A., Shrestha, R. R., Cannon, A. J., Zwiers, F. W., Dayon, G., & Anslow, F.
1311 (2019). A long-term, temporally consistent, gridded daily meteorological dataset for northwestern
1312 North America. *Scientific Data*, *6*(1), Article 1. https://doi.org/10.1038/sdata.2018.299
1313 Westra, S., Thyer, M., Leonard, M., Kavetski, D., & Lambert, M. (2014). A strategy for diagnosing and
1314 interpreting hydrological model nonstationarity. *Water Resources Research*, *50*(6), 5090–5113.
1315 https://doi.org/10.1002/2013WR014719
1316 Whitfield, P. H., Wang, J. Y., & Cannon, A. J. (2003). Modelling Future Streamflow Extremes—Floods
1317 and Low Flows in Georgia Basin, British Columbia. *Canadian Water Resources Journal / Revue*
1318 *Canadienne Des Ressources Hydriques*, *28*(4), 633–656. https://doi.org/10.4296/cwrj2804633
1319 Wood, S. K. (2021, December 21). 'The salmon will come back again': First Nations document
1320 devastating low returns on B.C.'s central coast. *The Narwhal*. https://thenarwhal.ca/bc-salmon-
1321 central-coast-2021-run/
1322 Woodhouse, C. A., Pederson, G. T., Morino, K., McAfee, S. A., & McCabe, G. J. (2016). Increasing
1323 influence of air temperature on upper Colorado River streamflow. *Geophysical Research Letters*,
1324 *43*(5), 2174–2181. https://doi.org/10.1002/2015GL067613
1325 YUE, S., PILON, P., & PHINNEY, B. (2003). Canadian streamflow trend detection: Impacts of serial and
1326 cross-correlation. *Hydrological Sciences Journal*, *48*(1), 51–63.
1327 https://doi.org/10.1623/hysj.48.1.51.43478

1328 Zambrano-Bigiarini, M. (2024). *hydroGOF: Goodness-of-Fit Functions for Comparison of Simulated and*
1329 *Observed Hydrological Time Series* (Version 0.5-4) [Computer software]. https://cran.r-
1330 project.org/web/packages/hydroGOF/index.html
1331 Zhang, M., & Wei, X. (2012). The effects of cumulative forest disturbance on streamflow in a large
1332 watershed in the central interior of British Columbia, Canada. *Hydrology and Earth System*
1333 *Sciences*, *16*(7), 2021–2034. https://doi.org/10.5194/hess-16-2021-2012
1334 Zhang, X., Harvey, K. D., Hogg, W. D., & Yuzyk, T. R. (2001). Trends in Canadian streamflow. *Water*
1335 *Resources Research*, *37*(4), 987–998. https://doi.org/10.1029/2000WR900357
1336

Water Resources Research

Supporting Information for

Rising temperatures drive lower summer minimum flows across hydrologically diverse catchments in British Columbia

S. W. Ruzzante[1] and T. Gleeson[1]

[1]University of Victoria, Victoria, BC, Canada

APPENDIX A: CATCHMENT CLASSIFICATION

CONTENTS

Tables

Algorithm

A variety of catchment classification schemes have been proposed in the literature for Pacific Northwest streams. Wade et al. (2001) classified streams by qualitatively analysing annual hydrographs and runoff calculations. Similarly, Fleming et al. (2007) used a qualitative evaluation of the average annual hydrograph of each river; hybrid regimes were those that "consistently display two seasonal peaks." Wenger et al. (2010) and later Kormos et al. (2016) classified streams by the centre of timing of streamflow (CT, days since start of water year) with CT<150, 150≤CT≤200, and CT>200 corresponding to pluvial, transitional, and nival regimes. Chang et al. (2012) classified catchments by mean basin elevation. Cooper et al. (2018) used the ratio of snow-water equivalent to total annual precipitation to distinguish rain-dominated and snow-dominated catchments. (Islam et al., 2019) use a snowmelt pulse detection technique based on the work of Cayan et al. (2001) and Fritze et al. (2011). Mohan et al. (2023) classified regions of BC as rainfall-dominant when low flows occur in late summer and snowfall-dominant when low flows occur in winter. Déry et al. (2009) qualitatively classified 9 BC streams as Pluvial, Nival, and Glacial.

For the purposes of low flow analysis, the definition proposed by Fleming et al. (2007) is the most relevant. The consistent appearance of two seasonal peaks also guarantees the appearance of two seasonal low flow periods. Thus, we define pluvial regimes as those with a single low flow period in the warm season. Nival regimes are those with a single low flow period in cold seasons, and hybrid regimes are those that have two distinct low flow period.

We define the warm season as the snow-free season, based on the monthly average snow-water-equivalent (SWE) for the period 1985-2014, using data from the ERA-5 Reanalysis (Muñoz Sabater, 2019). We define the snow disappearance date (SDD) and snow appearance date (SAD) as the first (last) month of the year for which the catchment-average SWE is less than 1 mm. For catchments with perennial snow or ice cover in parts, we define the SDD (SAD) as the first (last) month for which SWE is within the bottom

10% of the annual range. The snow maximum date (SMD) is the month with the highest average snow accumulation.

We designed an algorithm to classify the catchments by their annual hydrographs. We construct the annual hydrograph by averaging the 30-day flows (Q30) from all available years.

We define the *low-flow month* based on the timing of the minimum warm-season flow on the average annual hydrograph. We also define the *low-flow season* as the low-flow month ±1, as long as the neighboring months are within the previously defined warm season.

The following equations refer to the average Q30.

We define four variables:

$Q_{min.Winter}$ is the minimum cold-season flow.

$Q_{max.Freshet}$ is the maximum spring flow, which occurs after $Q_{min.Winter}$, during or after the month of maximum snow accumulation (SMD), and during or before the month of the snow disappearance date (SDD). This flow is attributed to the freshet peak.

$Q_{min.Summer}$ is the *low-flow season* minimum flow.

$Q_{max.Autumn}$ is the maximum Autumn-Winter flow (October to December). This flow is attributed to increased autumn-winter rainfall. $Q_{max.Autumn}$ is also constrained to occur after $Q_{min.Summer}$.

We define **snow-affected catchments** as those with a substantial freshet (at least 1.5X larger than the winter minimum flow):

$$snow.affected = Q_{max.Freshet} > 1.5 \times Q_{min.Winter}$$

We define **rain-affected catchments** as those with a substantial autumn rainfall peak (sometimes called an autumn freshet). In these catchments, increased autumn rainfall more than compensates for catchment drainage from summer to autumn. Autumn precipitation also typically falls as rain, rather than snow. Similar to the definition of snow-affected catchments, we require the peak to be 1.5X larger than the minimum.

$$rain.affected = Q_{max.Autumn} > 1.5 \times Q_{min.Summer}$$

If both $rain.affected$ and $snow.affected$ are true, then the catchment is classified as **hybrid**. If only $snow.affected$ is true, then the catchment is **snowmelt-dominated**, and if only $rain.affected$ is true then the catchment is **rainfall-dominated**.

Lastly, if over 5% of the catchment area is glaciated, we classify the catchment to be **glacial**, overriding any prior classification. We computed the average glacial coverage from 1991-2020 by spatially overlaying catchment polygons with glacial extent polygons (Bevington & Menounos, 2022)

Two catchments on the island of Haida Gwaii (Honna River Near the Mouth, 08OA004 and Tarundl Creek Near Queen Charlotte, 08HA005) have few years of winter data, so their annual hydrographs are noisier than the hydrographs for other catchments. These catchments are pluvial, but the algorithm incorrectly identified winter rainfall-induced runoff peaks as freshets, so the catchments were incorrectly classified as hybrid.

Sensitivity to snow data

The ERA5-Land SWE data, which are used to determine the SMD, SDD, and SAD, are provided at a grid resolution of 0.1 degrees (~10 km), which is larger than some of the catchments. The grid-cell SWE may thus not be representative of the catchment SWE. In particular, catchments with a mean elevation significantly higher than the ERA5-Land grid cell elevation may have a later SMD and SDD and an earlier SAD.

We tested the sensitivity of the algorithm to the SWE data by changing each variable (SMD, SDD, and SAD) by +/- 1 month, for 64 non-glacial catchments smaller than 100 km^2. Only 12 catchments changed classification under any of the changes. 11 hybrid catchments could be reclassified as snowmelt-dominated due to an earlier SAD (8 catchments), a later SDD (2 catchments) or a later SAD (1 catchment). 1 hybrid catchment could be reclassified as rainfall-dominated due to a later SMD.

Some of these changes are plausible. For example, two of these small catchments are located about 300 m above the mean ERA5-Land grid cell elevation, so it is likely that the SDD really is later,, and the SAD is earlier. However, for most of the catchments – 218 of 230 – the regime classification is insensitive to the large grid size of the SWE data.

Comparison to Previous Classification Schemes

The classification presented here differs somewhat from previous classifications. We implemented algorithms proposed by Wenger et al. (2010), Chang et al. (2012), and Cooper et al. (2018). The following contingency tables compare our classification algorithm with the algorithms used by these authors. We also compare our classification against the qualitative classifications published by Wade et al. (2001), Fleming et al. (2007), and Déry et al. (2009).

Wenger et al. (2010)

Table A1 presents a confusion matrix comparing the regimes as classified here against those predicted by the algorithm of Wenger et al. (2010), based on the centre of timing. Overall, there is 69% agreement. However, much of this disagreement occurs because our "hybrid" category is much more expansive than Wenger's "transitional" category (79 catchments in our hybrid category and only 7 in Wenger's classification). The two schemes generally agree on the rainfall-dominated regime, although 5 watersheds classified as hybrid in this scheme are classified as rainfall-dominated in Wenger's scheme.

Table A1: Contingency table for regime classification, comparison to Wenger et al. (2010). Cells denoting agreement are bolded.

		Wenger et al. (2010)		
		Rainfall	Transitional	Snowmelt
This study	Rainfall	**28**	0	0
	Hybrid	5	**7**	67
	Snowmelt	0	0	**89**
	Glacial	0	0	**34**

Chang et al. (2012)

Table A2 compares our classification to the elevation-based classification used by Chang et al. (2012). There is only 41% agreement between the two schemes and troublingly, Chang et al. classify as rainfall-

dominated 6 catchments that we classify as snowmelt-dominated or glacial. Also, their scheme classifies only six catchments as snowmelt-dominated (mean elevation above 2000 m above sea level).

Table A2: Contingency table for regime classification, comparison to Chang et al. (2010). Cells denoting agreement are bolded.

		Chang et al. (2012)		
		Rainfall	Hybrid	Snowmelt
This study	Rainfall	**28**	0	0
	Hybrid	18	**61**	0
	Snowmelt	5	81	**3**
	Glacial	1	30	**3**

Cooper et al. (2018)

Table A3 compares our classification to the scheme used by Cooper et al. (2018). They classified catchments according to the ratio of maximum snow water equivalent to annual precipitation. Catchments with a ratio greater than 0.2 were classified as snow-dominated. Although their scheme did not classify as rainfall-dominated any catchments that we classified as hybrid, snowmelt, or glacial, their scheme is highly skewed towards the snowmelt category for our sample. They also did not include a hybrid category. Overall there was 64% agreement.

Table A3: Contingency table for regime classification, comparison to Cooper et al (2018). Cells denoting agreement are bolded.

		(Cooper et al., 2018)	
		Rainfall	Snowmelt
This study	Rainfall	**24**	4
	Hybrid	1	78
	Snowmelt	0	**89**
	Glacial	0	**34**

Wade et al. (2001)

Twenty-three (23) catchments in our study were also classified by Wade et al. (2001) based on consideration of climate, hydrologic, and elevation data. We ran our classification algorithm on hydrometric data from the same stations up to the year 2000, to match the data available to Wade et al. Table A4 shows a comparison of their classification with ours. Overall, our classification agrees with Wade et al. (2001) in 18/23 (78%) of the catchments. There are no egregious differences (none of our 'rainfall-dominated' catchments were classified by Wade et al as Snowmelt/Glacial or vice versa).

Table A4: Contingency table for regime classification, comparison to Wade et al. (2001). Cells denoting agreement are bolded.

		(Wade et al., 2001)		
		Rainfall	Hybrid	Snowmelt/Glacial
This study	Rainfall	**8**	3	0
	Hybrid	0	**5**	1
	Snowmelt	0	0	**1**
	Glacial	0	1	**4**

Fleming et al. (2007)

Six catchments in our study were also classified by Fleming et al. (2007), based on a qualitative assessment of the hydrographs. We ran our classification algorithm on hydrometric data from the same stations up to the year 2003, in order to match the data available to Fleming et al. Table A5 shows a comparison of their classification with ours. Their classification combined snowmelt-dominated and glacial catchments into one 'nival' category but otherwise there is perfect (100%) agreement between our classification and theirs.

Table A5: Contingency table for regime classification, comparison to Fleming et al. (2007). Cells denoting agreement are bolded.

		Fleming et al. (2007)		
		Pluvial	Hybrid	Nival
This study	Rainfall	**3**	0	0
	Hybrid	0	**2**	0
	Snowmelt	0	0	0
	Glacial	0	0	**1**

Déry et al. (2009)

Eight catchments in our study were also qualitatively classified by Déry et al. (2009). We ran our classification algorithm on hydrometric data from the same stations up to the year 2006, in order to match the data available to Fleming et al. Table A6 shows a comparison of their classification with ours. They assigned pluvial, nival, and glacial categories (no hybrid category). There is perfect agreement between our classification and theirs.

Table A6: Contingency table for regime classification, comparison to Déry et al. (2009). Cells denoting agreement are bolded.

		Déry et al. (2009)		
		Pluvial	Nival	Glacial
This study	Rainfall	**2**	0	0
	Hybrid	0	0	0
	Snowmelt	0	**3**	0
	Glacial	0	0	**3**

Moore et al (2011)

Eight catchments in our study were also qualitatively classified by Moore et al. (2012). We ran our classification algorithm on hydrometric data from the same stations up to the year 2000, in order to match the data available to Moore et al. They assigned five categories, differentiating hybrid catchments into rain-dominant and snow-dominant subtypes. Our classification agrees in 7 of 8 catchments; one catchment that they classified as a rain-dominant hybrid catchment we classified as rain-dominated.

Table A7: Contingency table for regime classification, comparison to Moore et al (2012). Cells denoting agreement are bolded.

		Moore et al (2012)				
		Pluvial	Hybrid (rain dominant)	Hybrid (snow dominant)	Nival	Glacial
This study	Rainfall	**2**	1	0	0	0
	Hybrid	0	0	**2**	0	0
	Snowmelt	0	0	0	**1**	0
	Glacial	0	0	0	0	**2**

Our scheme relies on direct observations of the dominant processes, rather than somewhat arbitrary cutoffs based on the center of timing, elevation, or the ratio of maximum snow water equivalent to precipitation. Our classification agrees reasonably well with past qualitative assessments but has the benefit of reproducibility over qualitative assessments.

Regime changes

We also evaluated whether regimes have changed over time. We ran the classification algorithm on 30-year intervals beginning between 1951 and 2011. The last two intervals (beginning in 2001 and 2011) were necessarily shorter than 30 years. Of our 230 catchments, 112 had enough data to classify the regime in each interval (at least 10 years of data or glacial cover >5%). We also conducted the analysis over a shorter period, with intervals beginning between 1961 and 2001; 175 catchments were eligible for these years.

For glacial coverage, we used the annually resolved glacier extents developed by Bevington & Menounos (2022), which are available from 1984-2021. Glacier retreat In British Columbia stabilized and even reversed for some glaciers between 1950-1980 (Beedle et al., 2015; Koch et al., 2009; Moore et al., 2009; Osborn & Luckman, 1988), so we assumed that glacier extents from 1951-1983 were equal to the average extent from 1984-1990.

Figure A1 shows the evolution of the regime classification for both analyses. Over the last 70 years, many snowmelt-dominated catchments have transitioned to the hybrid regime.

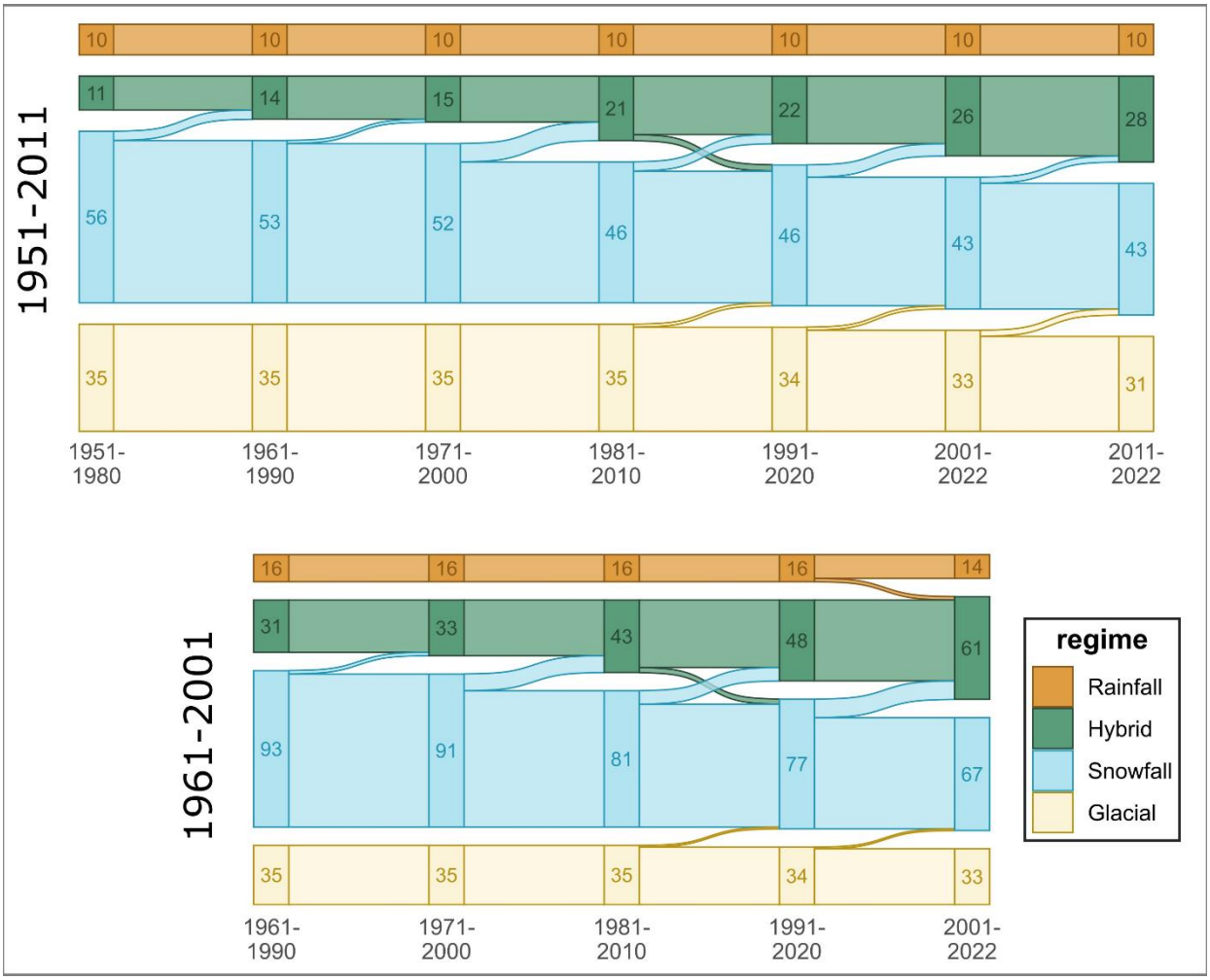

Figure A1: Regime changes for intervals starting from 1951-2011 for 122 catchments (top) and from 1961-2001 for 175 catchments (bottom).

References

Beedle, M. J., Menounos, B., & Wheate, R. (2015). Glacier change in the Cariboo Mountains, British Columbia, Canada (1952–2005). *The Cryosphere*, *9*(1), 65–80. https://doi.org/10.5194/tc-9-65-2015

Bevington, A. R., & Menounos, B. (2022). Accelerated change in the glaciated environments of western Canada revealed through trend analysis of optical satellite imagery. *Remote Sensing of Environment*, *270*, 112862. https://doi.org/10.1016/j.rse.2021.112862

Brunner, M. I., Melsen, L. A., Newman, A. J., Wood, A. W., & Clark, M. P. (2020). Future streamflow regime changes in the United States: Assessment using functional classification. *Hydrology and Earth System Sciences*, *24*(8), 3951–3966. https://doi.org/10.5194/hess-24-3951-2020

Cayan, D. R., Kammerdiener, S. A., Dettinger, M. D., Caprio, J. M., & Peterson, D. H. (2001). Changes in the Onset of Spring in the Western United States. *Bulletin of the American Meteorological Society*, *82*(3), 399–416. https://doi.org/10.1175/1520-0477(2001)082<0399:CITOOS>2.3.CO;2

Chang, H., Jung, I.-W., Steele, M., & Gannett, M. (2012). Spatial Patterns of March and September Streamflow Trends in Pacific Northwest Streams, 1958–2008. *Geographical Analysis*, *44*(3), 177–201. https://doi.org/10.1111/j.1538-4632.2012.00847.x

Cooper, M. G., Schaperow, J. R., Cooley, S. W., Alam, S., Smith, L. C., & Lettenmaier, D. P. (2018). Climate Elasticity of Low Flows in the Maritime Western U.S. Mountains. *Water Resources Research*, *54*(8), 5602–5619. https://doi.org/10.1029/2018WR022816

Déry, S. J., Stahl, K., Moore, R. D., Whitfield, P. H., Menounos, B., & Burford, J. E. (2009). Detection of runoff timing changes in pluvial, nival, and glacial rivers of western Canada. *Water Resources Research*, *45*(4). https://doi.org/10.1029/2008WR006975

Fleming, S. W., Whitfield, P. H., Moore, R. D., & Quilty, E. J. (2007). Regime-dependent streamflow sensitivities to Pacific climate modes cross the Georgia–Puget transboundary ecoregion. *Hydrological Processes*, *21*(24), 3264–3287. https://doi.org/10.1002/hyp.6544

Fritze, H., Stewart, I. T., & Pebesma, E. (2011). Shifts in Western North American Snowmelt Runoff Regimes for the Recent Warm Decades. *Journal of Hydrometeorology*, *12*(5), 989–1006. https://doi.org/10.1175/2011JHM1360.1

Islam, S. U., Curry, C. L., Déry, S. J., & Zwiers, F. W. (2019). Quantifying projected changes in runoff variability and flow regimes of the Fraser River Basin, British Columbia. *Hydrology and Earth System Sciences*, *23*(2), 811–828. https://doi.org/10.5194/hess-23-811-2019

Koch, J., Menounos, B., & Clague, J. J. (2009). Glacier change in Garibaldi Provincial Park, southern Coast Mountains, British Columbia, since the Little Ice Age. *Global and Planetary Change*, *66*(3), 161–178. https://doi.org/10.1016/j.gloplacha.2008.11.006

Kormos, P. R., Luce, C. H., Wenger, S. J., & Berghuijs, W. R. (2016). Trends and sensitivities of low streamflow extremes to discharge timing and magnitude in Pacific Northwest mountain streams. *Water Resources Research*, *52*(7), 4990–5007. https://doi.org/10.1002/2015WR018125

Mohan, C., Gleeson, T., Forstner, T., Famiglietti, J. S., & de Graaf, I. (2023). Quantifying Groundwater's Contribution to Regional Environmental-Flows in Diverse Hydrologic Landscapes. *Water Resources Research*, *59*(6), e2022WR033153. https://doi.org/10.1029/2022WR033153

Moore, R. D., Fleming, S. W., Menounos, B., Wheate, R., Fountain, A., Stahl, K., Holm, K., & Jakob, M. (2009). Glacier change in western North America: Influences on hydrology, geomorphic hazards and water quality. *Hydrological Processes*, *23*(1), 42–61. https://doi.org/10.1002/hyp.7162

Moore, R. D., Trubilowicz, J. w., & Buttle, J. m. (2012). Prediction of Streamflow Regime and Annual Runoff for Ungauged Basins Using a Distributed Monthly Water Balance Model. *JAWRA Journal of the American Water Resources Association*, *48*(1), 32–42. https://doi.org/10.1111/j.1752-1688.2011.00595.x

Muñoz Sabater, J. (2019). *ERA5-Land hourly data from 2001 to present* [Dataset]. Copernicus Climate Change Service (C3S) Climate Data Store (CDS). https://doi.org/10.24381/CDS.E2161BAC

Osborn, G., & Luckman, B. H. (1988). Holocene glacier fluctuations in the Canadian Cordillera (Alberta and British Columbia). *Quaternary Science Reviews*, *7*(2), 115–128. https://doi.org/10.1016/0277-3791(88)90002-9

Wade, N. L., Martin, J., & Whitfield, P. H. (2001). Hydrologic and Climatic Zonation of Georgia Basin, British Columbia. *Canadian Water Resources Journal / Revue Canadienne Des Ressources Hydriques*, *26*(1), 43–70. https://doi.org/10.4296/cwrj2601043

Wenger, S. J., Luce, C. H., Hamlet, A. F., Isaak, D. J., & Neville, H. M. (2010). Macroscale hydrologic modeling of ecologically relevant flow metrics. *Water Resources Research*, *46*(9). https://doi.org/10.1029/2009WR008839

APPENDIX B: WATER USE ESTIMATION

We estimated both surface water and groundwater use. The total water use for each year is the sum of the two estimates. We followed the estimation framework used by Barroso and Wainwright (2020).

Licensed Surface and Ground Water

Geo-located data on surface and ground water licenses were downloaded from British Columbia's data warehouse (BC Ministry of Forests, 2023) on August 29, 2023. We excluded licences for uses in the winter or early spring as well as licenses that represent non-consumptive use. Table B1 lists the license purpose codes for licenses located within the 230 studied catchments.

We assumed that all users draw the maximum licensed amount each year from the license priority date to the date when the licenses is cancelled or abandoned. We did not account for license expiry dates, but only 20 (less than 0.1%) of the licenses have expired.

Unlicensed Groundwater Use

Groundwater licensing began in British Columbia in 2016 but most groundwater users are not licensed. We estimated groundwater use for unlicensed wells based on provincial well records (BC Ministry of Environment and Climate Change Strategy, 2023) and property assessment data collected by the (BC Assessment Authority, 2022).

First, we spatially filtered wells to the 230 studied catchments and removed wells whose tag numbers were also found in the water license data. We then filtered to wells with "Well Class" of *Water Supply* or *Unknown*, and removed wells with an "Intended Use" of *Observation Well*, *Test,* or *Open Loop Geoexchange.* We spatially joined the remaining wells to the BC Asessment parcels (individual properties).

For wells with an "Intended Use" of *Private Domestic* we assumed water consumption of 1.75 m^3/day. For wells with an "Intended Use" of *Irrigation* we assumed a standard irrigation duty of 1 acre-foot per year, over a reference area of half the property size. These estimates are consistent with Barroso and Wainwright (2020).

For wells with other "Intended Use" codes, located within properties used as for a variety of commercial and community purposes, we assumed water consumption of 1-10 times the domestic rate. This included campgrounds, seasonal resorts, motels, restaurants, service stations, churches, and community halls.

For wells located within golf courses we assumed a standard irrigation duty of 1 acre-foot per year over the full property area.

At this point, we assumed any wells for which use had not already been estimated, and for which the property use was "Grain & Forage", "Vegetable & Truck" or other agricultural purposes, had a standard irrigation duty of 1 acre-foot per year, over half the property. For orchards and vineyards 0.5 acre-feet per year was assumed.

For other property uses, including sawmills, various types of mining operations, airports, sand and gravel quarries, concrete plants, we analysed water licenses located within the same property use type and assigned a reasonable value to unlicensed wells.

Lastly, for wells that were still not assigned an estimated water use rate we assumed private domestic use (1.75 m^3/day).

For properties with more than one well with the same intended use (*eg.* two irrigation wells) we divided the use for each well by the total number of wells.

We assumed water use started when the well was constructed.

References

Barroso, S., & Wainwright, M. (2020). *Water Use and Management Options in the Koksilah River Watershed: Preliminary analysis and recommendations for future work* (WSS2020-02; Water Science Series). https://a100.gov.bc.ca/pub/acat/documents/r59126/Koksilah_wateruse_1620692372737_E9980F7DAE.pdf

BC Assessment Authority. (2022). *BC Assessment Data Advice, 2022*- (Version V8) [dataset]. Abacus Data Network. https://hdl.handle.net/11272.1/AB2/NXRVP9

BC Ministry of Environment and Climate Change Strategy. (2023). *Groundwater Wells* [dataset]. BC Data Catalogue. https://catalogue.data.gov.bc.ca/dataset/e4731a85-ffca-4112-8caf-cb0a96905778

BC Ministry of Forests. (2023). *Water Rights Licences—Public* [dataset]. BC Data Catalogue. https://catalogue.data.gov.bc.ca/dataset/water-rights-licences-public

Table B1: Summary of included and excluded licences

Code	Purpose	# Licenses	Included?
01A	Domestic	10527	YES
03B	Irrigation: Private	6056	YES
02I31	Livestock & Animal: Stockwatering	960	YES
WSA08	Livestock & Animal	406	YES
WSA01	Domestic (WSA01)	391	YES
00A	Waterworks: Local Provider	383	YES
02D	Comm. Enterprise: Enterprise	342	YES
00B	Waterworks (other than LP)	154	YES
05D	Mining: Placer	149	YES
WSA03	Commercial Enterprise	133	YES
WSA02	Camps & Public Facilities	115	YES
02F	Lwn, Fairway & Grdn: Watering	114	YES
03A	Irrigation: Local Provider	106	YES
02E	Pond & Aquaculture	104	YES
02I42	Lwn, Fairway & Grdn: Res L/G	104	YES
02I08	Transport Mgmt: Dust Control	84	YES
02B	Processing & Mfg: Processing	47	YES
02I37	Camps & Pub Facil: Work Camps	40	YES
02I12	Misc Ind'l: Fire Protection	37	YES
05C	Mining: Processing Ore	33	YES
WSA11	Lawn, Fairway & Garden	33	YES
02I27	Misc Ind'l: Sediment Control	28	YES
02G	Fresh Water Bottling	27	YES
02I02	Camps & Pub Facil: Non-Work Camps	24	YES
02C	Cooling	21	YES
05A	Mining: Hydraulic	17	YES
02I25	Camps & Pub Facil: Public Facility	16	YES
WSA09	Processing & Manufacturing	16	YES
02I17	Grnhouse & Nursery: Grnhouse	15	YES
02I21	Camps & Pub Facil: Institutions	14	YES
WSA10	Well Drill/Transprt Mgmt	12	YES
02I35	Waterworks: Water Delivery	11	YES
WSA05	Greenhouse & Nursery	10	YES
WSA12	Vehicle & Equipment	9	YES
02I38	Fish Hatchery	8	YES
05B	Mining: Washing Coal	8	YES
09B	Mineralized Water: Comm. Pool	8	YES
02I24	Misc Ind'l: Overburden Disposal	7	YES
02I22	Grnhouse & Nursery: Nursery	6	YES
09A	Mineralized Water: Bottling & Dist	6	YES

Table B1 (continued)

Code	Purpose	# Licenses	Included?
02I03	Camps & Pub Facil: Church/Com Hall	5	YES
02I11	Processing & Mfg: Fire Prevention	4	YES
02I39	Vehicle & Eqpt: Mine & Quarry	4	YES
02I46	Transport Mgmt: Road Maint.	4	YES
02A	Pulp Mill	3	YES
02I07	Ind'l Waste Mgmt: Effluent	3	YES
02I33	Vehicle & Eqpt: Truck & Eqp Wash	3	YES
02I09	Camps & Pub Facil: Exhibition Grnds	2	YES
02I18	Heat Exchanger	2	YES
02I32	Swimming Pool	2	YES
02I47	Heat Exchanger, Residential	2	YES
WSA04	Crop: Harvest/Protect/Compost	2	YES
02H	Bulk Shipment for Marine Trans	1	YES
02I01	Vehicle & Eqpt: Brake Cooling	1	YES
02I04	Conveying (Inactiv	1	YES
02I09	Camp & Pub Facil: Exhibition Grnds	1	YES
02I16	Ind'l Waste Mgmt: Garbage Dump	1	YES
02I26	River Improvement	1	YES
02I28	Ind'l Waste Mgmt: Sewage Disposal	1	YES
02I43	Transport Mgmt: Tunnelling/Well Drilling	1	YES
04B	Land Improve: Rehab/Remed	1	YES
08A	Stream Storage: Non-Power	1026	NO
11A	Conservation: Storage	251	NO
04A	Land Improve: General	237	NO
07A	Power: Residential	166	NO
11B	Conservation: Use of Water	109	NO
07C	Power: General	74	NO
11C	Conservation: Construct Works	73	NO
WSA07	Misc Indust	47	NO
01A01	Incidental - Domestic	39	NO
07B	Power: Commercial	39	NO
02I30	Ice & Snow Making: Snow	21	NO
12A	Stream Storage: Power	17	NO
02I06	Misc Ind'l: Dewatering	5	NO
08B	Aquifer Storage: NP	4	NO
02I14	Crops: Frost Protection	1	NO
WSA06	Ice & Snow Making	1	NO

APPENDIX C: TREND TESTS

Table C1 shows the number positive and negative, and significant trends for all regimes and months, as well as for the low-flow season (*overall*). Figure B1 shows maps of the trends for the low flow in each month.

Table C1: Overall and month-specific trends in log($Q7_{min}$). The trend direction is based on Sen's slope. The numbers in parentheses indicate the number of significant trends, based on a Mann-Kendall trend test for autocorrelated data (Hamed & Ramachandra Rao, 1998).

Regime	Month	# Negative Trends (# significant)	# Positive Trends (# significant)	Total
All	Overall	174 (50)	56 (5)	230
	July	201 (58)	29 (5)	230
	August	210 (104)	20 (4)	230
	September	174 (50)	56 (6)	230
	October	131 (21)	97 (8)	228
Rainfall	Overall	27 (16)	1 (0)	28
	July	27 (14)	1 (0)	28
	August	27 (15)	1 (0)	28
	September	23 (11)	5 (0)	28
	October	16 (3)	10 (0)	28
Hybrid	Overall	74 (22)	5 (1)	79
	July	74 (22)	5 (2)	79
	August	75 (37)	4 (2)	79
	September	70 (26)	9 (2)	79
	October	49 (11)	30 (2)	79
Snowmelt	Overall	61 (11)	28 (3)	89
	July	76 (17)	13 (1)	89
	August	82 (41)	7 (1)	89
	September	69 (12)	20 (1)	89
	October	54 (7)	35 (4)	89
Glacial	Overall	12 (1)	22 (1)	34
	July	24 (5)	10 (2)	34
	August	26 (11)	8 (1)	34
	September	12 (1)	22 (3)	34
	October	12 (0)	22 (2)	34

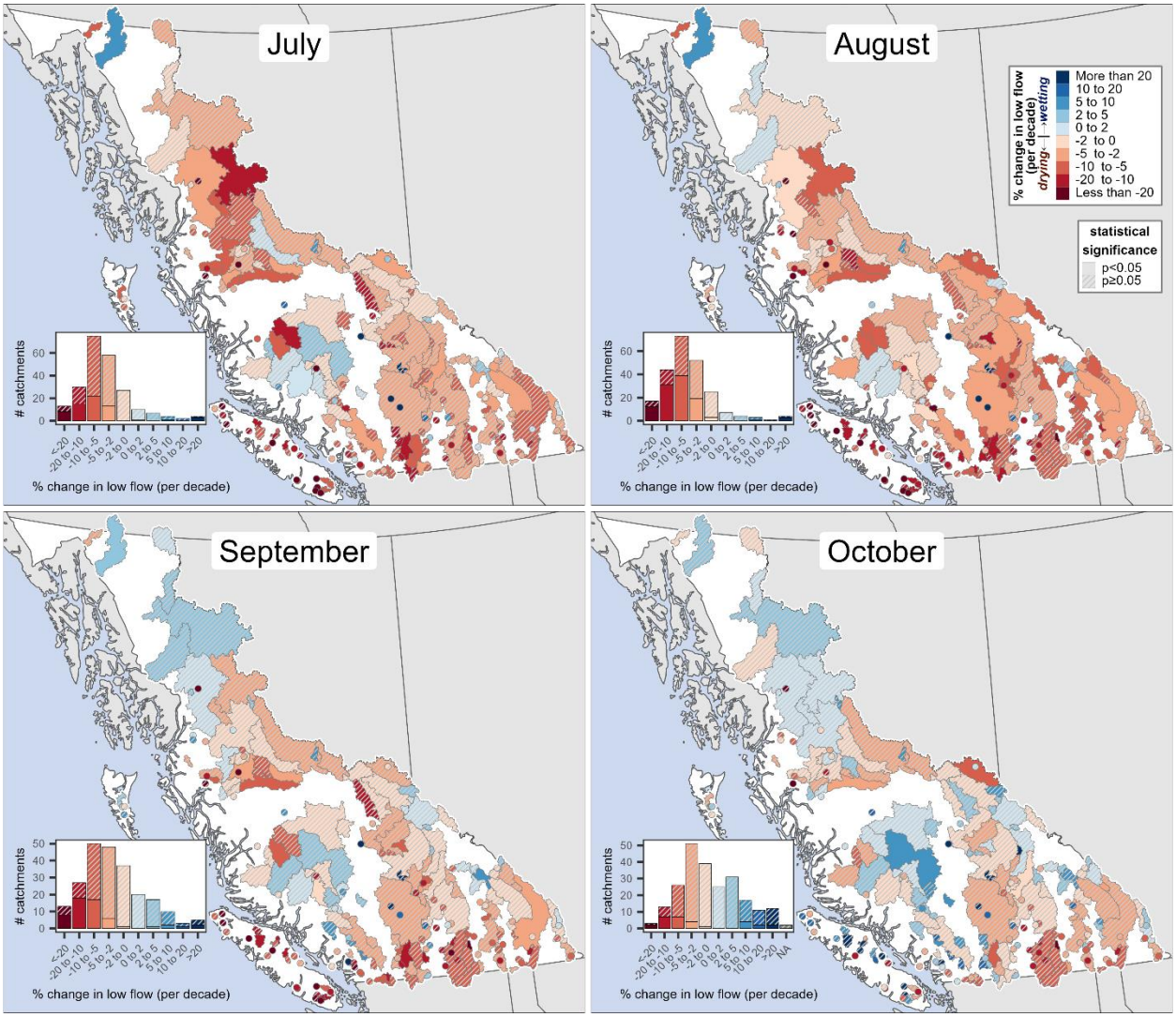

Figure C1: Trends for the overall monthly low flows in the 230 study catchments, using available data from 1950 to present. Hatched polygons denote non-significant trends. Red denotes drying trends and blue denotes wetting trends.

APPENDIX D: SENSITIVITY AND STATIONARITY

This appendix provides additional robustness checks for Section 3.2.

Figure D1 shows Pearson correlation coefficients for each of the eight tested variables. This differs from the analysis presented in Figure 3 in the main text, where we showed the coefficients from a multiple regression model with all variables standardized to mean of 0 and unit variance. We found correlations with SWE_{max} were generally slightly stronger but still not very large. Correlations with BF_{winter} were similarly small, and correlations with P_{summer} were similarly large or slightly larger. Pearson correlations with T_{summer} and T_7 were substantially larger than the standardized regression coefficients, due to multicollinearity with other variables in the multiple regression. Correlations with abstraction, ECA_I, and ECA_{III} varied somewhat but not predictably.

Figure D2 shows results using two alternatives to SWE_{max} (SWE_{fixed} and SDD). SWE_{fixed} is the SWE for a fixed month each year (rather than the maximum accumulation). The timing for each catchment is set to the median peak accumulation month (except when that month is January or February, in which case we used March SWE).

SDD is the snow disappearance date, calculated from ERA5-Land daily data. Since some catchments have glaciers and perennial or semi-perennial snow cover, we defined the SDD as the last day for which the catchment-average SWE was above a threshold $SWE_{threshold}$:

$$\mathrm{SWE}_{\mathrm{threshold}} = \overline{\mathrm{SWE}_{\mathrm{min}}} + (\overline{\mathrm{SWE}_{\mathrm{max}}} - \overline{\mathrm{SWE}_{\mathrm{min}}}) * 0.1$$

Where $\overline{\mathrm{SWE}_{\mathrm{min}}}$ and $\overline{\mathrm{SWE}_{\mathrm{max}}}$ are the average minimum and maximum SWE from 1991-2020. For years when the SWE was never below $SWE_{threshold}$ we set the SDD to day 275 (October 1st in non-leap years).

There were no major differences in the correlation strength between SWE_{max} and SWE_{fixed}. SDD is more highly correlated with $Q7_{min}$ in colder catchments, likely because it represents the effects of both winter snow accumulation and summer melting.

Figure D3 shows results using 18 different definitions of the baseflow variable. All results indicate minor effects of winter baseflow/groundwater storage on summer low flows.

Figure D4 shows a figure analogous to Figure 3 in the main text, but using P_{winter} and T_{winter} instead of BF_{winter} and SWE_{max}. The effect of these variables was similar.

Figure D5 shows figures analogous to Figure 3 in the main text but computed for each month between July and October (instead of using the overall $Q7_{min}$). SWE_{max} and T_{summer} have larger impacts on flows earlier in the season (July and August), while P_{summer} has a larger impact later in the season. The effect of all other variables is small in all seasons.

Tables D1-D4 show results of our stationarity tests, splitting the data at 1995, 1996, 1997, and 1998. Test 1 evaluates the percentage of catchments that show positive changes in each coefficient, while Tests 2 and 3 evaluate the percentage of catchments showing positive and significant changes. Overall there is little evidence of non-stationarity in most variables. However, in hybrid and snowmelt-dominated regimes, we do see consistent reductions in the effect of SWE_{max} (coefficients mostly decrease) and in T_{summer} (coefficients mostly become less negative).

Tables

Figures

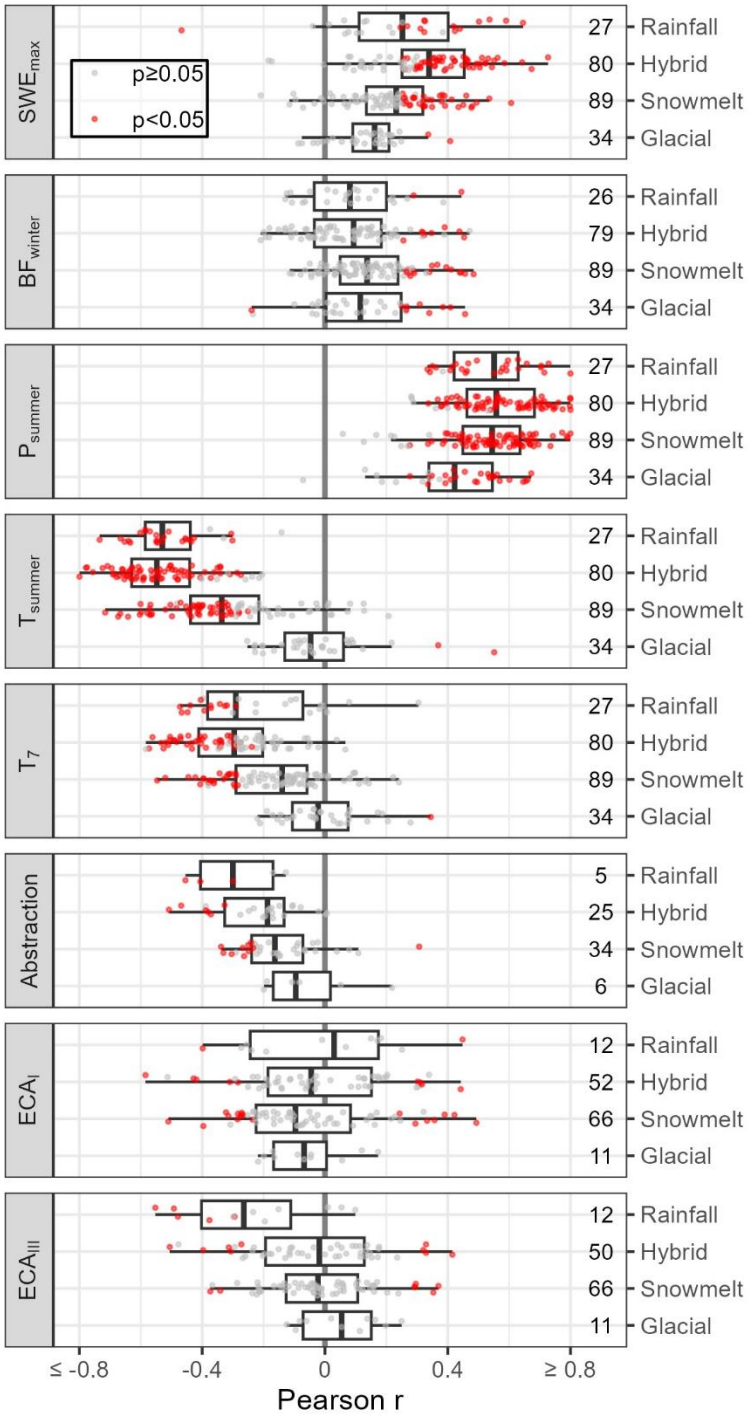

Figure D1: Bivariate Pearson correlation coefficients for log-transformed summer low flows with 8 explanatory variables.

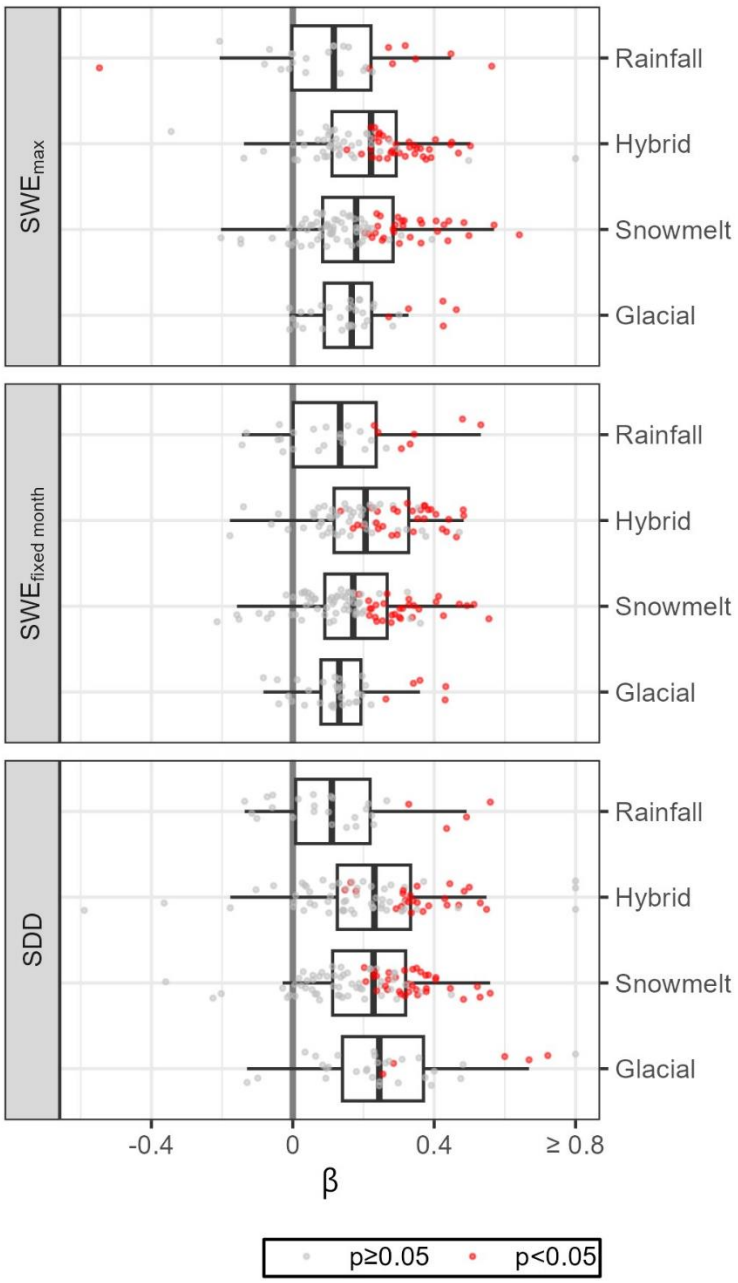

Figure D2: Standardized regression coefficients using three different variables related to winter snow accumulation. The top panel shows results using the maximum accumulation for each year (as in the manuscript). The bottom panel shows SWE_{fixed}, which is the monthly average SWE for the median peak accumulation month.

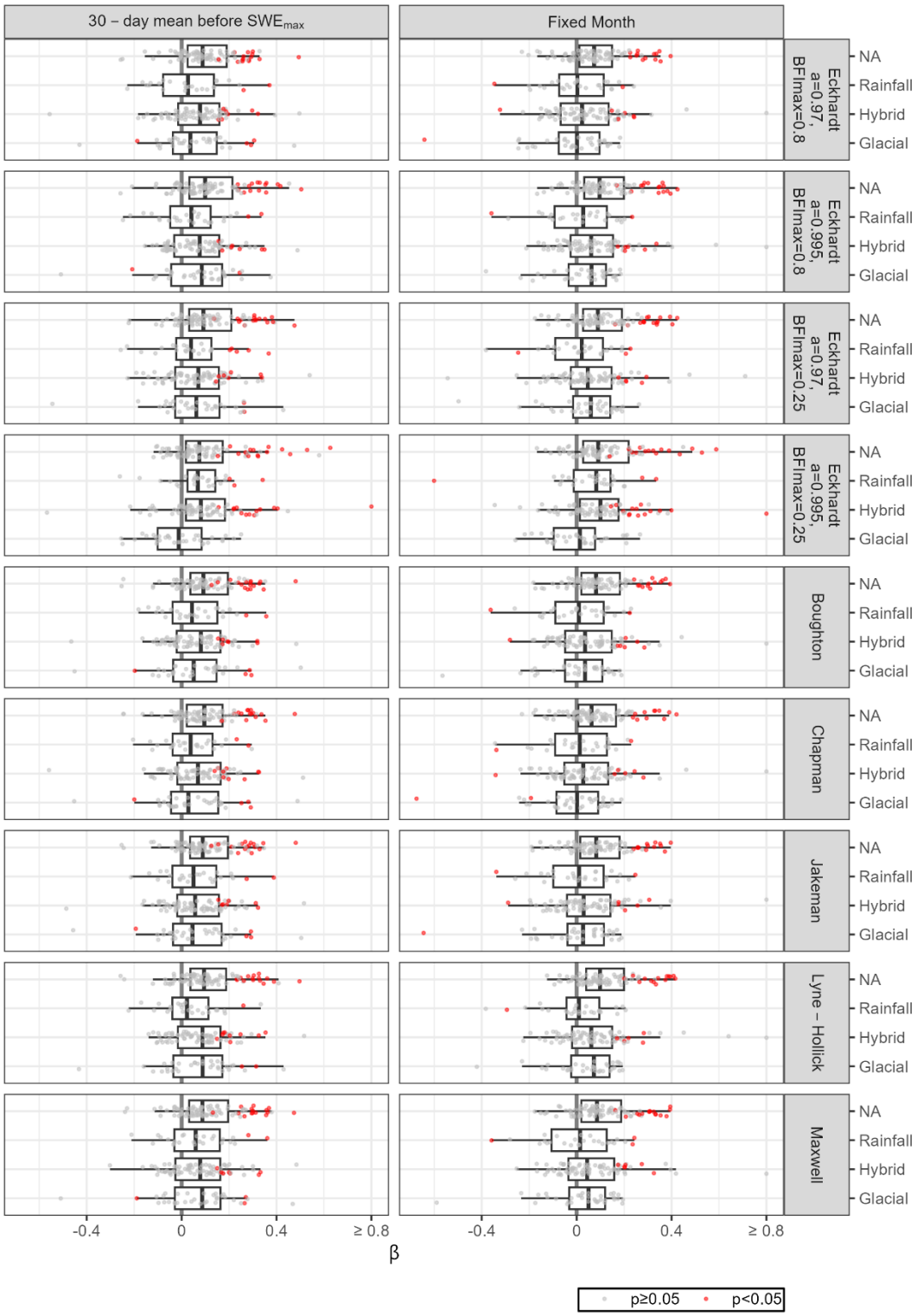

Figure D3: Eighteen different baseflow variables all show very small effects. The left column uses the average baseflow for 30 days prior to SWE$_{max}$. The right column uses the average baseflow over the same month as SWE$_{fixed}$. Each row is a different baseflow filtering algorithm. The top row (Eckhardt) is used in the manuscript, with $\alpha = 0.97$ and $\mathbf{BFI_{max}} = 0.8$.

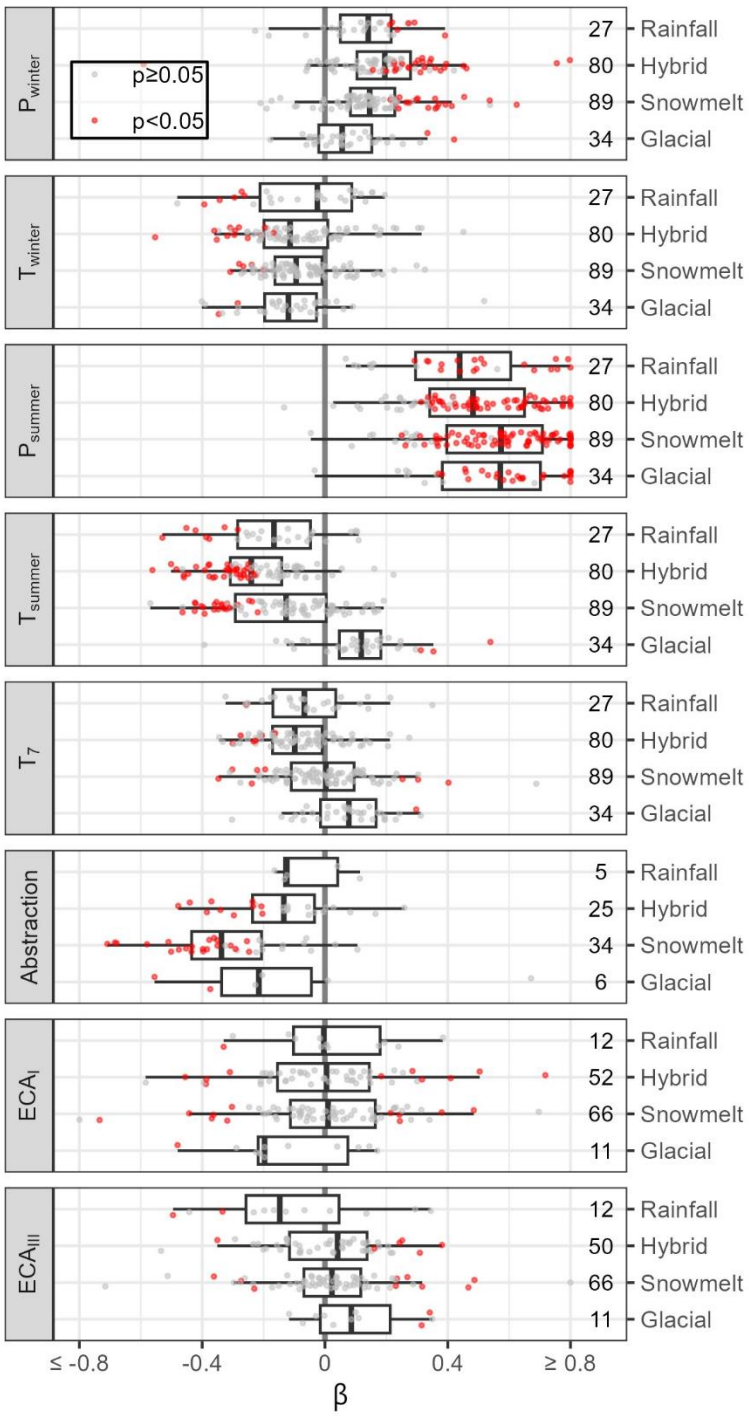

Figure D4: Standardized regression coefficients for log-transformed summer low flows with 8 explanatory variables. In contrast to Figure 3 in the manuscript here we use the winter temperature and precipitation instead of SWE_{max} and BF_{winter}.

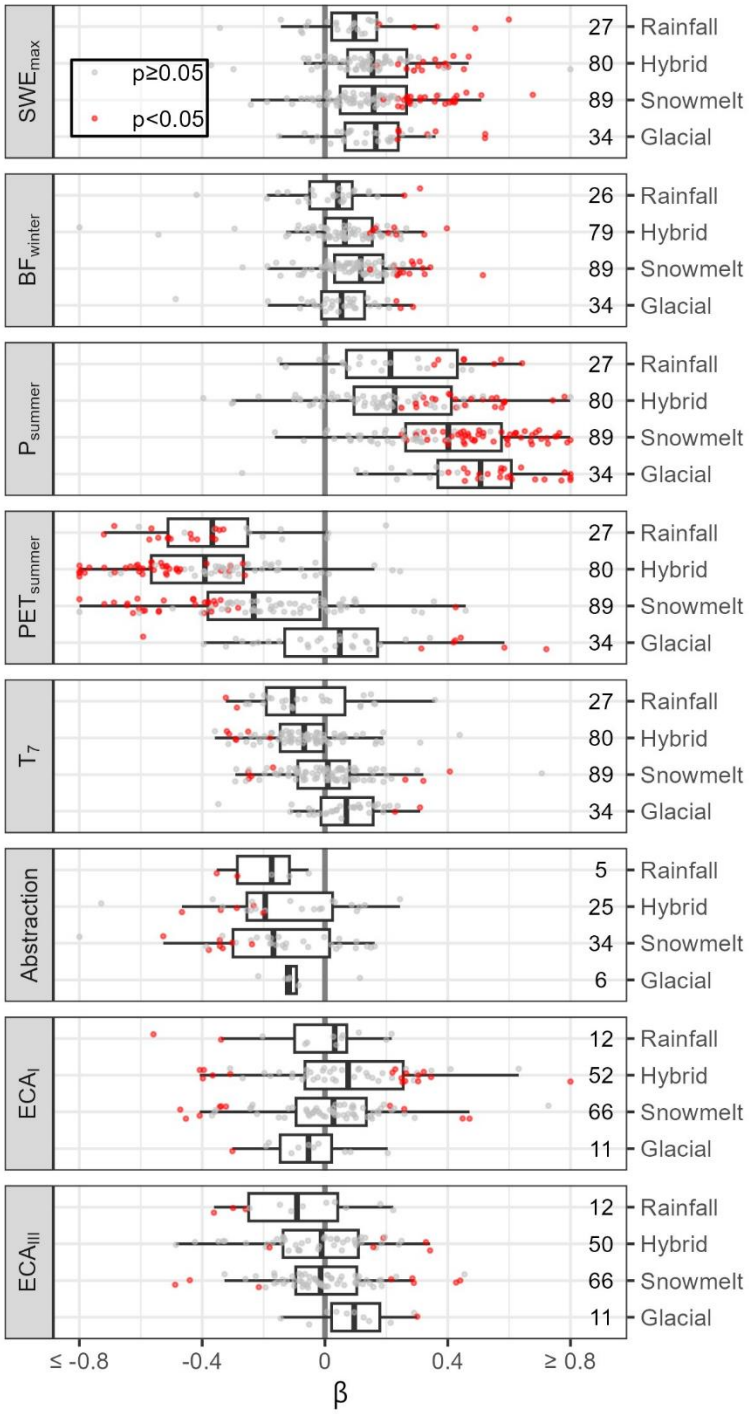

Figure D5: Standardized regression coefficients using P_{summer} and PET_{summer} (potential evapotranspiration) from the ERA5-Land reanalysis (Muñoz Sabater, 2019) in place of P_{summer} and T_{summer} from ANUSPLIN.

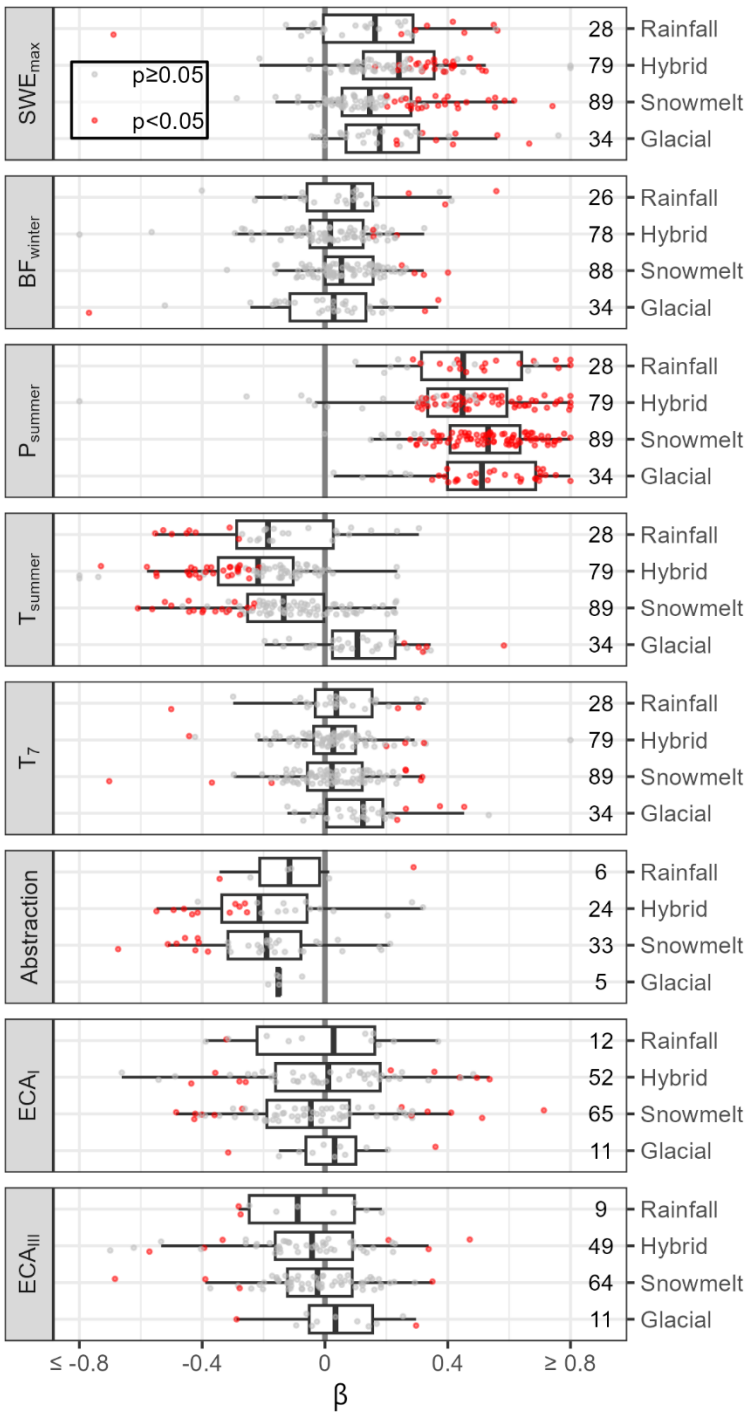

Figure D6: Standardized regression coefficients using P_{summer} and T_{summer} (potential evapotranspiration) from the PNWNAmet (Werner et al., 2019) in place of P_{summer} and T_{summer} from ANUSPLIN.

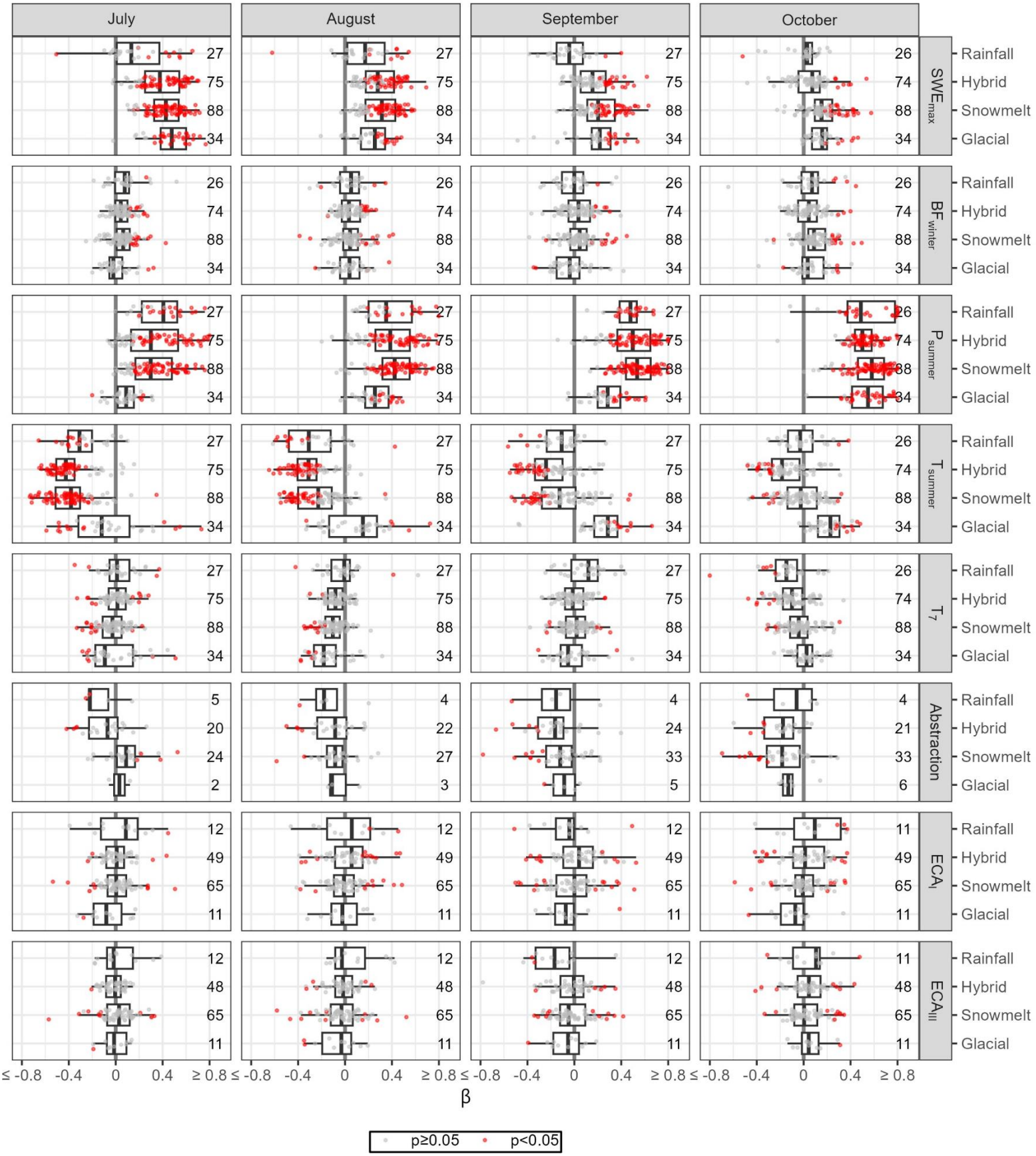

Figure D7: Standardized regression coefficients for log-transformed monthly low flows. The effect of SWE is larger earlier in the summer. The effect of BF_{winter} is minimal in all months. The effect of P_{summer} is largest in the later months, while the effect of temperature is strongest earlier in the season. The effects of the four other variables are small and mostly non-significant.

Table D1: Stationarity tests with split year 1995. The three tests correspond to the significance tests described in Section 2.4. The H-B test columns refer to the Holm-Bonferroni method. Significant results after applying the Holm-Bonferroni method are bolded.

Variable	Regime	N	Test 1 (positive)			Test 2 (positive, significant)			Test 3 (negative, significant)		
			% positive	p	H-B test	% positive & significant	p	H-B test	% negative & significant	p	H-B test
SWE_{max}	Rainfall	15	27%	0.12		0%	1.00		7%	0.54	15
	Hybrid	43	**16%**	**<0.0001**	***	0%	1.00		0%	1.00	43
	Snowmelt	68	34%	0.01		1%	0.97		3%	0.86	68
	Glacial	21	57%	0.66		0%	1.00		0%	1.00	21
BF_{winter}	Rainfall	15	13%	0.01		0%	1.00		0%	1.00	15
	Hybrid	43	65%	0.07		9%	0.17		0%	1.00	43
	Snowmelt	68	66%	0.01		3%	0.86		3%	0.86	68
	Glacial	21	71%	0.08		0%	1.00		0%	1.00	21
P_{summer}	Rainfall	15	67%	0.30		0%	1.00		0%	1.00	15
	Hybrid	43	42%	0.36		0%	1.00		7%	0.36	43
	Snowmelt	68	53%	0.72		1%	0.97		1%	0.97	68
	Glacial	21	81%	0.01		10%	0.28		0%	1.00	21
T_{summer}	Rainfall	15	60%	0.61		7%	0.54		0%	1.00	15
	Hybrid	43	63%	0.13		12%	0.06		2%	0.89	43
	Snowmelt	68	**76%**	**<0.0001**	***	0%	1.00		0%	1.00	68
	Glacial	21	62%	0.38		10%	0.28		0%	1.00	21
T_7	Rainfall	15	60%	0.61		0%	1.00		0%	1.00	15
	Hybrid	43	60%	0.22		2%	0.89		0%	1.00	43
	Snowmelt	68	**26%**	**0.0001**	**	0%	1.00		7%	0.25	68
	Glacial	21	38%	0.38		0%	1.00		10%	0.28	21

Holm-Bonferroni significance levels: * p<0.05, **p<0.01, ***p<0.001

Table D2: Stationarity tests with split year 1996. The three tests correspond to the significance tests described in Section 2.4. The H-B test columns refer to the Holm-Bonferroni method. Significant results after applying the Holm-Bonferroni method are bolded.

Variable	Regime	N	Test 1 (positive)			Test 2 (positive, significant)			Test 3 (negative, significant)		
			% positive	p	H-B test	% positive & significant	p	H-B test	% negative & significant	p	H-B test
SWE_{max}	Rainfall	15	33%	0.30		0%	1.00		7%	0.54	15
	Hybrid	47	**23%**	**0.0003**	*	0%	1.00		0%	1.00	47
	Snowmelt	69	**30%**	**0.001**	*	1%	0.97		3%	0.87	69
	Glacial	21	57%	0.66		0%	1.00		0%	1.00	21
BF_{winter}	Rainfall	15	13%	0.01		0%	1.00		0%	1.00	15
	Hybrid	47	72%	0.003		6%	0.42		0%	1.00	47
	Snowmelt	69	68%	0.003		3%	0.87		1%	0.97	69
	Glacial	21	71%	0.08		0%	1.00		0%	1.00	21
P_{summer}	Rainfall	15	73%	0.12		0%	1.00		0%	1.00	15
	Hybrid	47	53%	0.77		0%	1.00		6%	0.42	47
	Snowmelt	69	54%	0.63		6%	0.46		0%	1.00	69
	Glacial	21	81%	0.01		19%	0.02		0%	1.00	21
T_{summer}	Rainfall	15	60%	0.61		7%	0.54		0%	1.00	15
	Hybrid	47	68%	0.02		13%	0.03		2%	0.91	47
	Snowmelt	69	**80%**	**<0.0001**	***	3%	0.87		0%	1.00	69
	Glacial	21	76%	0.03		10%	0.28		0%	1.00	21
T_7	Rainfall	15	60%	0.61		0%	1.00		0%	1.00	15
	Hybrid	47	57%	0.38		2%	0.91		0%	1.00	47
	Snowmelt	69	**29%**	**0.0006**	*	0%	1.00		9%	0.13	69
	Glacial	21	43%	0.66		0%	1.00		10%	0.28	21

Holm-Bonferroni significance levels: * p<0.05, **p<0.01, ***p<0.001

Table D3: Stationarity tests with split year 1997. The three tests correspond to the significance tests described in Section 2.4. The H-B test columns refer to the Holm-Bonferroni method. Significant results after applying the Holm-Bonferroni method are bolded.

Variable	Regime	N	Test 1 (positive)			Test 2 (positive, significant)			Test 3 (negative, significant)		
			% positive	p	H-B test	% positive & significant	p	H-B test	% negative & significant	p	H-B test
SWE_{max}	Rainfall	15	27%	0.12		0%	1.00		13%	0.17	
	Hybrid	47	**26%**	**0.001**	*	0%	1.00		0%	1.00	
	Snowmelt	67	**22%**	**<0.0001**	***	1%	0.97		1%	0.97	
	Glacial	21	52%	1.00		0%	1.00		0%	1.00	
BF_{winter}	Rainfall	15	13%	0.01		0%	1.00		0%	1.00	
	Hybrid	47	70%	0.01		6%	0.42		0%	1.00	
	Snowmelt	67	67%	0.01		6%	0.43		1%	0.97	
	Glacial	21	71%	0.08		0%	1.00		0%	1.00	
P_{summer}	Rainfall	15	67%	0.30		7%	0.54		0%	1.00	
	Hybrid	47	53%	0.77		0%	1.00		4%	0.69	
	Snowmelt	67	48%	0.81		1%	0.97		1%	0.97	
	Glacial	21	81%	0.01		10%	0.28		0%	1.00	
T_{summer}	Rainfall	15	67%	0.30		7%	0.54		0%	1.00	
	Hybrid	47	**79%**	**0.0001**	**	11%	0.08		2%	0.91	
	Snowmelt	67	**76%**	**<0.0001**	***	0%	1.00		0%	1.00	
	Glacial	21	67%	0.19		0%	1.00		0%	1.00	
T_7	Rainfall	15	60%	0.61		0%	1.00		0%	1.00	
	Hybrid	47	51%	1.00		0%	1.00		0%	1.00	
	Snowmelt	67	34%	0.01		1%	0.97		7%	0.24	
	Glacial	21	43%	0.66		0%	1.00		10%	0.28	

Holm-Bonferroni significance levels: * p<0.05, **p<0.01, ***p<0.001

Table D4: Stationarity tests with split year 1998. The three tests correspond to the significance tests described in Section 2.4. The H-B test columns refer to the Holm-Bonferroni method. Significant results after applying the Holm-Bonferroni method are bolded.

Variable	Regime	N	Test 1 (positive)			Test 2 (positive, significant)			Test 3 (negative, significant)		
			% positive	p	H-B test	% positive & significant	p	H-B test	% negative & significant	p	H-B test
SWE_{max}	Rainfall	14	29%	0.18		0%	1.00		0%	1.00	
	Hybrid	44	27%	0.003		0%	1.00		0%	1.00	
	Snowmelt	66	**24%**	**<0.0001**	**	0%	1.00		2%	0.97	
	Glacial	22	50%	1.00		0%	1.00		0%	1.00	
BF_{winter}	Rainfall	14	14%	0.01		0%	1.00		0%	1.00	
	Hybrid	44	68%	0.02		2%	0.90		0%	1.00	
	Snowmelt	66	62%	0.06		6%	0.42		0%	1.00	
	Glacial	22	68%	0.13		0%	1.00		0%	1.00	
P_{summer}	Rainfall	14	64%	0.42		7%	0.51		0%	1.00	
	Hybrid	44	52%	0.88		0%	1.00		5%	0.65	
	Snowmelt	66	50%	1.00		2%	0.97		0%	1.00	
	Glacial	22	82%	0.004		9%	0.30		0%	1.00	
T_{summer}	Rainfall	14	64%	0.42		7%	0.51		0%	1.00	
	Hybrid	44	61%	0.17		7%	0.38		0%	1.00	
	Snowmelt	**66**	**73%**	**0.0003**	**	2%	0.97		2%	0.97	
	Glacial	22	64%	0.29		0%	1.00		0%	1.00	
T_7	Rainfall	14	64%	0.42		0%	1.00		0%	1.00	
	Hybrid	44	50%	1.00		0%	1.00		0%	1.00	
	Snowmelt	66	32%	0.004		2%	0.97		3%	0.85	
	Glacial	22	41%	0.52		0%	1.00		9%	0.30	

Holm-Bonferroni significance levels: * p<0.05, **p<0.01, ***p<0.001

APPENDIX E: EFFECT OF FORESTRY ON LOW FLOWS

CONTENTS

Figures

Tables

Introduction

Forest disturbance (wildfire, harvest, and/or insect-caused mortality) has been observed to both increase and decrease warm-season low flows in the Pacific Northwest (Coble et al., 2020; Goeking & Tarboton, 2020; Moore et al., 2020). Here we aim to apply longitudinal analysis techniques that have been used on individual catchments by others (*eg*. Zhang & Wei, 2012). We aim to investigate the effect that forest disturbance may have had on our 230 catchments.

Data & Methods

Hypothesis Testing

For each year from 1900-2022 we calculated forest age on a 30 m raster grid across British Columbia, based on wildfire and forest harvest polygons (cutblocks). The cutblocks data includes forest harvest records from crown land (95.5% of British Columbia), but not Private Managed Forests. For this analysis we excluded 30 watersheds for which private lands constitute more than 10% of the watershed area. We also excluded 97 watersheds for which less than 10% of the drainage area is recorded as having been logged or burned since 1900.

Zhang and Wei (2012) calculated ECA coefficients based on tree age-height relationships that decrease monotonically (but not linearly) from 100% at year 0 to between 0 and 15% at year 60. However, there is evidence of a range of recovery times, as well as non-monotonic recovery curves (Coble et al., 2020; Moore et al., 2020), so we chose to test four ECA coefficients which decrease from 100% to 0% over 5, 10, 20 and 60 years, respectively. We calculated the Equivalent Clearcut Area (ECA) for each watershed and each year, based on these four ECA coefficients. This allows us to test a variety of hydrologic recovery times.

We assess the Spearman rank correlation between ECA and $\log(Q7_{min})$ after applying three data filtering routines:

A) Jassby & Powell (1990) describe a method of drawing causal inferences from two autocorrelated, possibly non-stationary time series. This method has applied in British Columbia and elsewhere to study forestry effects on streamflow (Duan et al., 2017; Giles-Hansen et al., 2019; Li et al., 2018; Zhang & Wei, 2012). First, both the independent variable time series (ECA) and the dependent variable ($\log(Q7_{min})$) are pre-whitened using an ARIMA model. We use the ARIMA model with the best Akaike Information Criterion using the automated routine implemented in R by Hyndman & Khandakar (2008).
B) We use the same pre-whitening strategy as 1) but for the dependent variable we use the residuals from the optimized regression models (Section 3.4) instead of the time series of $\log(Q7_{min})$. This should remove the variability associated with climate from the dependent variable.
C) We use the residuals from the optimized regression models (same as 2) but skip the pre-whitening of both time series. This is done because pre-whitening can result in low-powered statistical tests.

For each routine above, we then evaluate three hypotheses that, if true, would suggest a consistent effect of forest disturbance on low flows:

H1: The number of significant ($p<0.05$) correlations will be greater than expected by chance (5%). This is evaluated using a one-sided binomial test with probability = 0.05.

H2: The fraction of positive/negative correlations will be greater than expected by chance. This is evaluated using a two-sided binomial test with probability = 0.5.

H3: The strength of the effect will be largest in catchments that have been most disturbed. This is evaluated by regressing the estimated correlation coefficients on the fraction of the catchment that has been harvested or burned since 1900. The regression is specified with no intercept such than the effect for an undisturbed catchment is 0.

Power Analysis

The pre-whitening strategy used in routines 1 and 2 lacks statistical power if there is a causal relationship between the two time series variables and a trend in the independent variable causes a trend in the dependent variable (Jassby & Powell, 1990). This is because the pre-whitening has the express purpose of removing trends and other non-stationarities in the time series. Many of ECA times series in our sample do show strong trends (mostly increasing since the 1950s), so it is likely that these analyses have low statistical power. We therefore tested the statistical power of hypotheses H1 and H2 using Monte Carlo analysis.

First, we found the Type I (false positive) error rate. For each catchment we:

1) Reordered the time series of $\log(Q7_{min})$ 1000 times.
2) Fit ARIMA models to each reordered series.
3) For each of the 1000 simulations, we calculated Spearman's rank correlation coefficient between the filtered ECA time series and the filtered $\log(Q7_{min})$ series.
4) We noted the fraction of simulations resulting in significant (H1) and negative (H2) correlations.

We then evaluated H1 and H2 for each regime:

5) We simulated 10000 tests of H1 and H2 using the fractions derived in step 4. The number of significant results for H1 and H2 is the Type I error rate.

We then explicitly included a causal relationship between ECA and $\log(Q7_{min})$. After step 1 above, we subtract a value proportional to the ECA from the reordered $\log(Q7_{min})$ time series:

$$\log(\mathrm{Q7_{min}})'_t = \log(\mathrm{Q7_{min}})_t - \sigma \times \mathrm{ECA_t} \times k \quad \text{(A1)}$$

Where $'$ denotes the perturbed value, t is the time step, σ is the standard deviation of $\log(\mathrm{Q7_{min}})$, $\mathrm{ECA_t}$ is the value of ECA at time t, and k is a scaling factor which we term the 'Harvest Effect'.

After perturbation, we repeat steps 1-5. The result of step 5 is now the statistical power (1- Type II error rate) for a particular Harvest Effect. We test Harvest Effects from 1 to 100.

Results

Hypothesis Testing

Figure A1 shows the Spearman correlations disaggregated by regime, and by ECA coefficient (60, 20, 10, and 5 year recovery times), for routines A, B, and C. Table A1 shows the results of the hypothesis testing. Each row of Table A1 corresponds to a panel in Figure A1.

For rainfall regimes, we cannot reject the null hypothesis for any of H1, H2, or H3, using any of the ECA recovery times.

For hybrid regimes, we found little evidence of any effect. Using routine A, we could reject H2 and H3 for the 10-year recovery time (more negative correlations than expected by chance), suggesting a downwards effect on low flows. On the other hand, using routine C we could also reject H1 for the 10-year recovery time (more significant positive correlations than expected by chance), which implies the opposite inference. We note that if we were to correct for the family-wise error rate using the Holm-Bonferroni method, these results would not be considered statistically significant.

For snowmelt regimes, we found some evidence for both H1 and H2 using all three routines, suggesting that forest disturbance tends to reduce low flows in these catchments. We found at least one significant result for each recovery time except the shortest (5 years). We note that the regressions against total disturbed area suggest are mostly negative (though not significant), supporting the inference that disturbance reduces low flows.

For glacial catchments we found limited evidence that forest disturbance reduces low flows. H1 has significant for 10 and 20 year recovery times using routine C, and both H2 and H3 were significant for a 5-year recovery time using routine A.

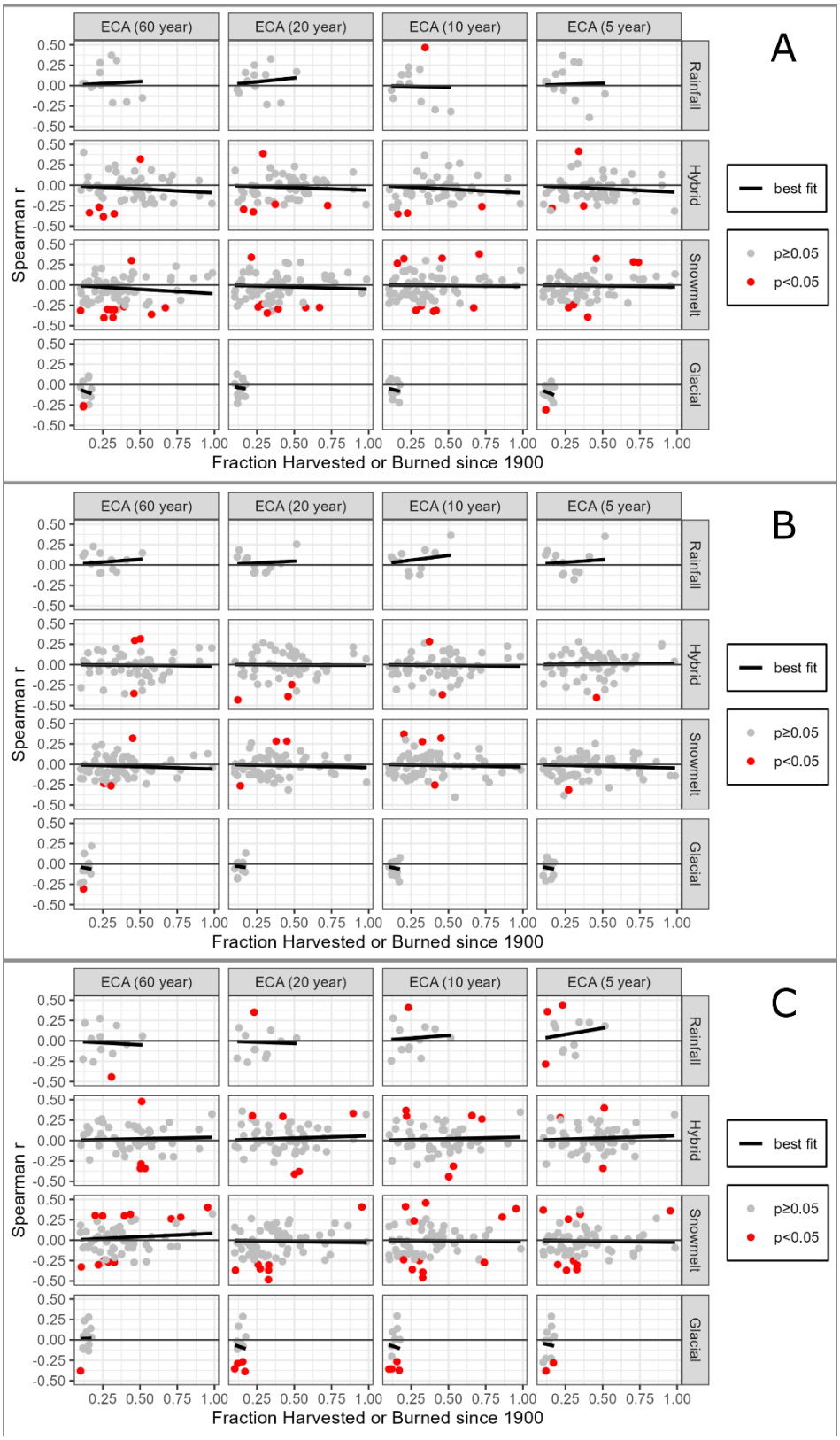

Figure E1: Spearman r correlations between filtered ECA coefficients and filtered log($Q7_{min}$). Panel A corresponds to filtering routine A, panel B to routine B, and panel C to routine C.

Table E 1 Results of hypothesis testing for H1, H2, and H3. H1: Binomial test for more significant (p<0.05) correlations than expected by chance. H2: Binomial test for more positive/negative correlations than expected by chance. H3: linear regression between Spearman r and fraction harvested or burned since 1900.

Filtering Routine	Regime	ECA Recovery Time	H1 (+ve)	H1 (-ve)	H2		H3		N
		(years)	p-value	p-value	% positive	p-value	slope	p-value	
A	Rainfall	60	1	1	67	0.39	0.10	0.63	12
		20	1	1	58	0.77	0.19	0.31	12
		10	0.46	1	58	0.77	-0.03	0.89	12
		5	1	1	58	0.77	0.06	0.80	12
	Hybrid	60	0.93	0.26	38	0.13	-0.09	0.06	52
		20	0.93	0.26	40	0.21	-0.06	0.17	52
		10	1	0.49	**27**	**0.001**	**-0.09**	**0.03**	52
		5	0.93	0.74	37	0.07	-0.08	0.06	52
	Snowmelt	60	0.97	**0.01**	38	0.06	-0.11	0.03	66
		20	0.97	0.11	41	0.18	-0.05	0.28	66
		10	0.42	0.23	42	0.27	-0.02	0.72	66
		5	0.65	0.65	39	0.11	-0.02	0.56	66
	Glacial	60	1	0.10	27	0.23	-0.64	0.06	11
		20	1	1	45	1	-0.28	0.27	11
		10	1	1	27	0.23	-0.47	0.04	11
		5	1	0.43	**9**	**0.01**	**-0.73**	**0.01**	11
B	Rainfall	60	1	1	67	0.39	0.14	0.26	12
		20	1	1	50	1	0.09	0.43	12
		10	1	1	58	0.77	0.23	0.13	12
		5	1	1	58	0.77	0.13	0.41	12
	Hybrid	60	0.74	0.93	48	0.89	-0.02	0.70	52
		20	1	0.49	44	0.49	-0.01	0.88	52
		10	0.93	0.93	42	0.33	-0.02	0.66	52
		5	1	0.93	58	0.33	0.01	0.73	52
	Snowmelt	60	0.97	0.85	**30**	**0.002**	-0.06	0.11	66
		20	0.85	0.97	42	0.27	-0.04	0.29	66
		10	0.65	0.97	38	0.06	-0.03	0.43	66
		5	1	0.97	47	0.71	-0.05	0.19	66
	Glacial	60	1	0.43	27	0.23	-0.36	0.32	11
		20	1	1	36	0.55	-0.24	0.25	11
		10	1	1	45	1	-0.36	0.10	11
		5	1	1	45	1	-0.36	0.12	11
C	Rainfall	60	1	0.46	50	1	-0.10	0.66	12
		20	0.46	1	42	0.77	-0.06	0.73	12
		10	0.46	1	58	0.77	0.13	0.51	12
		5	0.12	0.46	58	0.77	0.31	0.20	12
	Hybrid	60	0.93	0.49	54	0.68	0.04	0.40	52
		20	0.26	0.74	54	0.68	0.08	0.15	52
		10	**0.04**	0.74	50	1	0.10	0.09	52
		5	0.49	0.93	54	0.68	0.10	0.06	52
	Snowmelt	60	**0.02**	0.11	50	1	0.08	0.17	66
		20	0.85	**0.05**	41	0.18	-0.03	0.59	66
		10	0.23	**0.05**	44	0.39	-0.03	0.56	66
		5	0.42	0.11	39	0.11	-0.04	0.42	66
	Glacial	60	1	0.43	55	1	0.13	0.76	11
		20	1	**0.002**	27	0.23	-0.63	0.21	11
		10	1	**0.002**	45	1	-0.61	0.25	11
		5	1	0.10	36	0.55	-0.43	0.38	11

Power Analysis

Figure A2 shows the results of the power analysis for 60-year and 5-year ECA coefficients. The x-axis of each plot is the Harvest Effect (k) in Equation A1. This is the number of standard deviations by which an ECA of 1 would be expected to perturb the low flow time series. For example, a harvest effect of 1 suggests that a clearcut of the entire catchment would reduce log($Q7_{min}$) by 1 standard deviation. The y-axis is the Type II error (false negative) error rate, or 1-(statistical power). For a Harvest Effect of 0 there is no genuine effect, so the x-intercept can be interpreted as 1-(Type I error rate).

Routine A results in very low statistical power. This is the pre-whitening strategy suggested by Jassby & Powell (1990) and used extensively by Zhang & Wei (2012), Li et al. (2018), and others. The test will almost always fail to detect a true effect, except for Harvest Effects exceeding about 10. Hybrid and snowmelt-dominated regimes are slightly more likely to produce a significant result, even when there is no genuine effect (harvest effect = 0).

Routine B is only slightly more powerful than routine A. However, most of the statistical tests will still fail to detect a true effect for all but the largest Harvest Effects.

Routine C (no pre-whitening) has better statistical power than routines A and B. For a Harvest Effect of 2, the Type II error rate drops to almost 0 for the hybrid and snowmelt-dominated regimes, for a 60-year recovery time, for both H1 and H2. The x-intercept for routine C is similar to the x-intercept for routines A and B, which suggests that the pre-whitening strategy does not reduce the Type I error rate (false positives).

In general, the statistical power is greatest for the Hybrid and snowmelt-dominated regimes and weakest for the Rainfall and Glacial regimes, because there are many hybrid and snowmelt-dominated catchments (52 and 66, respectively) and few Rainfall (12) and Glacial (11) catchments. The power also tends to be greater for a 60-year recovery time than a 5-year recovery time because ECA (60 year) is always larger than ECA (5 year), so the perturbation applied in Equation A1 is larger than for ECA (60 year). However, ECA (60 year) also tends to show stronger autocorrelation, so the pre-whitening strategy in routines A and B removes more of the variance, reducing the statistical power.

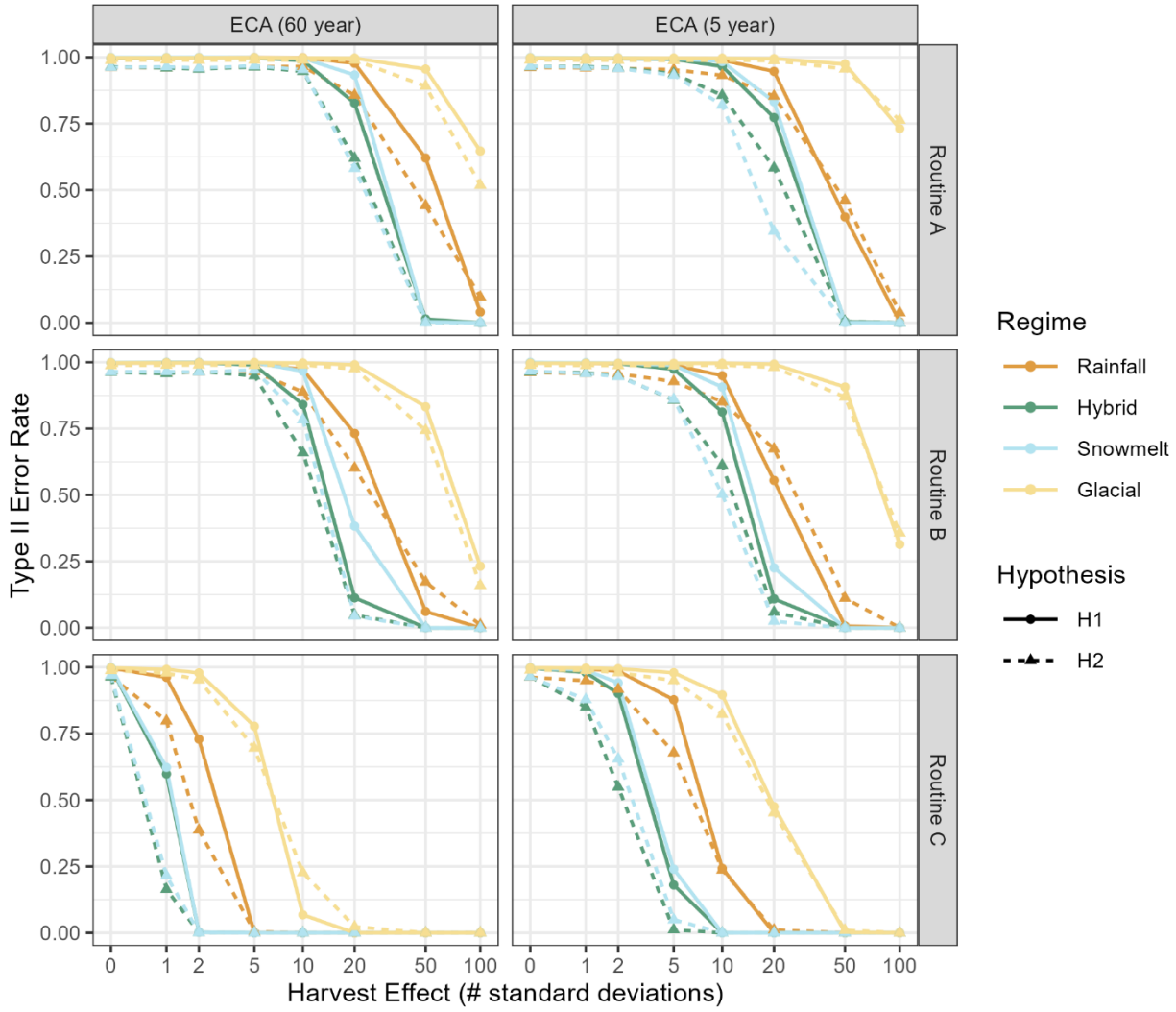

Figure E2: The Type II (false negative) error rate for hypotheses H1 and H2.

Discussion

Overall, the evidence of increases or decreases in low flows following forest disturbance is weak. We tried many statistical tests here and few produced significant results. This could be due to a genuine absence of substantial effects, or because the tests applied are statistically weak.

The weak statistical power found in the power analysis arises for several reasons. First, the pre-whitening strategy is recognized to reduce power where a trend in the independent variable manifests as a trend in the dependent variable (Jassby & Powell, 1990). Second, most of the catchments analysed here have only been moderately disturbed, so the signal to noise ratio in these data is smaller than in studies of small catchments that have been entirely harvested. Third, for many of the catchments studied here, harvesting has progressed at a relatively consistent pace, so there are few 'shocks' that would produce dramatic changes in low flows from year to year.

Despite these shortcomings, we found relatively consistent evidence of low-flow reductions in snowmelt-dominated catchments. We found weaker evidence of reductions in glacial catchments. Despite high

statistical power in hybrid catchments, we did not find consistent evidence of low-flow increases or decreases in these catchments.

These results contrast somewhat with the literature. First, we did not observe short-term increases in low flows that have been reported, particularly for warmer catchments (Coble et al., 2020; Moore et al., 2020). Second, we found the most consistent evidence of decreases to low flows in colder, snowmelt-dominated catchments, which contrasts with the findings of Moore et al. (2020) that results in colder catchments are the most mixed.

In the main text we found that snowmelt-dominated catchments are most sensitive to summer precipitation, so we hypothesize that quicker runoff is the primary mechanism that causes a reduction in low flows following forest disturbance in these catchments. Given that low flows in these catchments are not very sensitive to temperature or winter snow accumulation, we argue that disturbance-induced changes to spring snowmelt and to summer evapotranspiration probably have minor impacts.

References

Altman, D. G., & Bland, J. M. (1995). Absence of evidence is not evidence of absence. *BMJ : British Medical Journal*, *311*(7003), 485.

Coble, A. A., Barnard, H., Du, E., Johnson, S., Jones, J., Keppeler, E., Kwon, H., Link, T. E., Penaluna, B. E., Reiter, M., River, M., Puettmann, K., & Wagenbrenner, J. (2020). Long-term hydrological response to forest harvest during seasonal low flow: Potential implications for current forest practices. *Science of The Total Environment*, *730*, 138926. https://doi.org/10.1016/j.scitotenv.2020.138926

Duan, L., Man, X., Kurylyk, B. L., Cai, T., & Li, Q. (2017). Distinguishing streamflow trends caused by changes in climate, forest cover, and permafrost in a large watershed in northeastern China. *Hydrological Processes*, *31*(10), 1938–1951. https://doi.org/10.1002/hyp.11160

Giles-Hansen, K., Li, Q., & Wei, X. (2019). The Cumulative Effects of Forest Disturbance and Climate Variability on Streamflow in the Deadman River Watershed. *Forests*, *10*(2), Article 2. https://doi.org/10.3390/f10020196

Goeking, S. A., & Tarboton, D. G. (2020). Forests and Water Yield: A Synthesis of Disturbance Effects on Streamflow and Snowpack in Western Coniferous Forests. *Journal of Forestry*, *118*(2), 172–192. https://doi.org/10.1093/jofore/fvz069

Hou, Y., Wei, X., Hui, J., Xu, Z., Qiu, M., Zhang, M., Li, Q., & Chen, Q. (2024). Forest disturbance thresholds on summer low flows in the interior of British Columbia, Canada. *CATENA*, *243*, 108173. https://doi.org/10.1016/j.catena.2024.108173

Hyndman, R. J., & Khandakar, Y. (2008). Automatic Time Series Forecasting: The forecast Package for R. *Journal of Statistical Software*, *27*, 1–22. https://doi.org/10.18637/jss.v027.i03

Jassby, A. D., & Powell, T. M. (1990). Detecting Changes in Ecological Time Series. *Ecology*, *71*(6), 2044–2052. https://doi.org/10.2307/1938618

Li, Q., Wei, X., Zhang, M., Liu, W., Giles-Hansen, K., & Wang, Y. (2018). The cumulative effects of forest disturbance and climate variability on streamflow components in a large forest-dominated watershed. *Journal of Hydrology*, *557*, 448–459. https://doi.org/10.1016/j.jhydrol.2017.12.056

Moore, R. D. (Dan), Gronsdahl, S., & McCleary, R. (2020). Effects of Forest Harvesting on Warm-Season Low Flows in the Pacific Northwest: A Review: *Confluence: Journal of Watershed Science and Management*, *4*(1), Article 1. https://doi.org/10.22230/jwsm.2020v4n1a35

Zhang, M., & Wei, X. (2012). The effects of cumulative forest disturbance on streamflow in a large watershed in the central interior of British Columbia, Canada. *Hydrology and Earth System Sciences*, *16*(7), 2021–2034. https://doi.org/10.5194/hess-16-2021-2012

APPENDIX F: MODEL PERFORMANCE FOR LONG TIME SERIES

These figures show the results of historical simulations for individual stations along with measured data for select stations. For hybrid, snowmelt-dominated, and glacial regimes we show stations with mostly continuous data beginning before 1950. No rainfall-dominated stations have continuous data beginning before 1950, so we show four stations with time series beginning in the 1950's.

The figures show the 10-year running mean of $Q7_{min}$ for both predicted and measured time series. We allow up to 5 years of missing data in the 10-year mean, and show the degree of missingness by the transparency of the lines.

Table of Figures

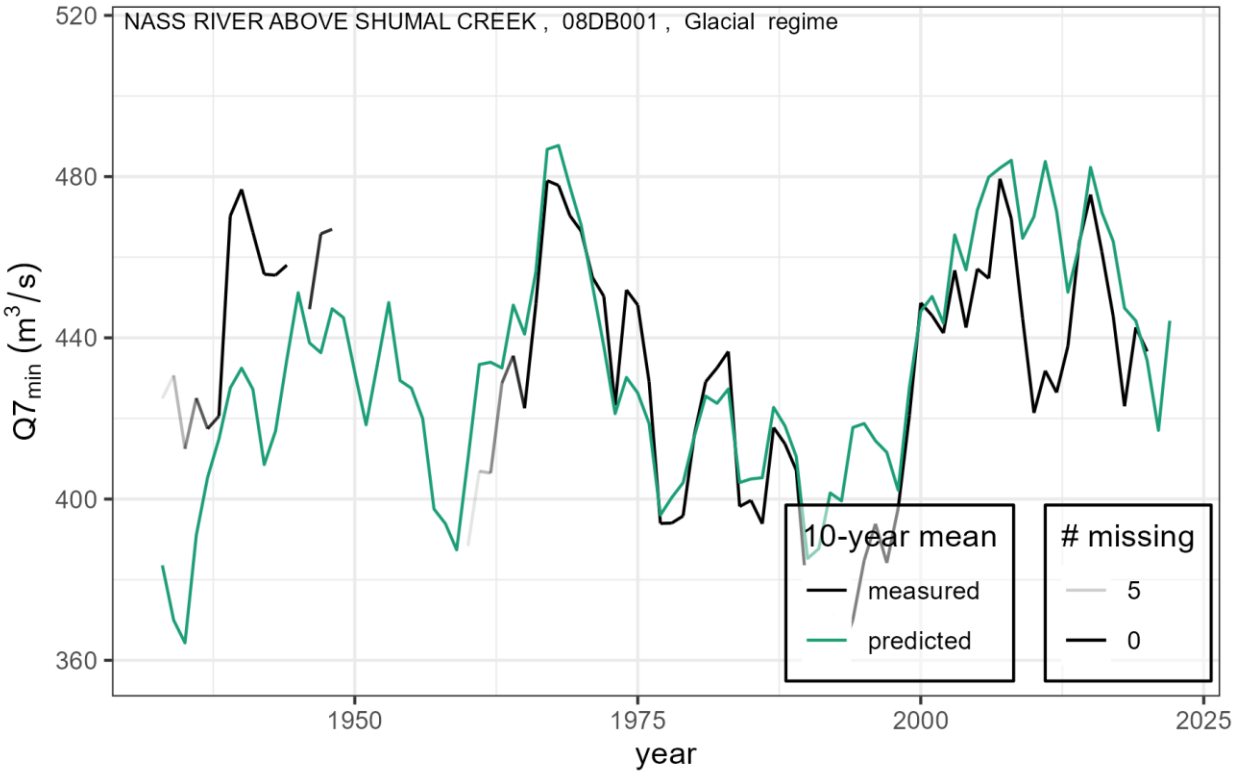

Figure F1: Gauge ID 08DB001, Nass River Above Shumal Creek

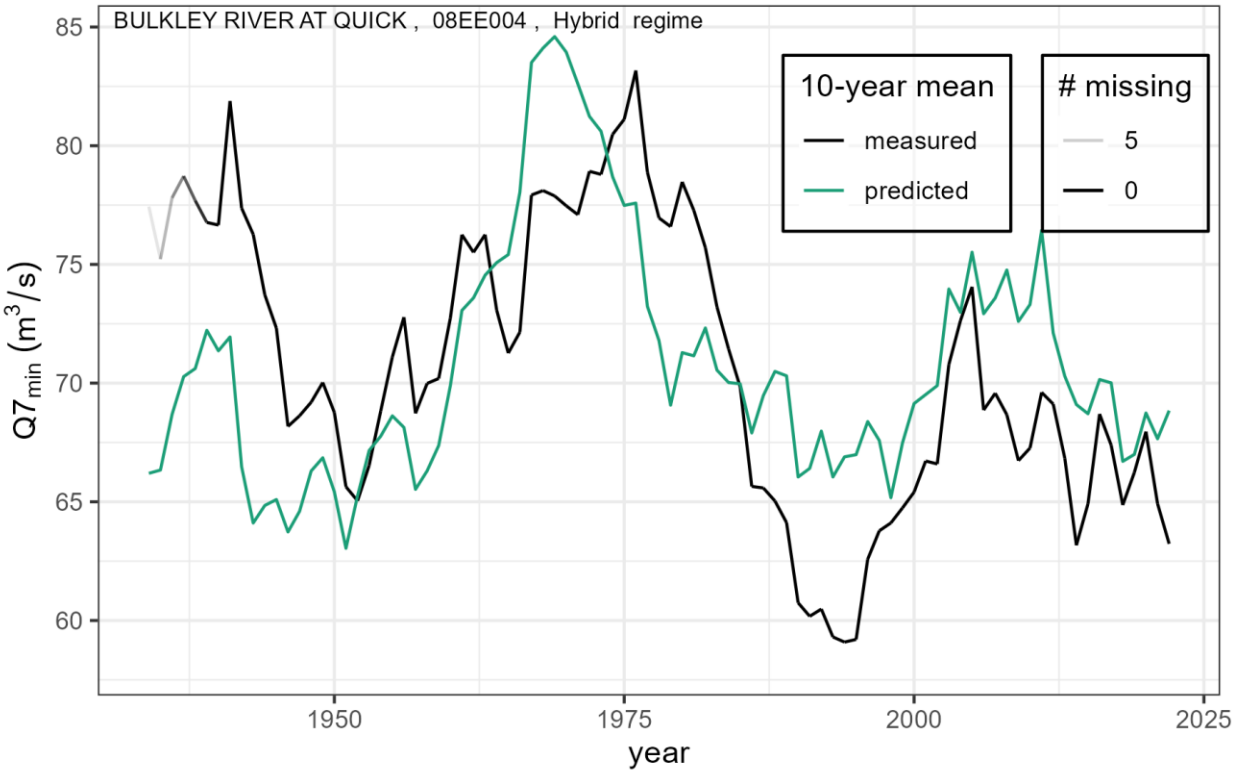

Figure F2: Gauge ID 08EE004, Bulkley River at Quick

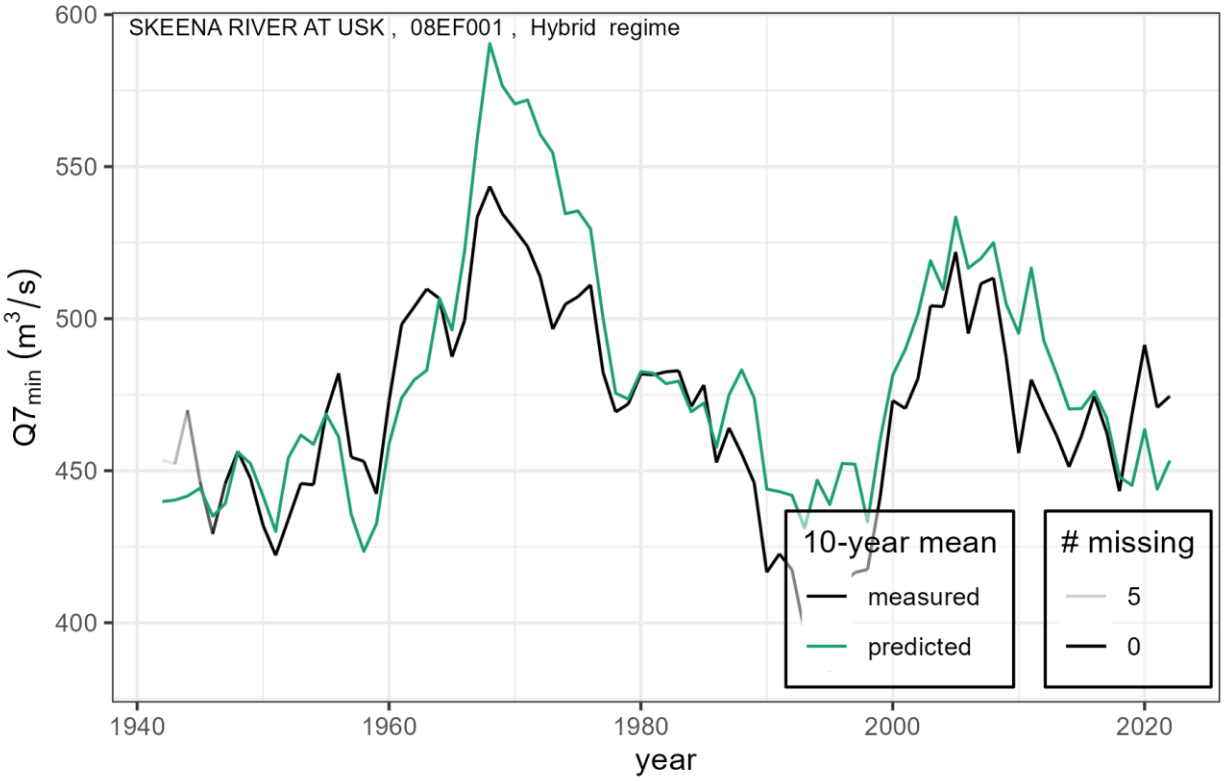

Figure F3: Gauge ID 08EF001, Skeena River at Usk

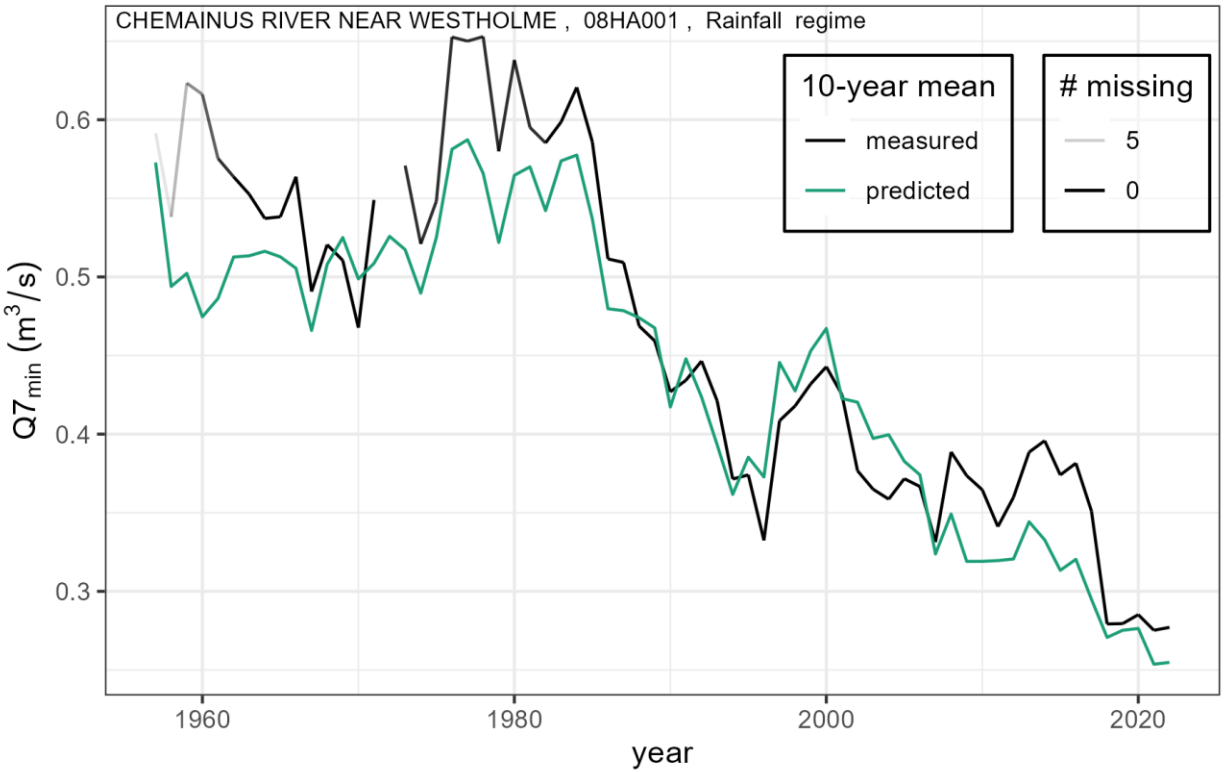

Figure F4: Gauge ID 08HA001, Chemainus River near Westholme

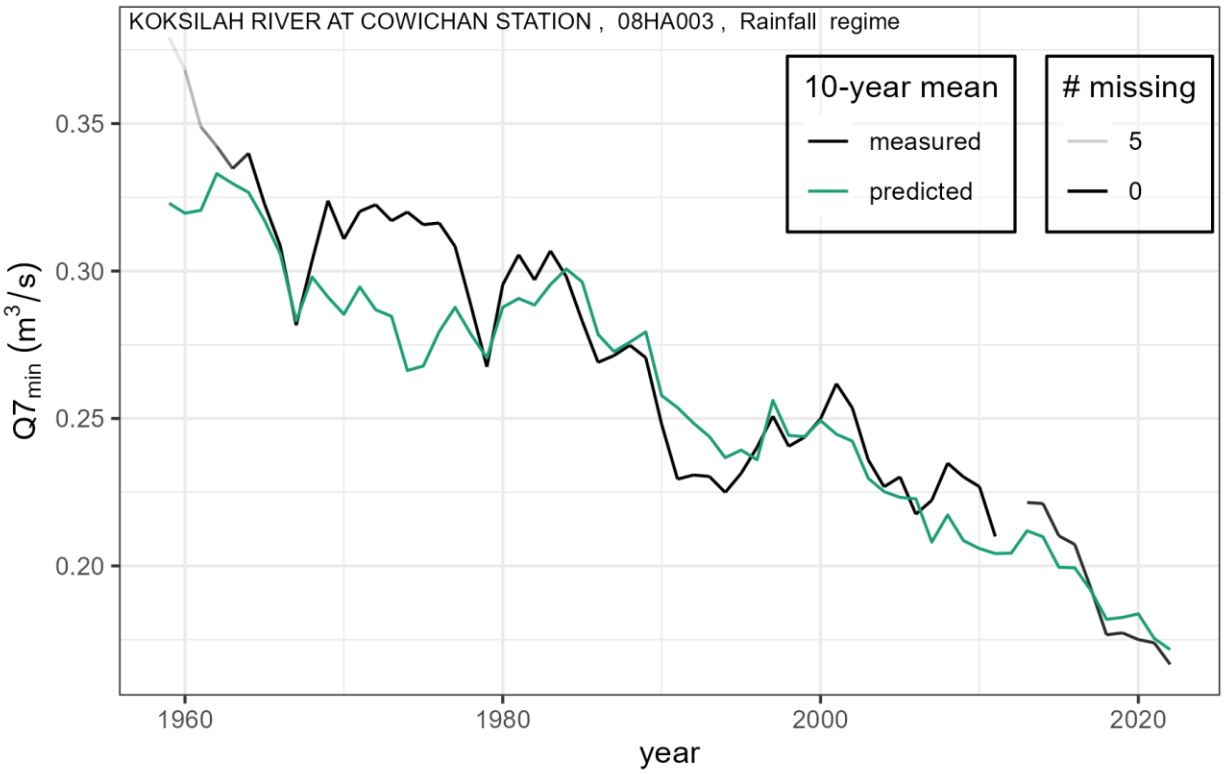

Figure F5: Gauge ID 08HA003, Koksilah River at Cowichan Station

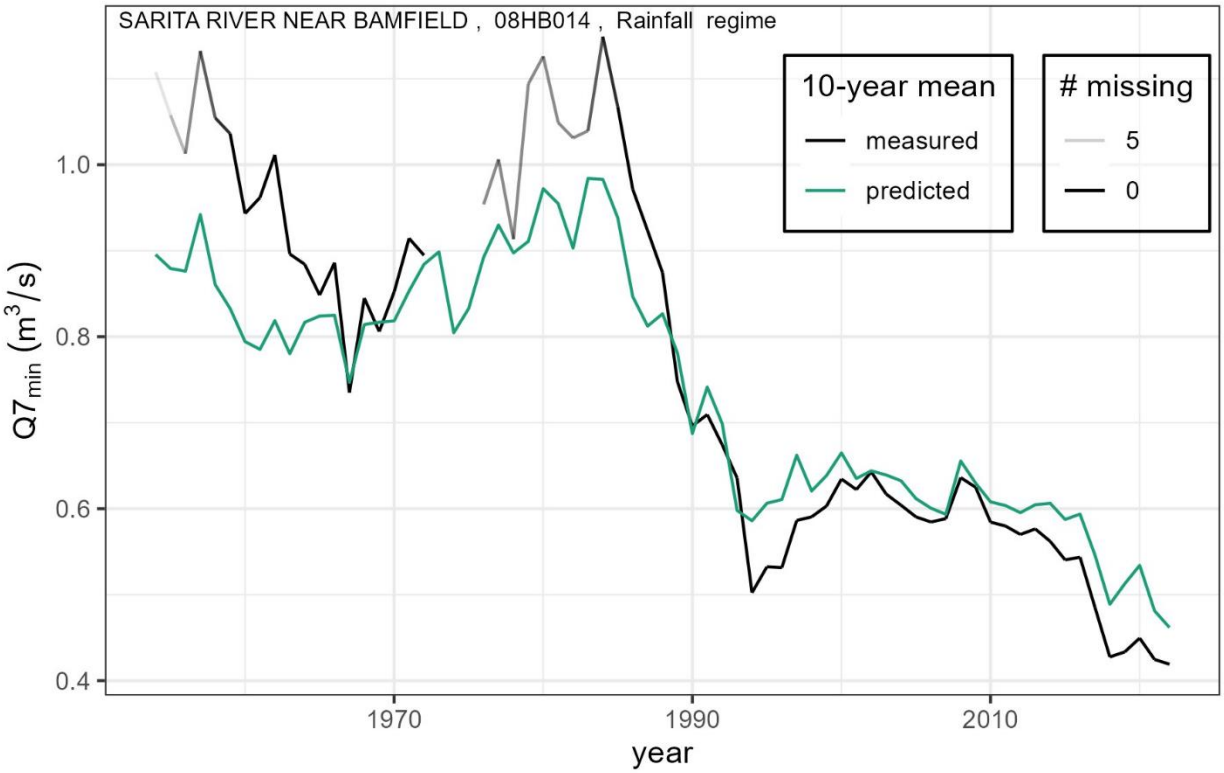

Figure F6: Gauge ID 08HB014, Sarita River near Bamfield

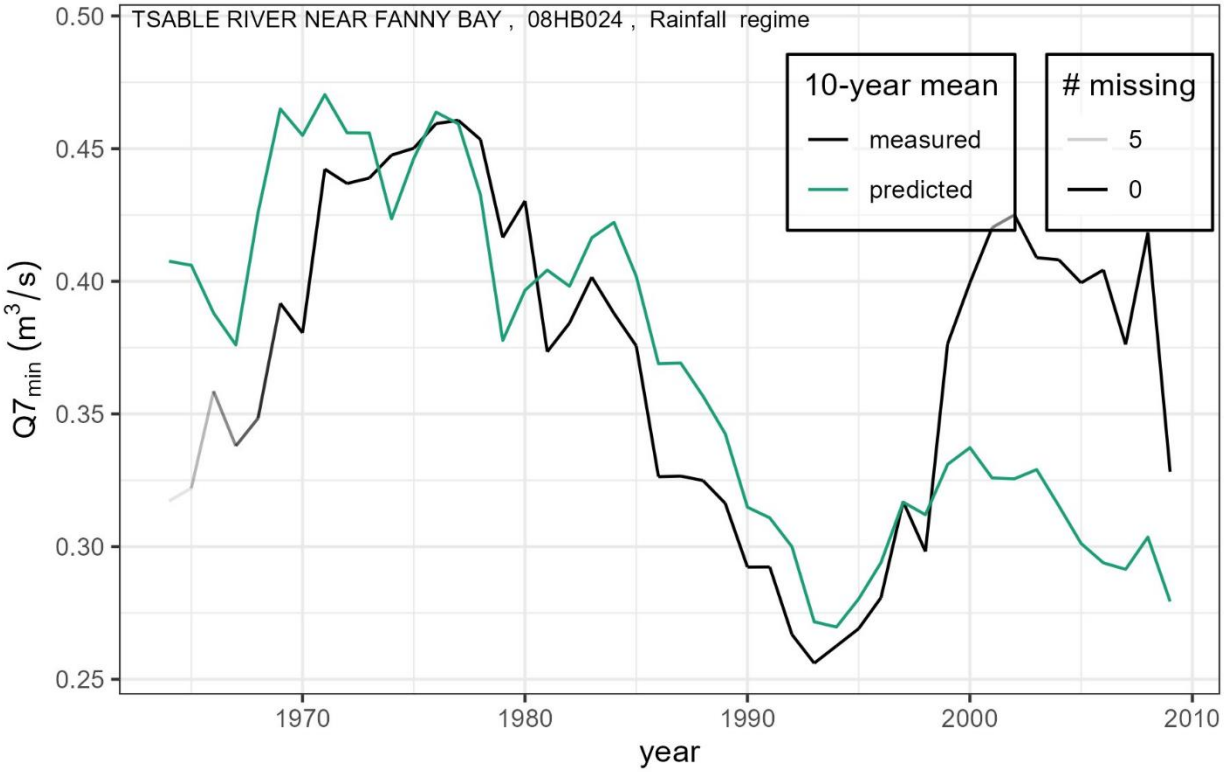

Figure F7: Gauge ID 08HB024, Tsable River near Fanny Bay

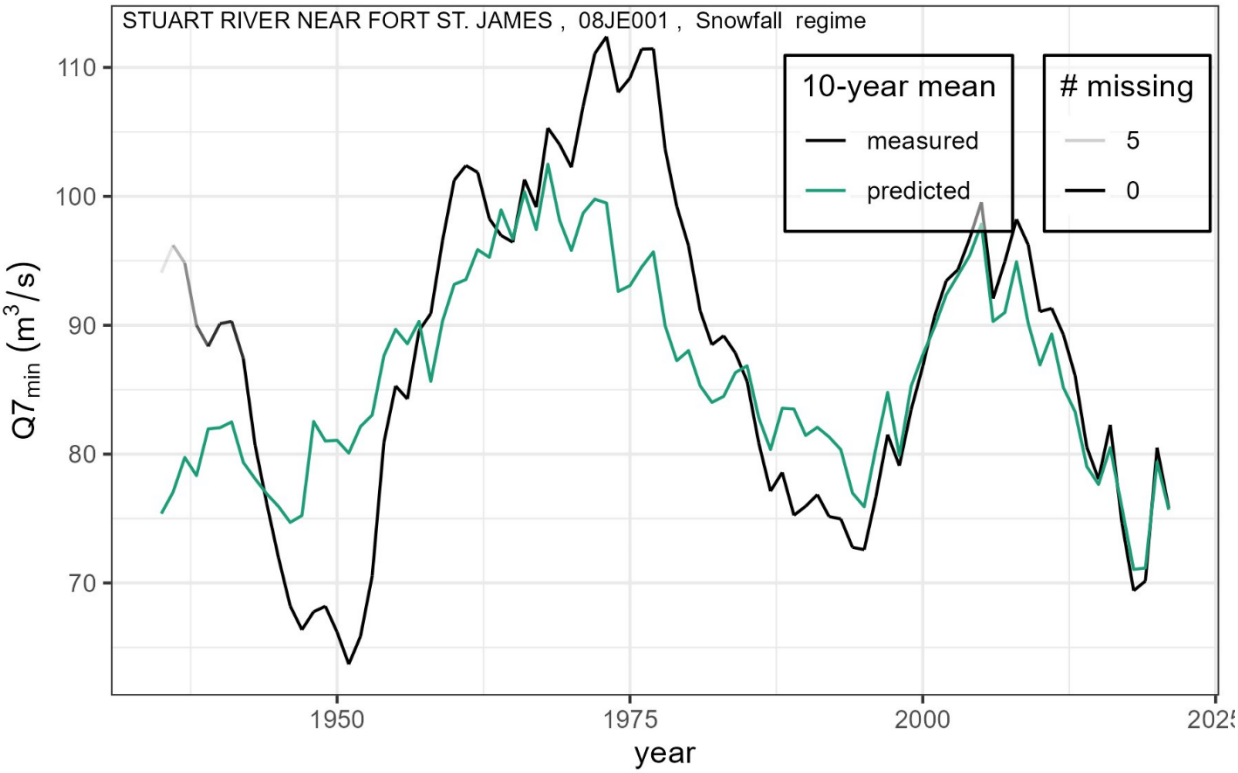

Figure F8: Gauge ID 08JE001, Stuart River near Fort St. James

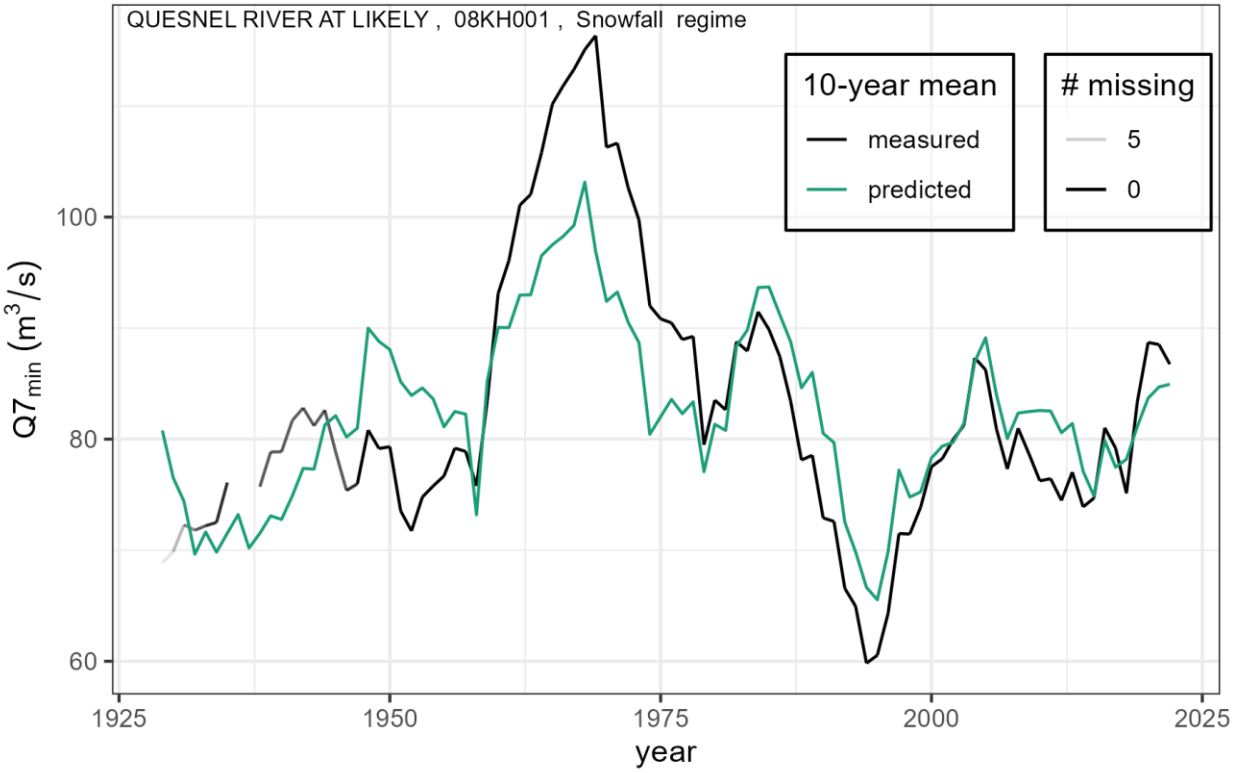

Figure F9: Gauge ID 08KH001, Quesnel River at Likely

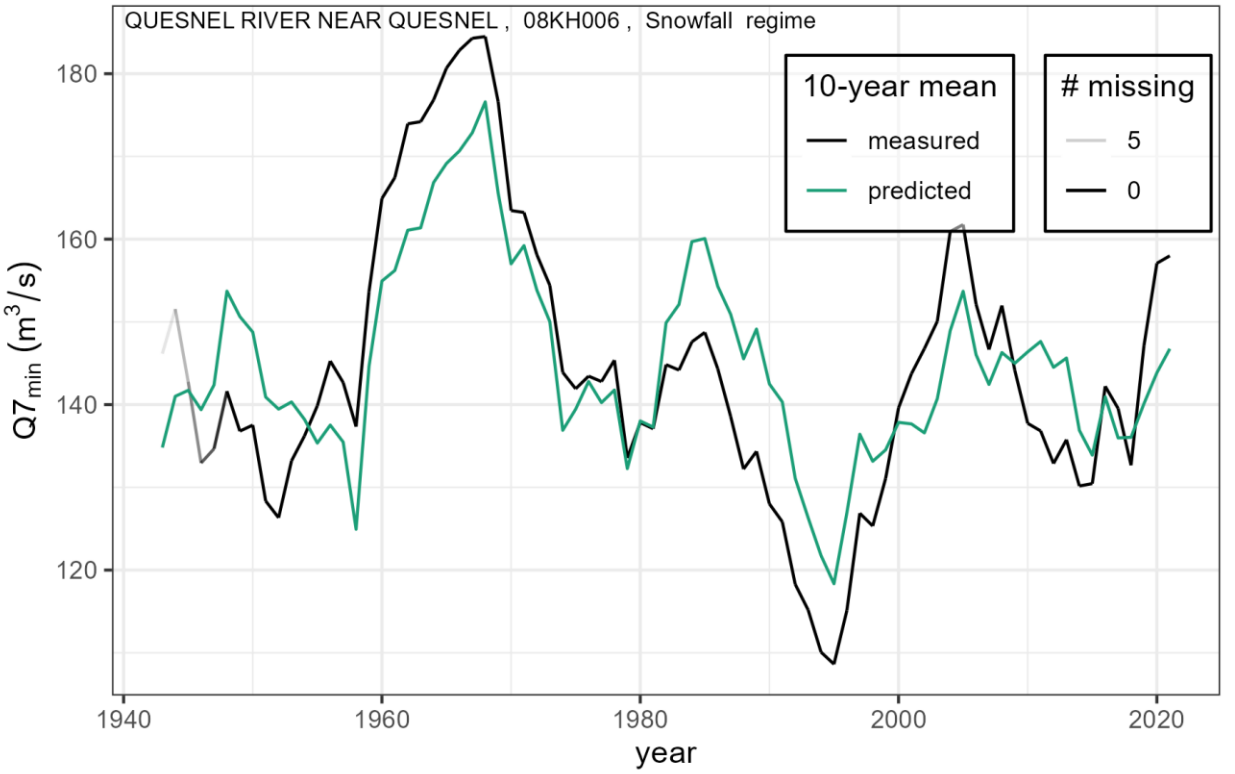

Figure F10: Gauge ID 08KH006, Quesnel River near Quesnel

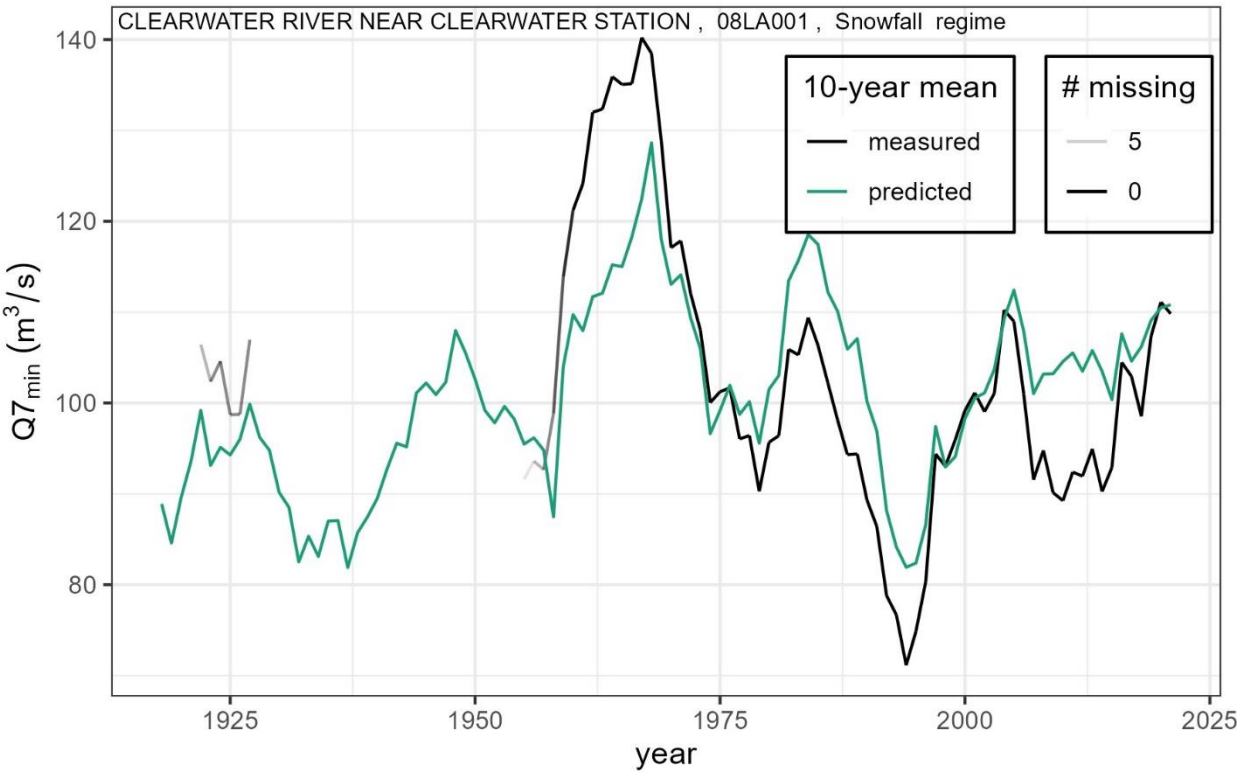

Figure F11: Gauge ID 08LA001, Clearwater River near Clearwater Station

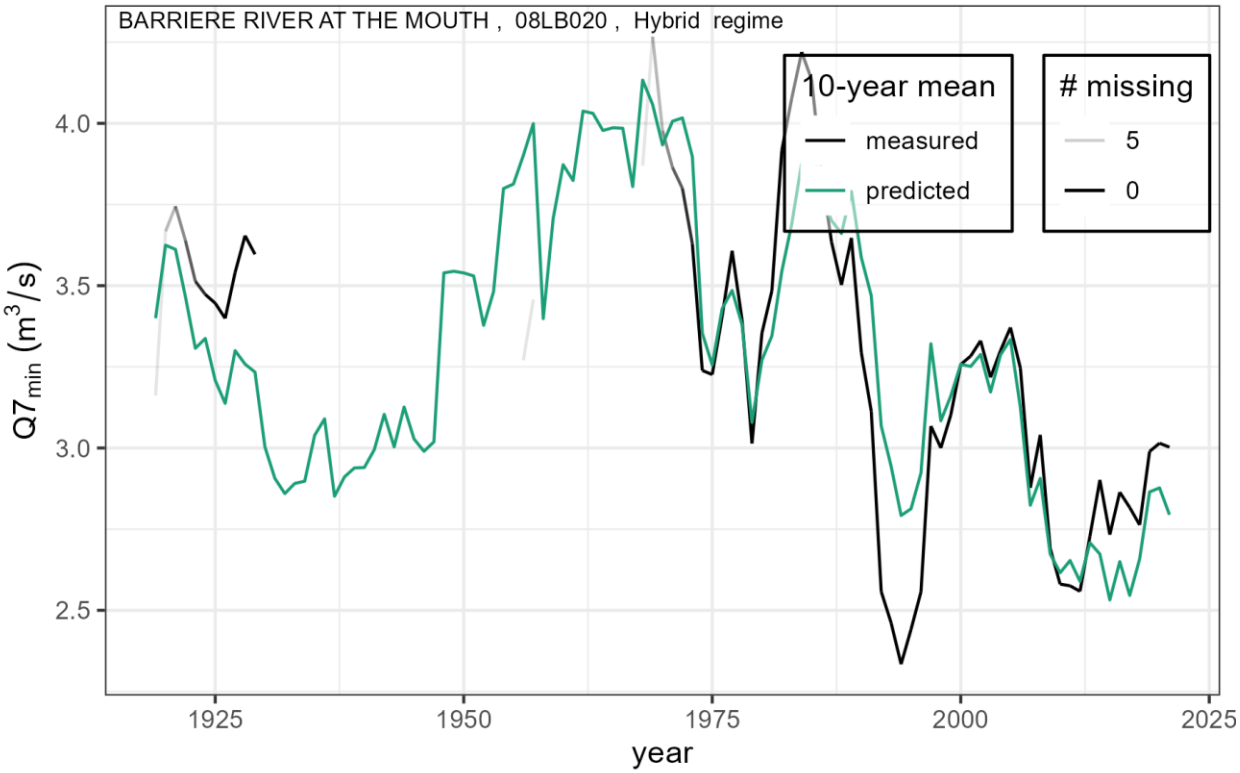

Figure F12: Gauge ID 08LB020, Barriere River at the Mouth

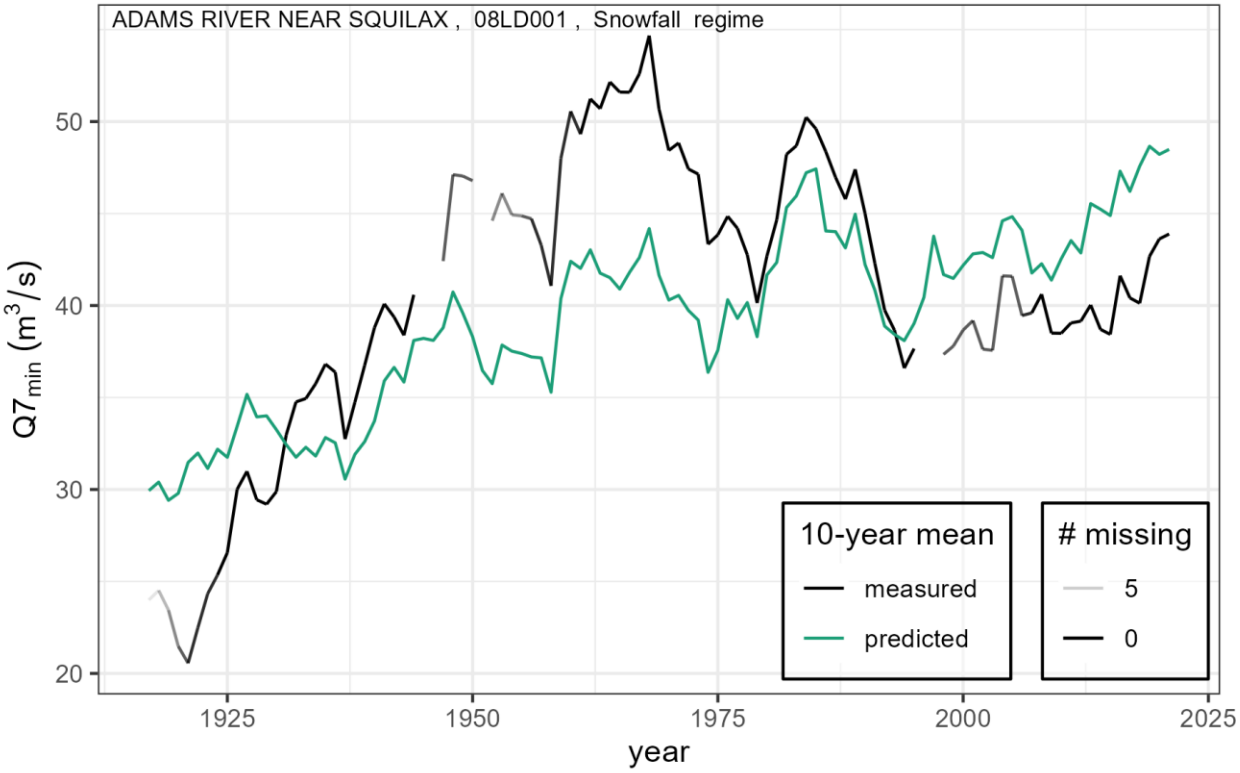

Figure F13: Gauge ID 08LD001, Adams River near Squilax

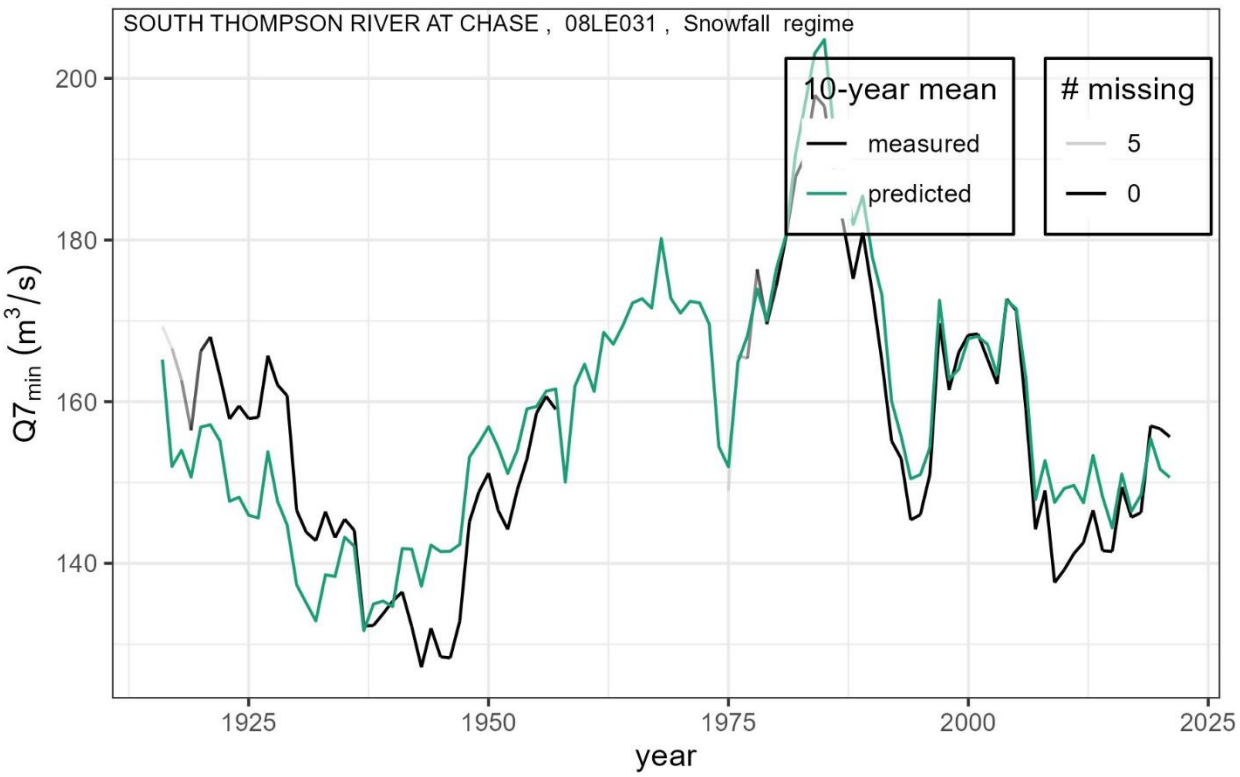

Figure F14: Gauge ID 08LE031, South Thompson River at Chase

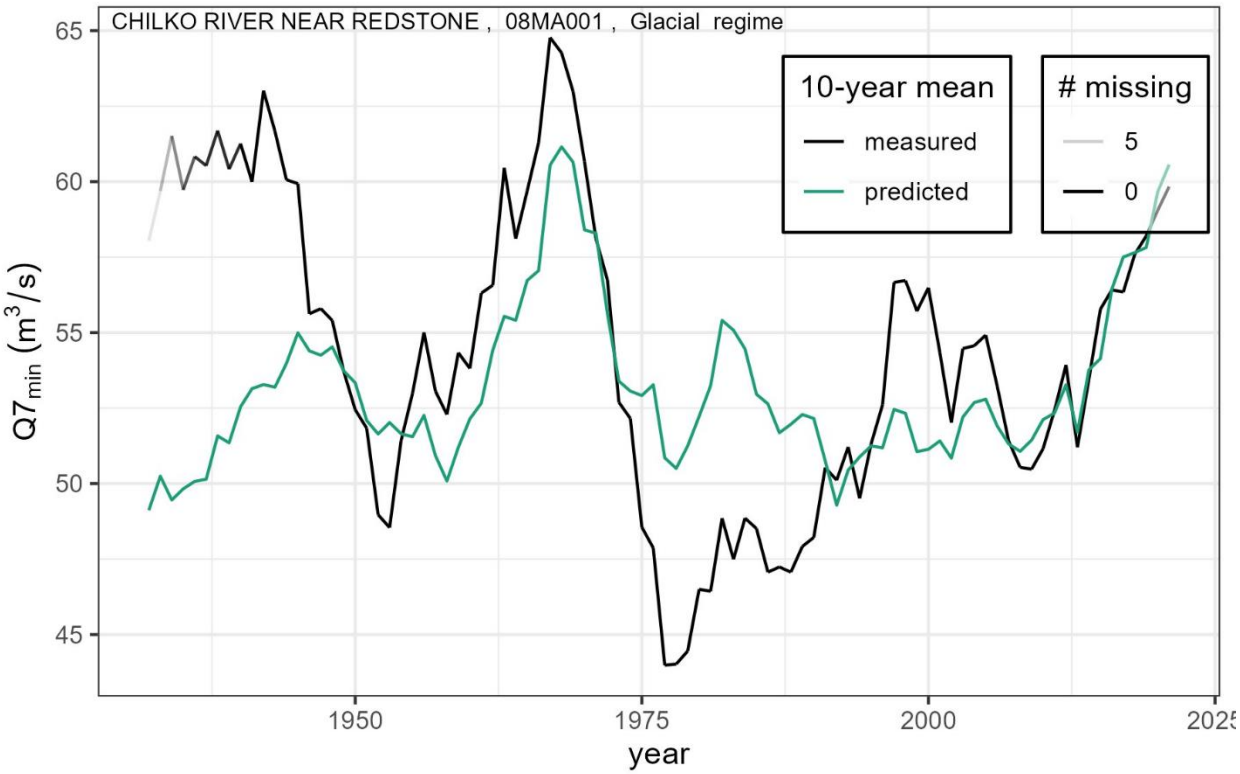

Figure F15: Gauge ID 08MA001, Chilko River near Redstone

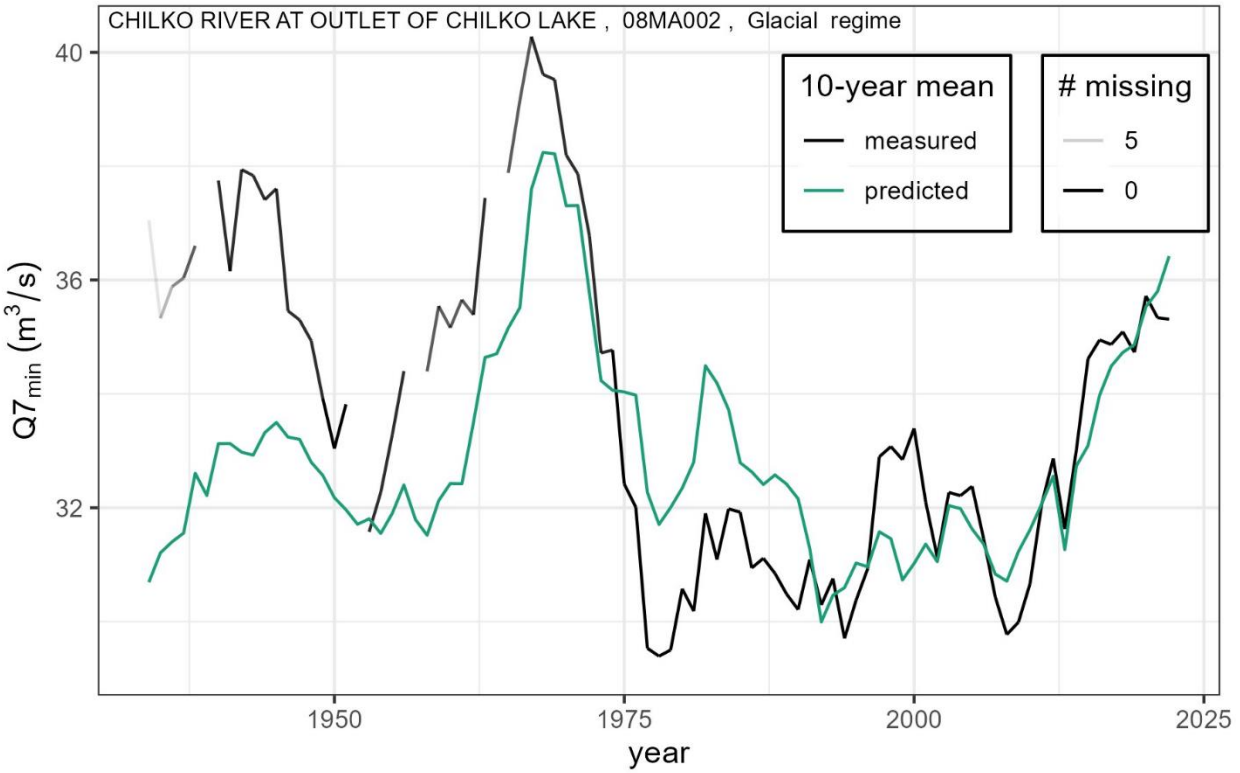

Figure F16: Gauge ID 08MA002, Chilko River at Outlet of Chilko Lake

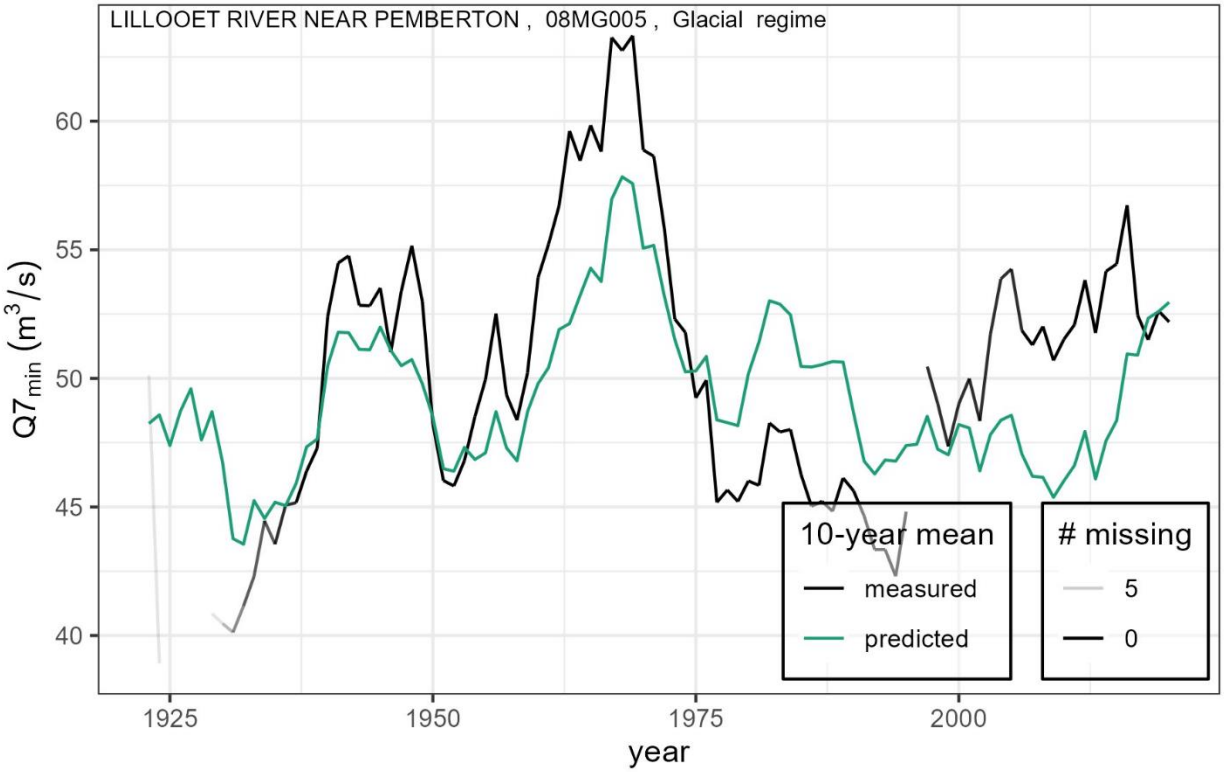

Figure F17: Gauge ID 08MG005, Lillooet River near Pemberton

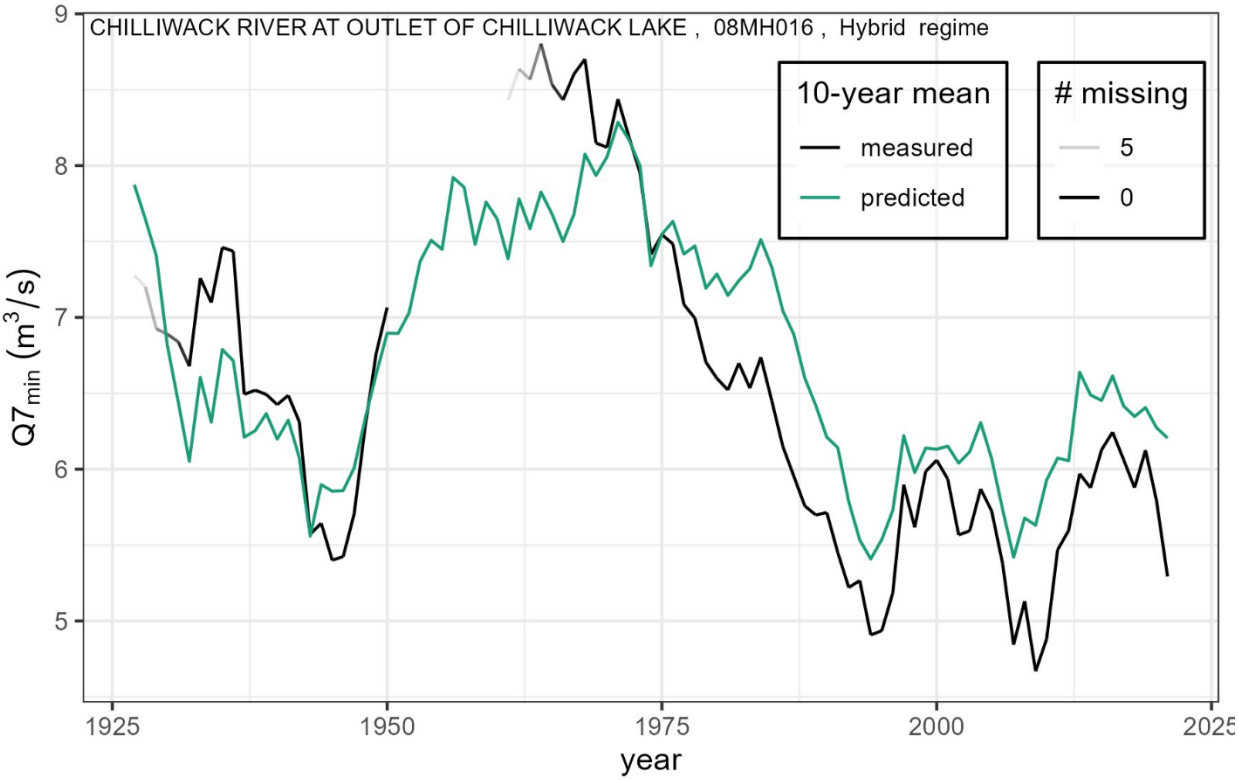

Figure F18: Gauge ID 08MG016, Chilliwack River at Outlet of Chilliwack Lake

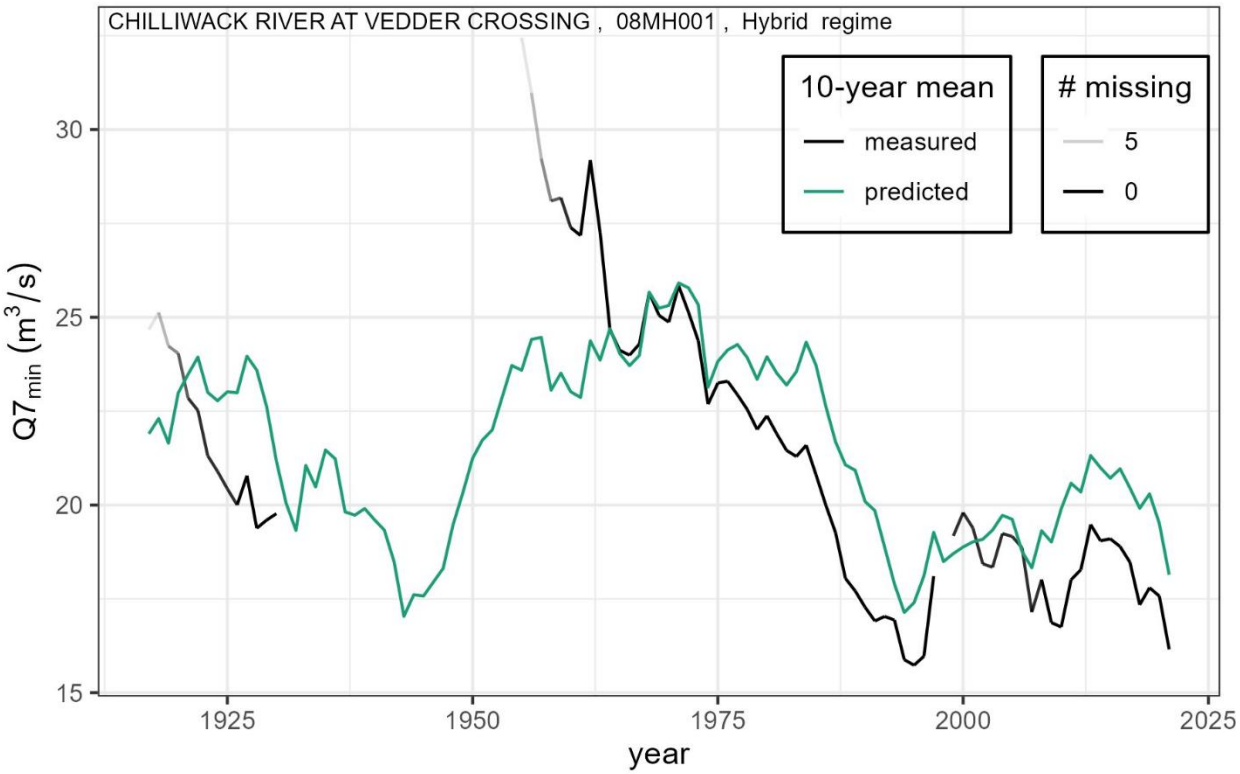

Figure F19: Gauge ID 08MH001, Chilliwack River at Vedder Crossing

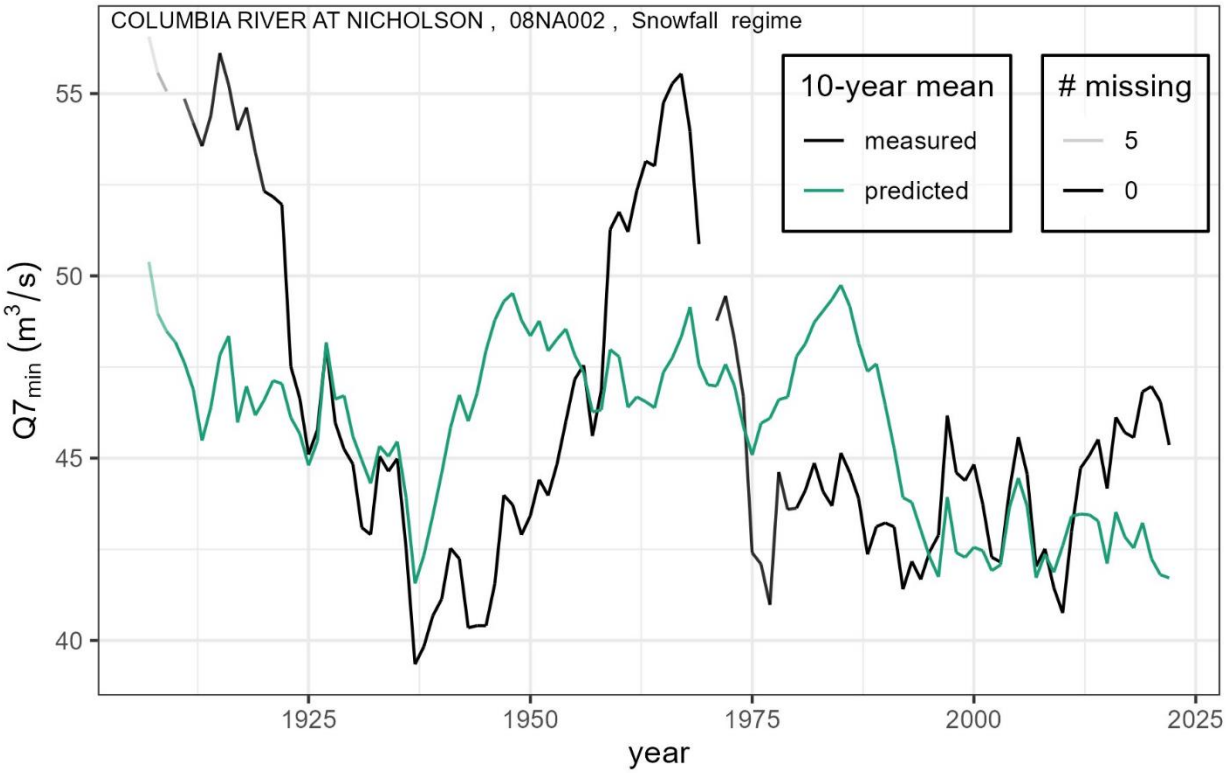

Figure F20: Gauge ID 08NA002, Columbia River at Nicholson

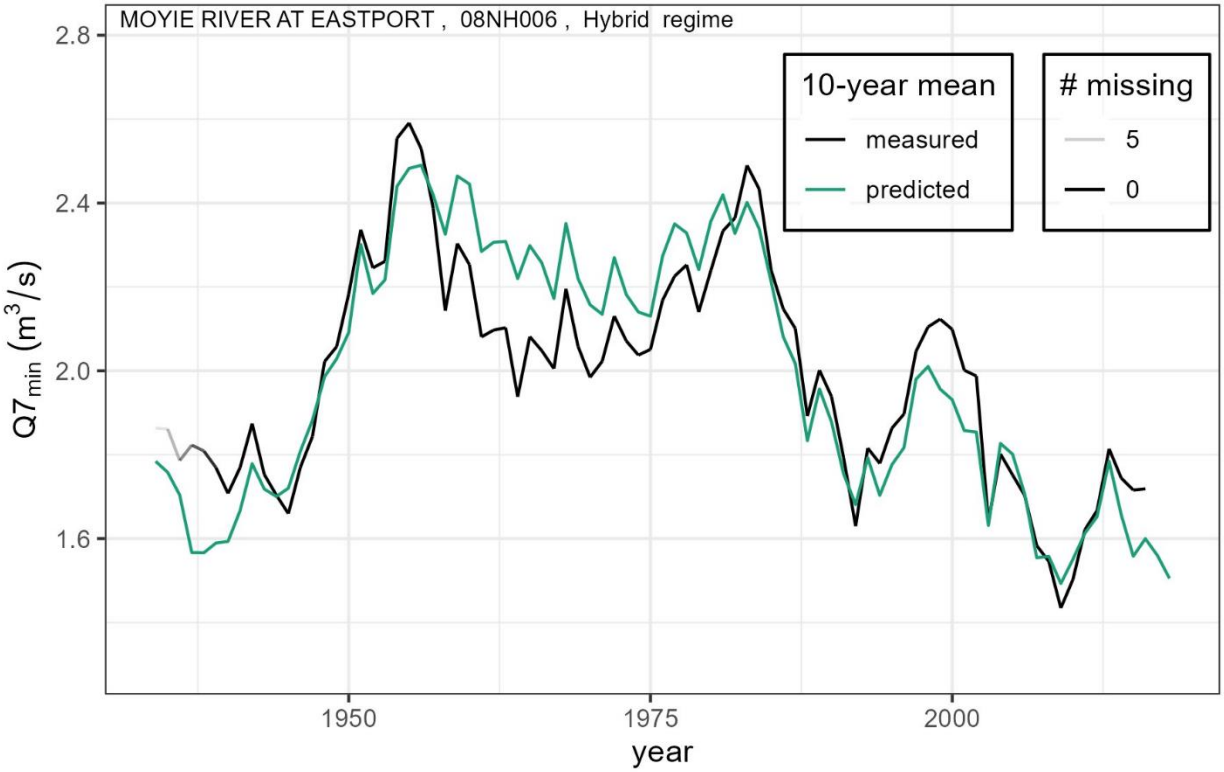

Figure F21: Gauge ID 08NH006, Moyie River at Eastport

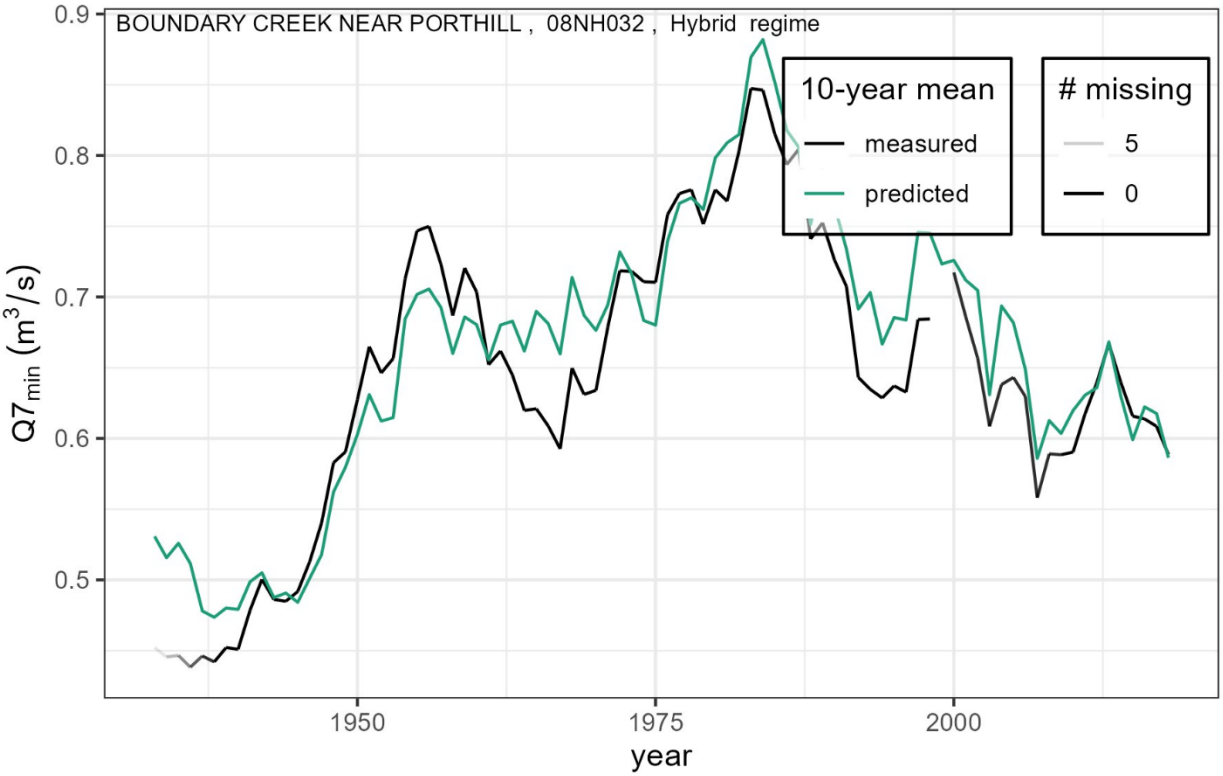

Figure F22: Gauge ID 08NH032, Boundary Creek near Porthill

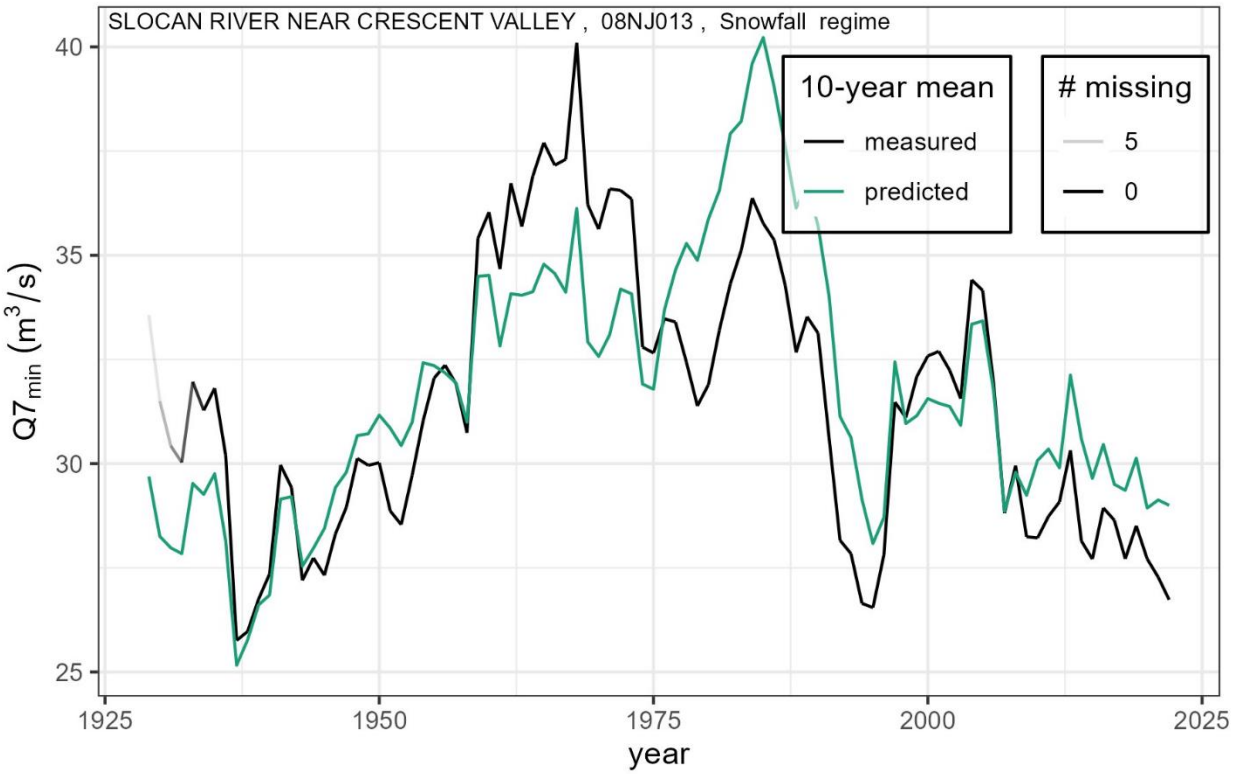

Figure F23: Gauge ID 08NJ013, Slocan River near Crescent Valley

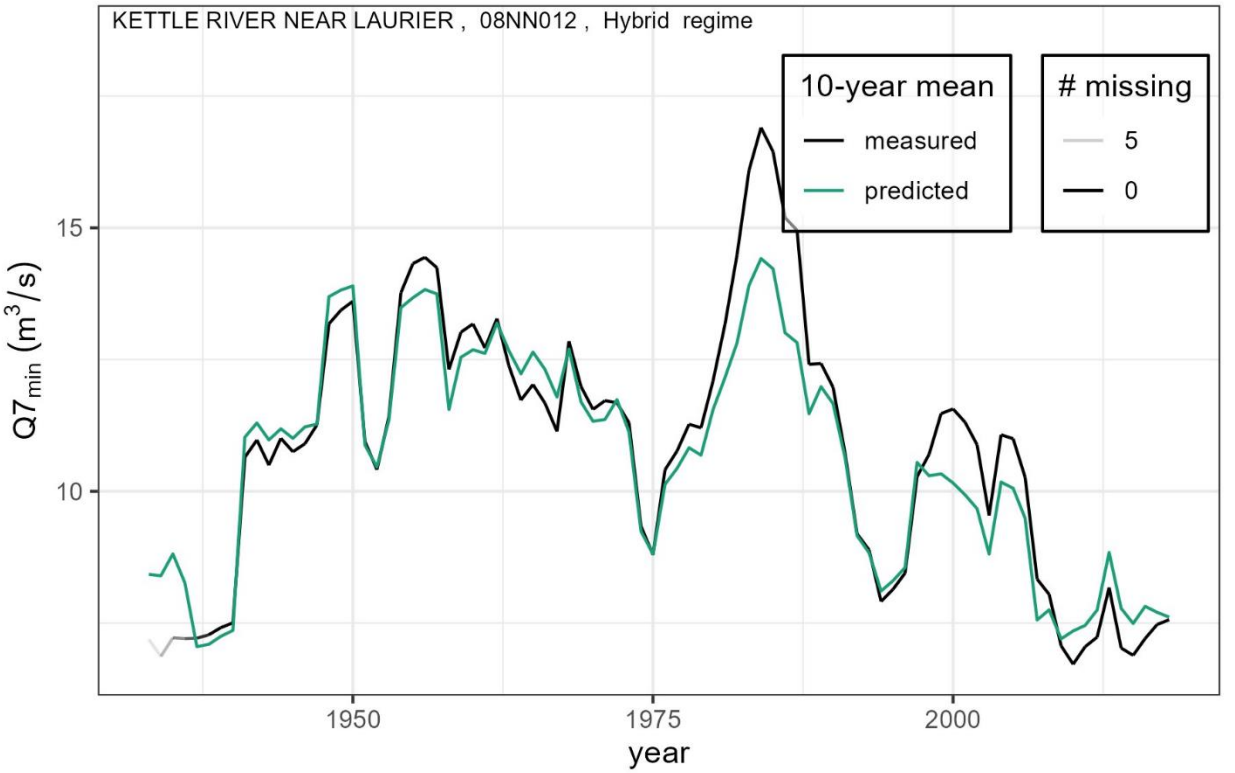

Figure F24: Gauge ID 08NN012, Kettle River Near Laurier

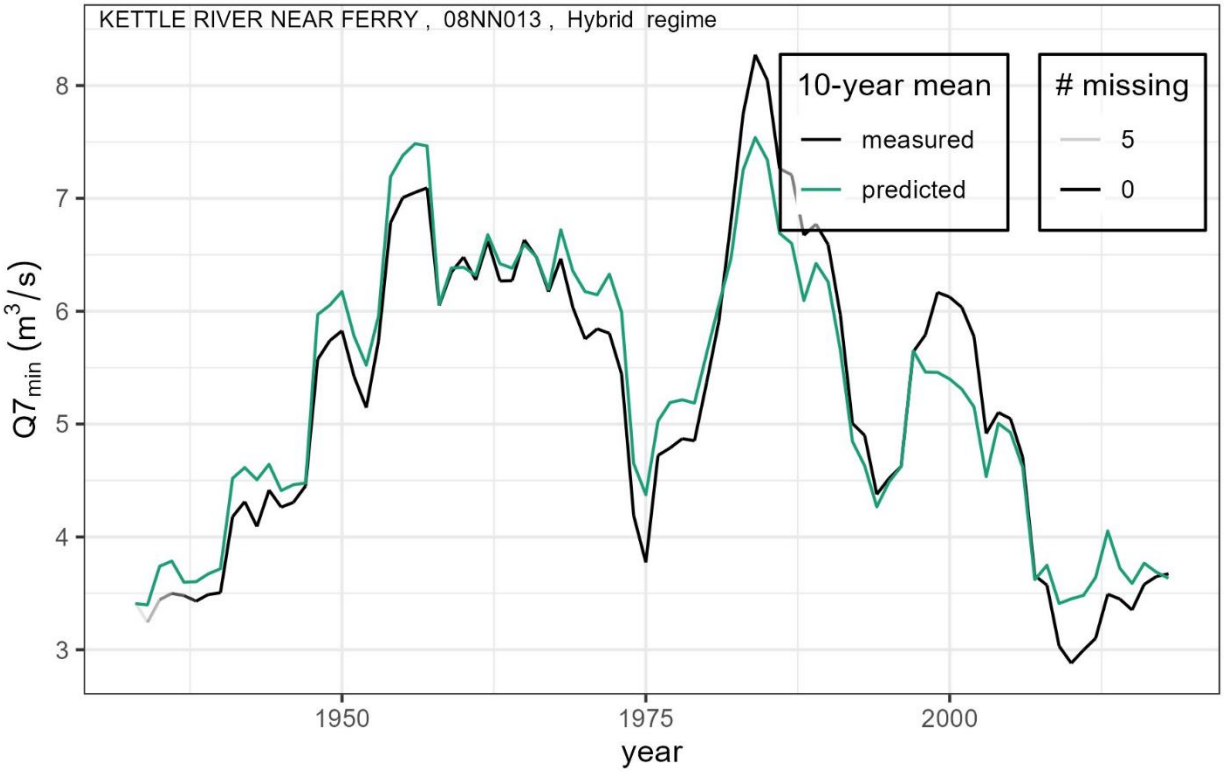

Figure F25: Gauge ID 08NN013, Kettle River Near Ferry

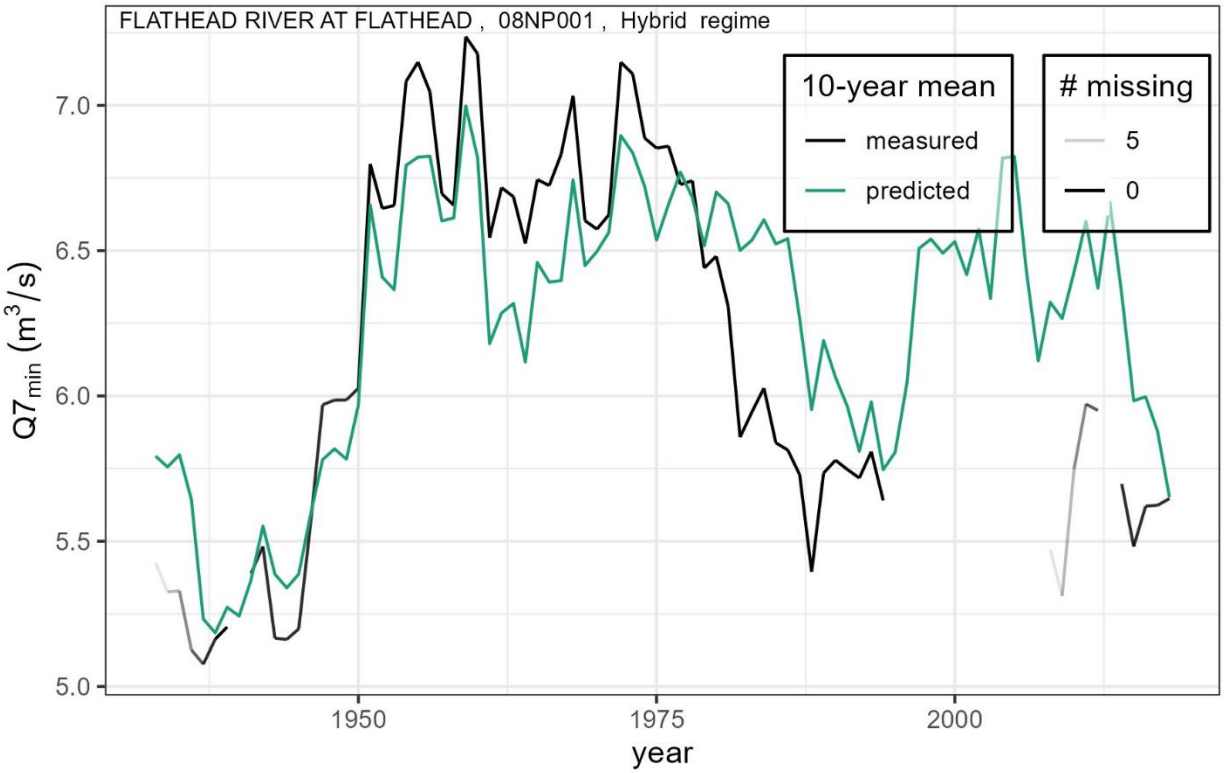

Figure F26: Gauge ID 08NP001, Flathead River at Flathead

APPENDIX G: TEMPORAL CONSISTENCY OF ANUSPLIN AND OTHER CLIMATE DATA

Introduction

We extensively use ANUSPLIN monthly data (MacDonald et al., 2020) to determine sensitivities, test stationarity, develop predictive regression models, and hindcast low-flow conditions in this study. However, the suitability of the ANUSPLIN data for these types of long-term sensitivity and trend analyses has not been established.

MacDonald et al. (2020) validated their dataset using leave-one-out cross-validation on 160 'test' stations, 11 of which were in western BC. They found that coastal stations (both Pacific and Atlantic) had the highest error in precipitation. They also found a negative significant trend in the mean error for July precipitation across the 160 stations.

Another potential issue with the ANUSPLIN dataset is that it is based on unadjusted and unhomogenized precipitation data (although the temperature records were homogenized). Operating procedures, instrumentation, and station locations have changed over time, potentially biasing trend analyses. Another ANUSPLIN dataset for adjusted precipitation is available (MacDonald et al., 2021) but it does not extend past 2015 and is provided at a lower spatial resolution.

In this appendix we evaluate whether there are indeed biases in the ANUSPLIN monthly data that could in turn bias our analyses of sensitivity and/or our hindcasts of low flow conditions. We will compare ANUSPLIN P and T to station data that have been adjusted to more accurately represent trends over time. We will also directly compare the unadjusted ANUSPLIN to the adjusted ANUSPLIN dataset. Lastly, we will assess whether runoff ratios, and changes in runoff ratios, are realistic in the two ANUSPLIN datasets for 23 catchments.

Data & Methods

Environment and Climate Change Canada have developed datasets of temperature and precipitation records that have been adjusted and harmonized for known measurement issues, changes to instrumentation, changes to instrument location, and changes to standard operating procedures, referred to as Adjusted and Harmonized Canadian Climate Data (AHCCD) (Mekis & Vincent, 2011; Vincent et al., 2020). These data include 780 temperature and 463 precipitation stations across Canada.

We extract ANUSPLIN data at the point location for each AHCCD station within 50 km of our study region and compare to the AHCCD data. For both ANUSPLIN and AHCCD data we calculate the monthly mean temperature T as the average of the monthly mean minimum and maximum temperatures.

We define the bias for temperature (T) and precipitation (P):

$$bias_T = T_{ANUSPLIN} - T_{AHCCD}$$
$$bias_P = \frac{P_{ANUSPLIN} - P_{AHCCD}}{P_{AHCCD}}$$

We analyse trends in $bias_T$ and $bias_P$ using Sen's slope and a Mann-Kendall trend test to test the magnitude, direction, and significance. We analyse trends over four time periods: 1900-2017, 1925-2017, 1950-2017, and 1975-2017. 2017 is the last year of data in the AHCCD. For each period we use only AHCCD stations that began recording on or before the first year in the period, and which have at least 30 years of data within the period. For precipitation we estimate trends in the logarithm of $bias_p$ and then calculate the trend in the same way that we calculate trends in low flows (equation 1 of this paper).

We analyse bias trends in annual mean temperature, total annual precipitation, summer (June – September) precipitation, and winter (December - April) precipitation.

We also analyse bias trends in temperature and precipitation for each month of the year. For each period and month, we use binomial tests to test whether the number of positive/negative trends is greater than expected by chance. We apply the Holm-Bonferroni method to correct for the family-wise error rate.

Note that we are interested in the bias trend, not the magnitude of the bias itself. The magnitude of bias may be a result of local topographic factors, as the station may be located substantially higher or lower than the mean elevation of the ANUSPLIN grid cell. Moreover, a stable bias will not affect the regression analyses performed in this study, but changes to the bias over time will.

We also note that we are comparing three interpolated datasets against station data that were also used to perform the interpolations. We do not have the option to evaluate out-of-sample performance. Our evaluation thus serves as a upper bound on the reliability of the ANUSPLIN data; the gridded data farther from climate stations are likely to be less reliable.

Next, we compare the gridded annual precipitation from ANUSPLIN and ANUSPLIN-adjusted across the province in two periods: 1900-1949, 1950-2015. These periods were chosen because we noted a distinct shift in the difference between the two datasets around 1950.

Lastly, we calculate annual runoff ratios for 23 unglaciated (<1% glacial cover) catchments that have at least one complete water year (October 1-September 30) of hydrometric data before 1950. We calculate the mean annual runoff ratio using both the ANUSPLIN and ANUSPLIN-adjusted data, for 1900-1950 and 1950-2015. We then evaluate whether the runoff ratios are realistic, and whether the change over time in the runoff ratio is realistic. Although some change in runoff ratio is possible due to land cover changes or changes in evapotranspiration, runoff ratios greater than 1 are not possible in the absence of large changes in catchment storage, which are unlikely in unglaciated catchments.

Results

Figure G1 shows the bias trends for annual temperature. Most trends are smaller than 0.1°C per decade, and all but one are smaller than 0.2°C per decade. The ratio of positive to negative trends is roughly balanced for all periods except 1900-2017, and there is no clear regional pattern. For 1900-2017 most trends are negative.

Table G1 shows the results of binomial tests applied to the number of positive/negative temperature bias trends in each month and period. We find that in the first period (1900-2017) there are significantly more negative trends than expected by chance, for February, March, October, and December. This implies that the beginning of the ANUSPLIN time series (1900-1925) has a positive bias in temperature; actual temperatures were probably colder than represented in the ANUSPLIN data.

For illustrative purposes, Figures G2 and G3 show the bias through time for the long-term stations with the largest negative and positive bias trends. 'Long-term' stations are arbitrarily defined as those with more than 90 years of data.

At Kelowna Airport (Climate ID 1123939, Figure G2) the bias trend is -0.13°C per decade, resulting in about 1.6°C bias between the start and end of the dataset. Actual temperatures in the early 20th century were probably colder than the ANUSPLIN data for this location. At Salmon Arm (Climate ID 1167337, Figure G3) the bias trend is 0.10°C per decade, resulting in about 1.0°C bias between the start and end of the dataset. Actual temperatures in the early 20th century were probably warmer than the ANUSPLIN data for this location. While the bias trend at Kelowna reflects a steady decrease in bias over time, the trend at Salmon Arm is related to a step change at 1982, when the original climate station was discontinued and a new climate station was installed at the Salmon Arm airport.

Figure G4 shows the bias trends in annual precipitation across the province, and Figures G7 and G8 show trends in summer and winter precipitation, respectively. For the longest period (1900-2017) all trends are smaller than 3% per decade. However, during the 1950-2017 and 1975-2017 periods there are several strong and significant trends of more than 5% per decade, especially for winter precipitation. Although positive and negative trends are roughly balanced in each period, there appear to be more positive trends in coastal locations, including Vancouver Island and Haida Gwaii, particularly from 1950-2017. This is a salient detail for this study, because these regions are home to most of the rainfall-dominated watersheds. Positive trends indicate that the early part of the period was wetter than is represented in the ANUSPLIN data.

Winter precipitation bias trends are more positive than summer trends. There are also more large (>5%, positive and negative) trends in the winter than the summer, possibly because of large adjustments to snow ruler measurements (Mekis & Vincent, 2011). There are clusters of large positive bias trends for winter precipitation on Vancouver Island and in the Southern Interior for the period 1975-2017.

Table G2 shows the results of binomial tests applied to the number of positive/negative precipitation trends in each month and period. No months show significant biases for the longest period (1900-2017) although only 15 stations are available for this period. April trends are more likely to be positive for the 1925-2017 and 1950-2017 periods, although no other months are significant. For 1975-2017, August bias trends are more likely to be positive and October trends are more likely to be negative.

Figures G5 and G6 show bias trends in annual precipitation for the long-term stations with the largest negative and positive bias trends. At Vancouver International Airport the trend from 1900-2017 is -2.6% per decade, meaning that the period from 1900-1950 was probably somewhat drier than represented by ANUSPLIN. At Estevan Point the trend is 1.2% per decade, implying that the beginning of the time series was probably wetter than represented by ANUSPLIN.

Figures G9 and G10 show bias trends in annual total precipitation and mean temperature for the adjusted ANUSPLIN data (MacDonald et al., 2021), the ERA5-Land data (Muñoz Sabater, 2019), and PNWNAmet data (Werner et al., 2019). Surprisingly, we found that the two datasets based on adjusted precipitation data (ANUSPLIN-adjusted and PNWNAmet) had stronger bias trends in (more stations with bias trends greater than 3%) than the unadjusted ANUSPLIN data. For temperature PNWNAmet performed as well or slightly better than ANUSPLIN, but some stations still had significant bias trends greater than 0.1°C per decade.

The ERA5-Land data performed worst, with most stations showing positive bias trends in temperature and negative bias trends in precipitation from 1950-2017. This implies that the ERA5-land data may represent the period from 1950 to about 1975 as colder and wetter than it actually was.

Figures G11, and G12, show the ratio of ANUSPLIN/ANUSPLIN-adjusted mean annual precipitation for two periods (1900-1949, 1950-2015). For 1900-1949 there are enormous differences in the two datasets, with some coastal regions receiving less than half of the annual precipitation in the adjusted ANUSPLIN data as in the unadjusted data. The largest differences are primarily in the interpolated regions between climate stations as well as near the Washington and Alaska borders where the unadjusted ANUSPLIN data had the benefit of using US stations.

Figure G13 shows runoff ratios in 23 catchments for two periods (1900-1949 and 1950-2015) for two datasets (ANUSPLIN and ANUSPLIN-adjusted. Several catchments have impossibly high runoff ratios (>1), probably indicating that precipitation is underpredicted. This is especially true for 1900-2015 and for the ANUSPLIN-adjusted precipitation data.

Between the early and late periods, the runoff ratio in the unadjusted ANUSPLIN dataset remains similar for most catchments. However, for ANUSPLIN-adjusted, runoff ratios in the 1900-1949 period are much higher than for 1950-2015, indicating that precipitation is underpredicted in the early period. Six catchments have runoff ratios larger than 1.5 in the early period using the ANUSPLIN-adjusted data, 4 of which are in the southwest of the province.

Discussion

The preceding analyses demonstrate some weaknesses in the ANUSPLIN data. In some locations there are significant bias trends, relative to adjusted and harmonized temperature and precipitation data. Trends as large as 0.2°C per decade were observed in the temperature data, and some trends larger than 5% per decade were observed in the precipitation data. Over the span of a century, these trends result in significant biases.

These biases have implications for our low flow analyses. First, if there is a change to the bias over the period for which we conduct our sensitivity analyses, this could in turn bias our estimates of sensitivity to temperature and/or precipitation. The direction of this bias is uncertain and could be different for each catchment.

Second, if there are regionally clustered long-term trends in the ANUSPLIN bias, our hindcasted low-flow conditions will also be biased. This could affect catchments in the rainfall regime in particular, since we noted that many of the precipitation bias trends on Vancouver Island were positive; we also noted that for the period 1900-2017, temperature bias trends are predominantly negative. This implies that the beginning of the 20th century was colder and wetter than represented in the ANUSPLIN data for Vancouver Island.

For the rest of the province, we note that most bias trends from 1900-2017 and 1925-2017 are small, and positive/negative bias trends appear to be spatially random (they do not cluster together). This means that some catchments in our study probably exhibit a positive bias, and some exhibit a negative bias. Therefore, our regime-averaged hindcasts (Figures 5 and 6 of the manuscript) are probably reasonable.

It is surprising that the ordinary ANUSPLIIN data performed better than the ANUSPLIN-adjusted data, and as well as the PNWNAmet datasets for precipitation. PNWNAmet, in particular, is an interpolation using the very same AHCCD data that we validated against. The existence of bias trends in the PNWNAmet data illustrates that interpolation can result in unexpected trends at some locations, probably related to discontinuities when nearby stations turn on or off.

Our comparisons of ANUSPLIN and ANUSPLIN-adjusted precipitation over two periods (1900-1949 and 1950-2015, Figures G11 and G12) indicate that the ANUSPLIN-adjusted precipitation may be underestimated for the period 1900-1949. These underestimations occur mainly far away from climate stations. Our analysis of runoff ratios also indicates that both datasets may underestimate precipitation in coastal watersheds, although the underestimation is generally larger in the ANUSPLIN-adjusted data (Figure G13). Runoff ratios are more temporally consistent in the ANUSPLIN data than in the ANUSPLIN-adjusted data.

Overall these results indicate that the unadjusted ANUSPLIN dataset is a good choice for the analyses in this study. It has the longest time series and appears to be no more biased than other datasets available for the region. The unadjusted ANUSPLIN data are more temporally consistent than the adjusted ANUSPLIN data.

Figures and Tables

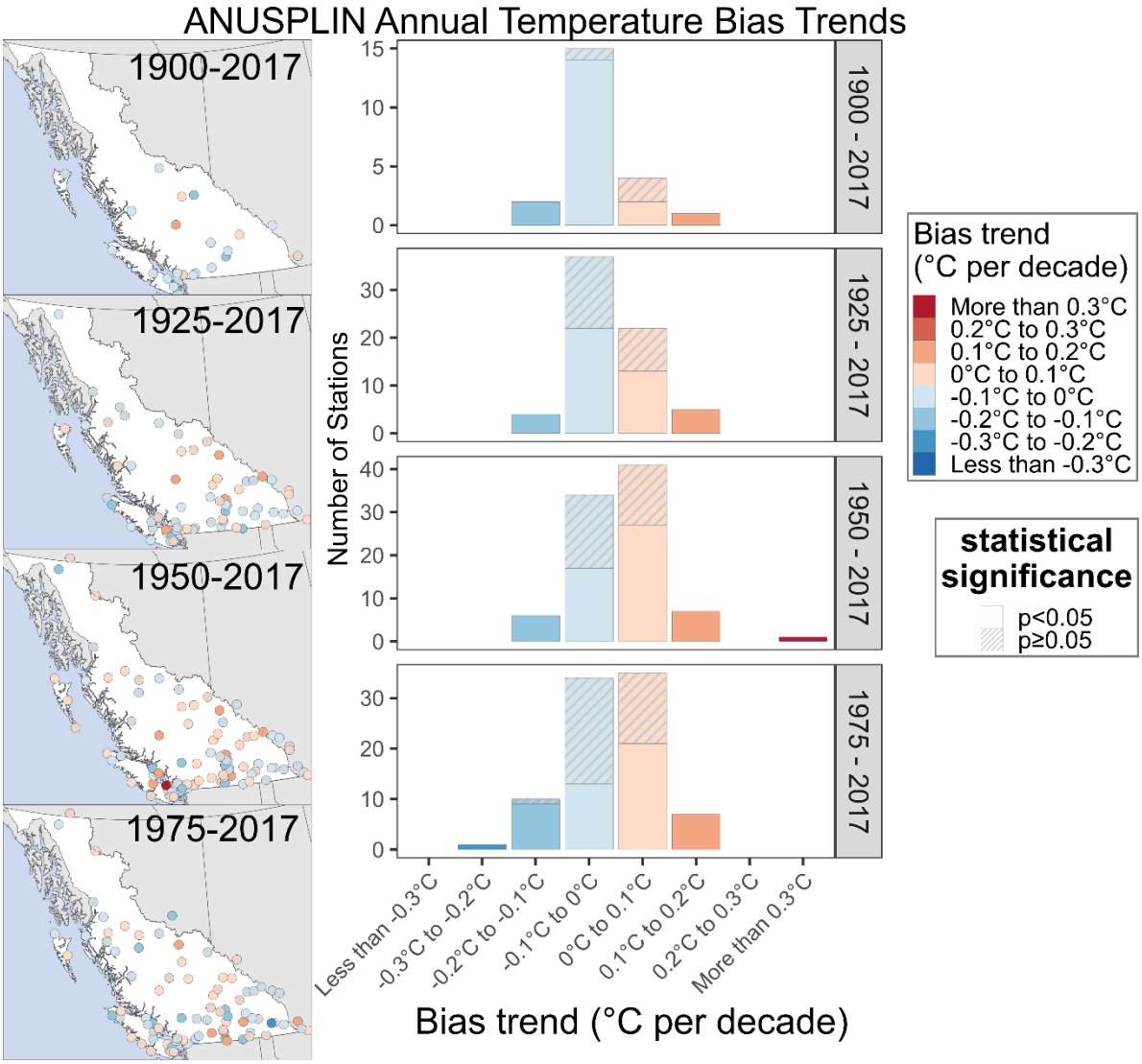

Figure G1: Bias trends in annual temperature. The panels (left) indicate the spatial distribution of the trends, also shown as histograms (right).

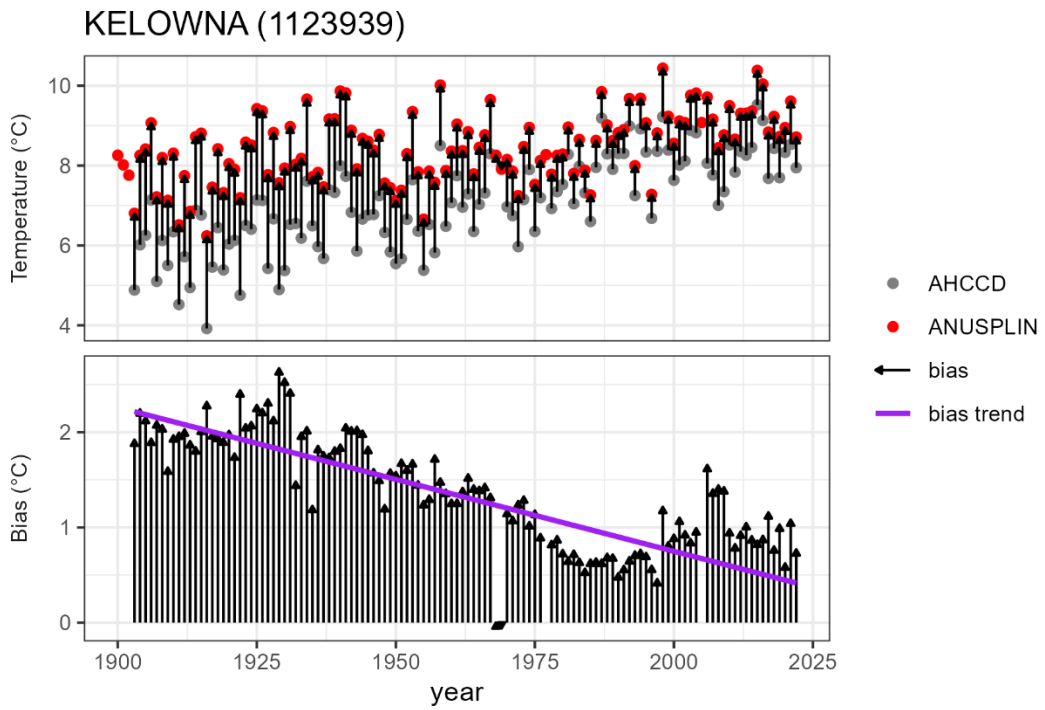

Figure G2: Annual mean temperature from AHCCD and ANUSPLIN (top) and bias (bottom) for Kelowna airport. The bias trend -0.13°C per decade.

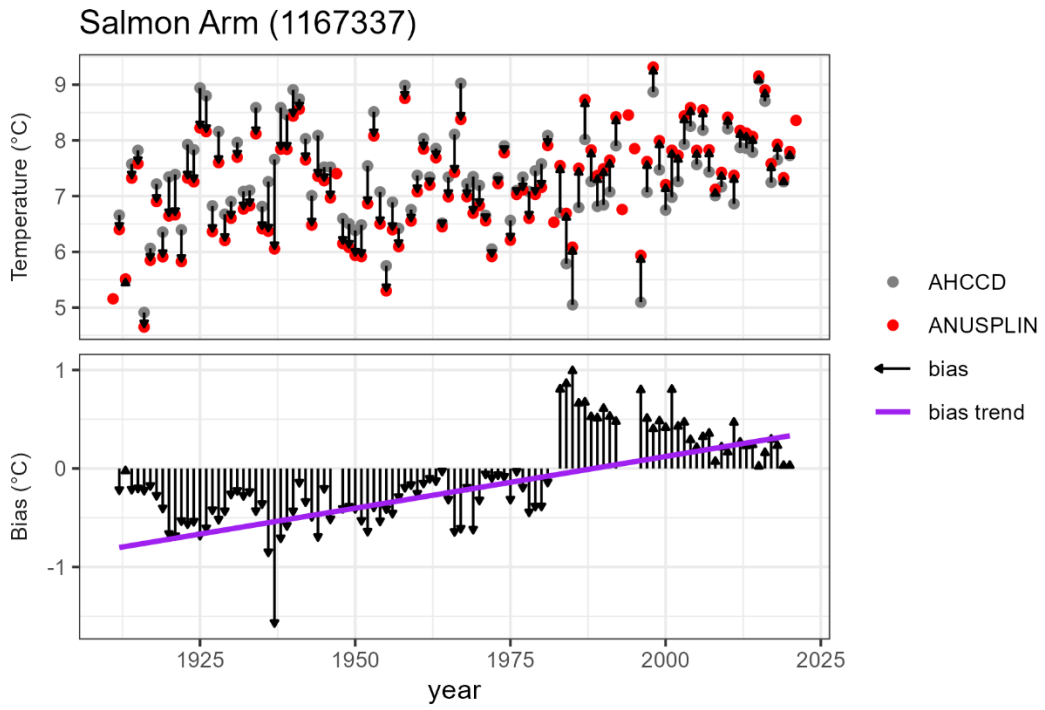

Figure G3: Annual mean temperature from AHCCD and ANUSPLIN (top) and bias (bottom) for Salmon Arm. The bias trend is +0.10°C per decade.

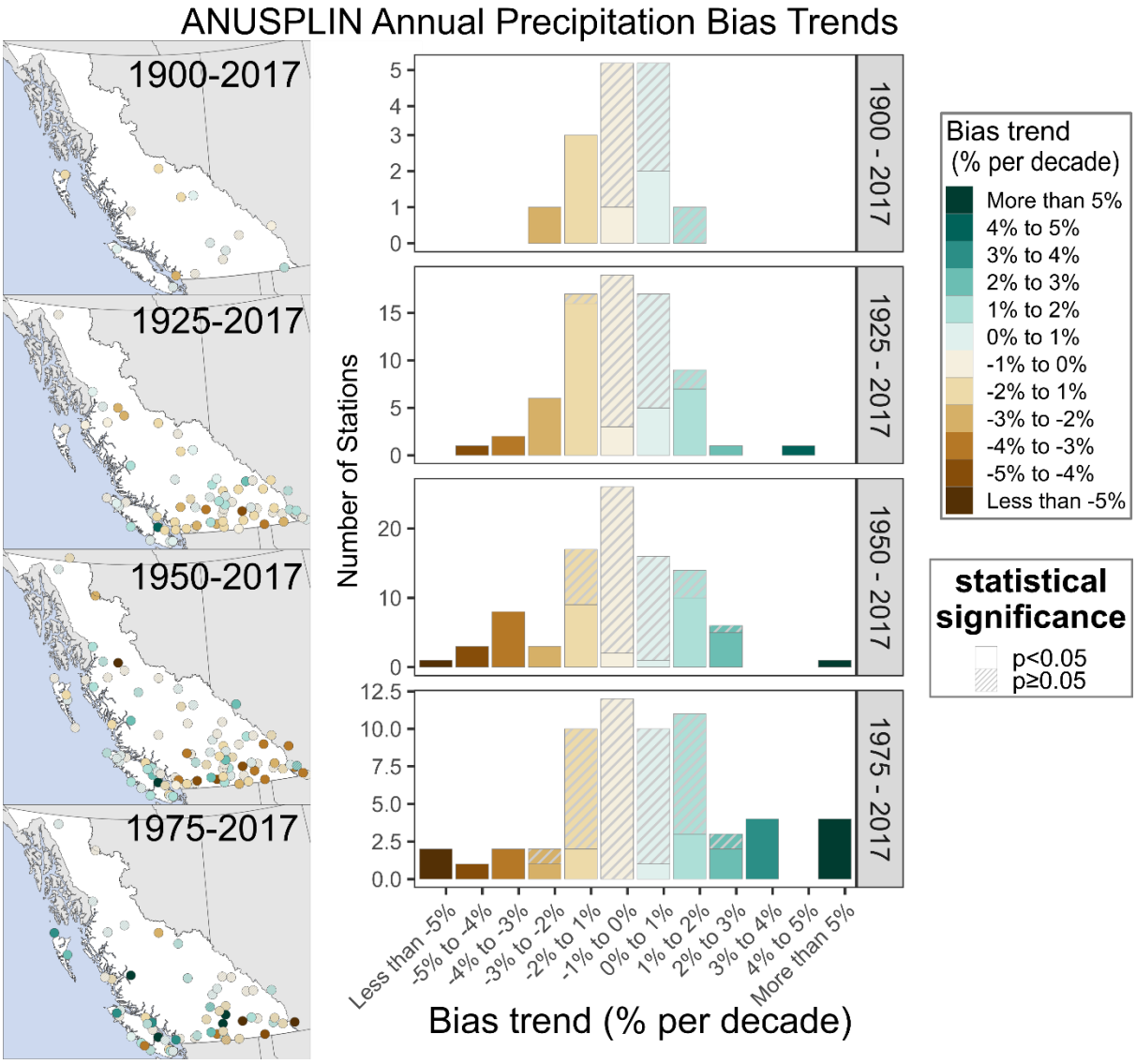

Figure G 4: Bias trends in annual total precipitation. The panels (left) indicate the spatial distribution of the trends, also shown as histograms (right).

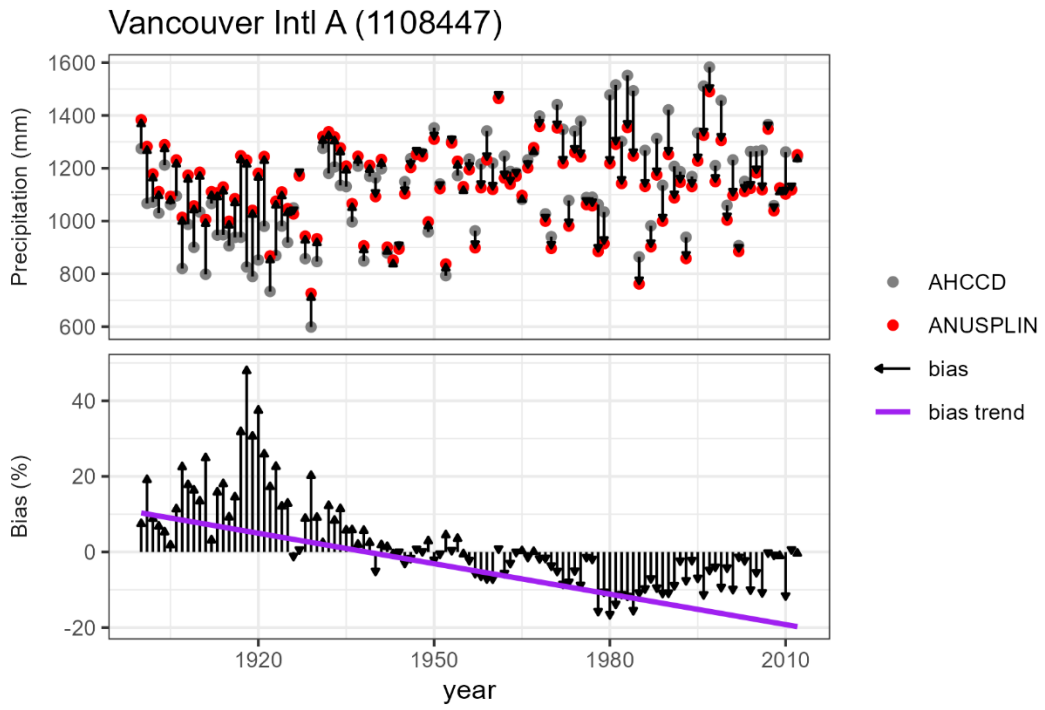

Figure G5: Annual total precipitation from AHCCD and ANUSPLIN (top) and bias (bottom) for Vancouver International Airport. The bias trend is -2.6% per decade.

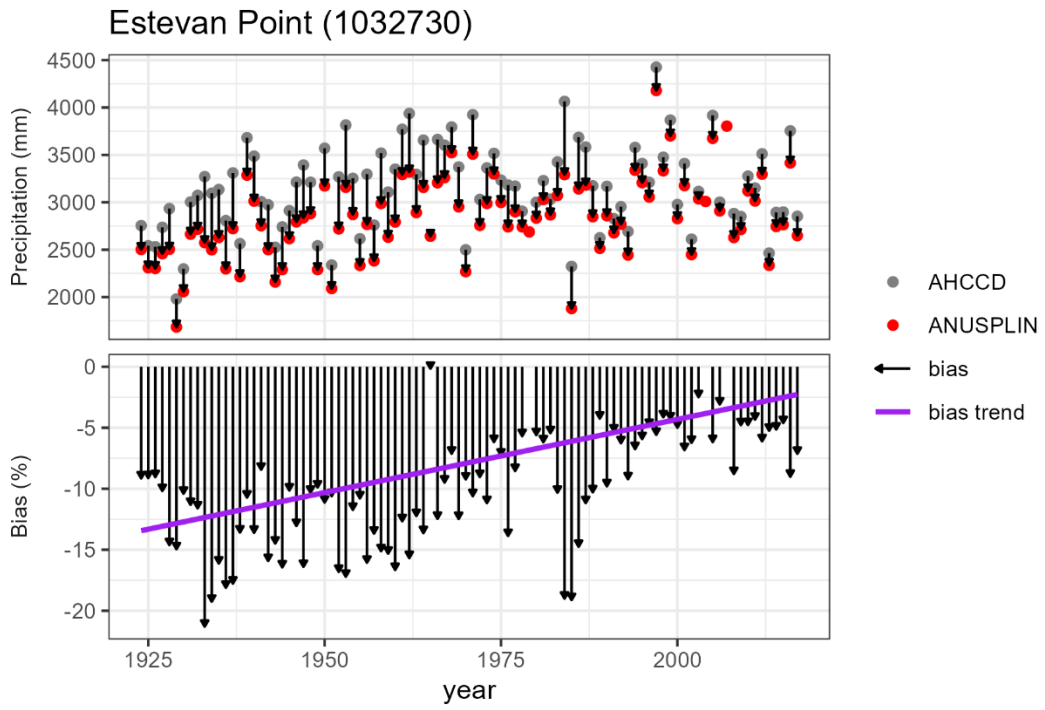

Figure G6: Annual total precipitation from AHCCD and ANUSPLIN (top) and bias (bottom) for Estevan Point. The bias trend is 1.2% per decade.

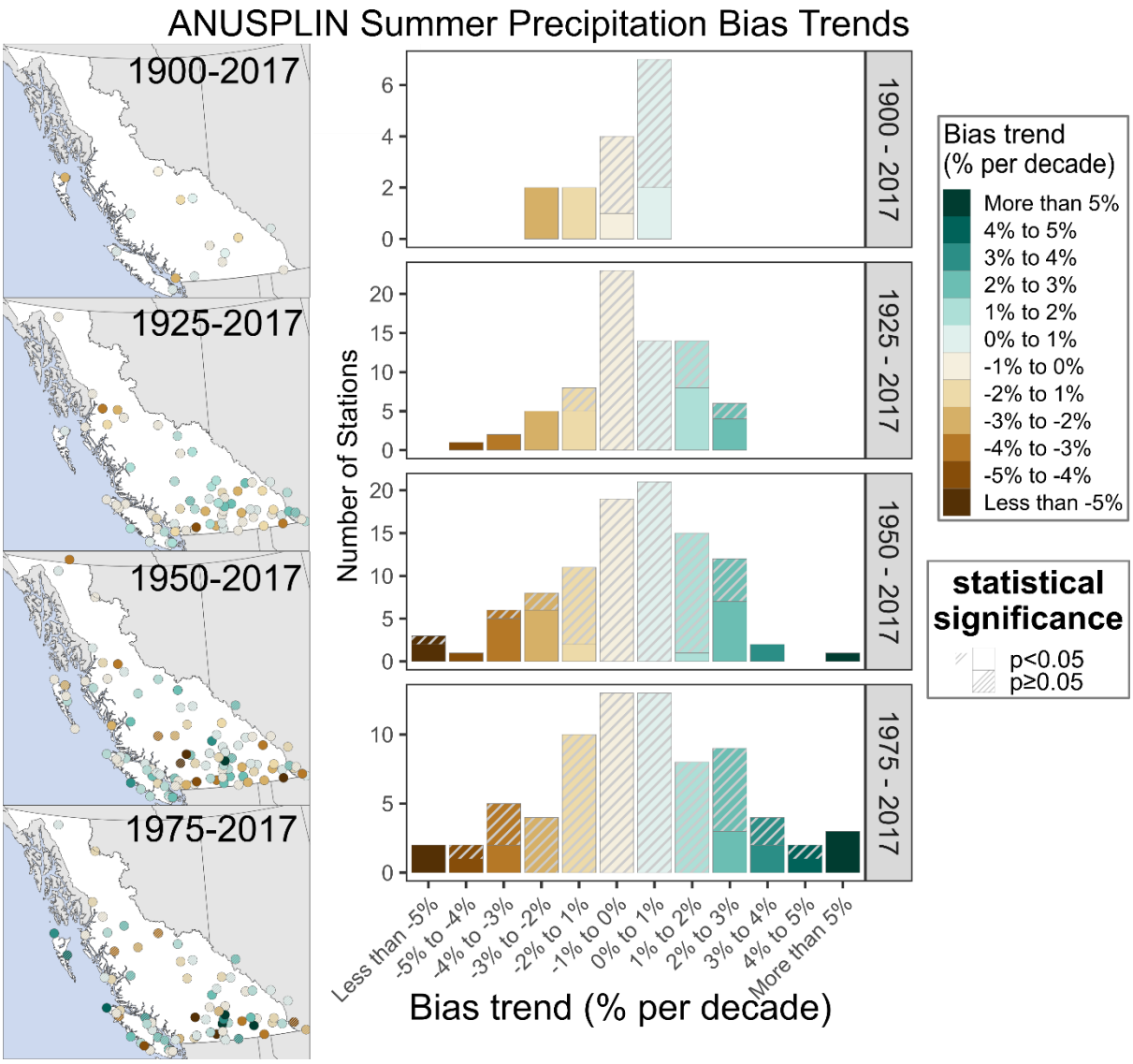

Figure G 7: Bias trends in summer (June-September) precipitation. The panels (left) indicate the spatial distribution of the trends, also shown as histograms (right).

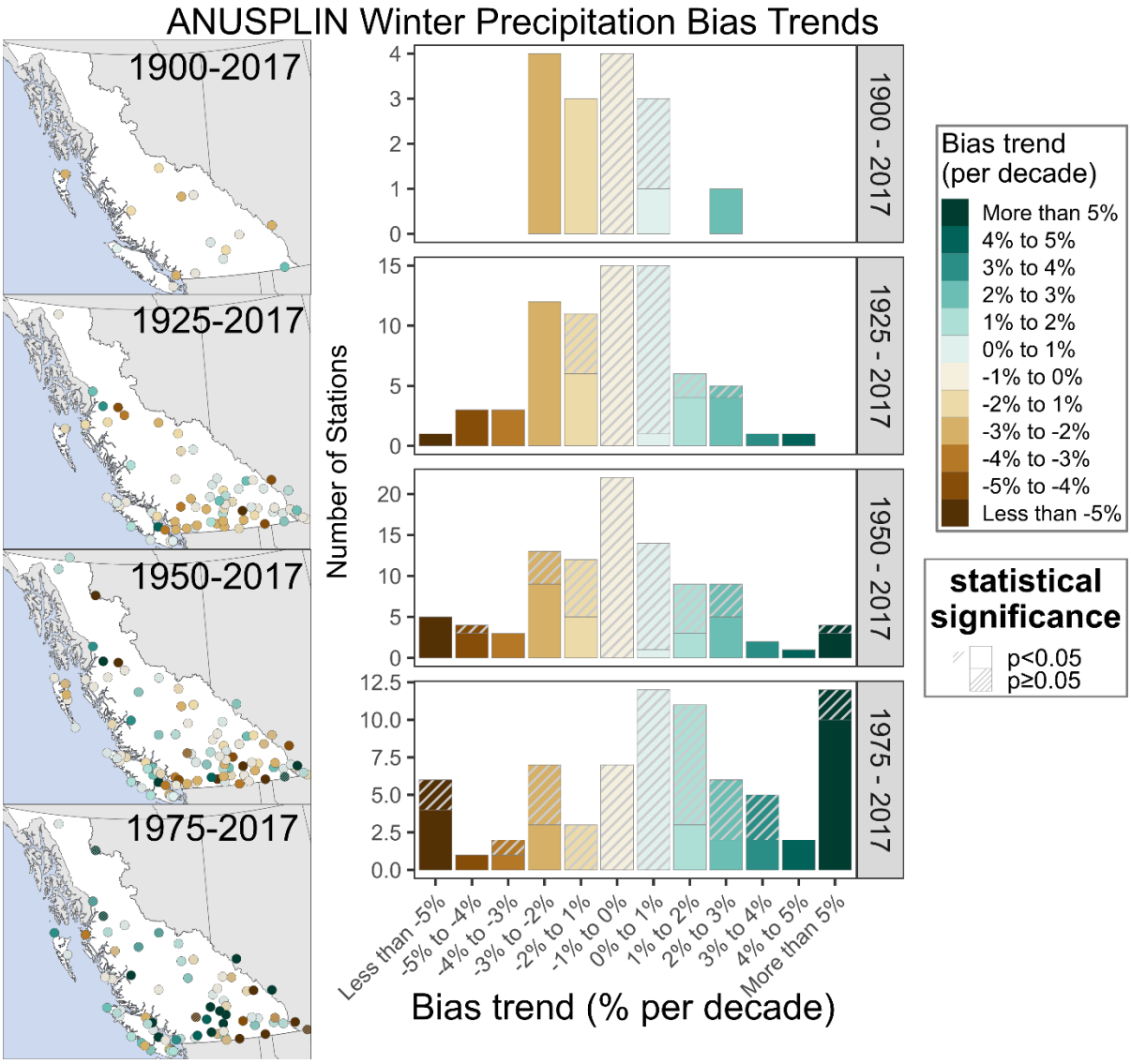

Figure G 8: Bias trends in winter (December - April) precipitation. The panels (left) indicate the spatial distribution of the trends, also shown as histograms (right).

Table G1: Summary of bias trends in mean temperature for each month, for all four periods. Bolded rows indicate that the number of positive or negative trends is greater than expected by chance, after applying a Holm-Bonferroni correction.

Period	month	N	N(trend>0)	N(trend<0)	p	H-B test
1900-2017	1	22	5	17	0.02	
1900-2017	**2**	**22**	**3**	**19**	**<0.0001**	*
1900-2017	**3**	**22**	**3**	**19**	**<0.0001**	**
1900-2017	4	22	5	17	0.02	
1900-2017	5	22	7	15	0.13	
1900-2017	6	22	6	16	0.05	
1900-2017	7	22	6	16	0.05	
1900-2017	8	22	6	16	0.05	
1900-2017	9	22	5	17	0.02	
1900-2017	**10**	**22**	**4**	**18**	**0.004**	*
1900-2017	11	22	5	17	0.02	
1900-2017	**12**	**22**	**4**	**18**	**0.004**	*
1925-2017	1	68	28	40	0.18	
1925-2017	2	68	22	46	0.005	
1925-2017	3	68	31	37	0.54	
1925-2017	4	68	29	39	0.27	
1925-2017	5	68	35	33	0.9	
1925-2017	6	68	32	36	0.72	
1925-2017	7	68	34	34	1	
1925-2017	8	68	32	36	0.72	
1925-2017	9	68	29	39	0.27	
1925-2017	10	68	30	38	0.4	
1925-2017	11	68	31	37	0.54	
1925-2017	12	68	31	37	0.54	
1950-2017	1	92	39	53	0.17	
1950-2017	2	93	51	42	0.41	
1950-2017	3	93	48	45	0.84	
1950-2017	4	93	56	37	0.06	
1950-2017	5	93	51	42	0.41	
1950-2017	6	93	56	37	0.06	
1950-2017	7	93	53	40	0.21	
1950-2017	8	93	53	40	0.21	
1950-2017	9	91	53	38	0.14	
1950-2017	10	92	49	43	0.6	
1950-2017	11	92	50	42	0.47	
1950-2017	12	92	54	38	0.12	
1975-2017	1	101	52	49	0.84	
1975-2017	2	101	54	47	0.55	
1975-2017	3	102	56	46	0.37	
1975-2017	4	103	53	50	0.84	
1975-2017	5	103	53	50	0.84	
1975-2017	6	102	51	51	1	
1975-2017	7	102	54	48	0.62	
1975-2017	8	102	46	56	0.37	
1975-2017	9	102	49	53	0.77	
1975-2017	10	103	54	49	0.69	
1975-2017	11	102	56	46	0.37	
1975-2017	12	101	63	38	0.02	

Table G 2: Summary of bias trends in precipitation for each month, for all four periods. Bolded rows indicate that the number of positive or negative trends is greater than expected by chance, after applying a Holm-Bonferroni correction.

Period	month	N	N(trend>0)	N(trend<0)	p	H-B test
1900-2017	1	15	5	10	0.3	
1900-2017	2	15	6	9	0.61	
1900-2017	3	15	4	11	0.12	
1900-2017	4	15	6	9	0.61	
1900-2017	5	15	5	10	0.3	
1900-2017	6	15	8	7	1	
1900-2017	7	15	8	7	1	
1900-2017	8	15	7	8	1	
1900-2017	9	15	7	8	1	
1900-2017	10	15	5	10	0.3	
1900-2017	11	15	8	7	1	
1900-2017	12	15	4	11	0.12	
1925-2017	1	73	31	42	0.24	
1925-2017	2	73	24	49	0.005	
1925-2017	3	73	26	47	0.02	
1925-2017	**4**	**73**	**21**	**52**	**<0.0001**	**
1925-2017	5	73	28	45	0.06	
1925-2017	6	73	35	38	0.82	
1925-2017	7	73	34	39	0.64	
1925-2017	8	73	28	45	0.06	
1925-2017	9	73	29	44	0.1	
1925-2017	10	73	30	43	0.16	
1925-2017	11	73	35	38	0.82	
1925-2017	12	73	28	45	0.06	
1950-2017	1	99	46	53	0.55	
1950-2017	2	99	43	56	0.23	
1950-2017	3	99	38	61	0.03	
1950-2017	**4**	**99**	**34**	**65**	**0.002**	*
1950-2017	5	99	46	53	0.55	
1950-2017	6	99	50	49	1	
1950-2017	7	99	49	50	1	
1950-2017	8	99	50	49	1	
1950-2017	9	99	46	53	0.55	
1950-2017	10	99	38	61	0.03	
1950-2017	11	99	51	48	0.84	
1950-2017	12	99	41	58	0.11	
1975-2017	1	81	51	30	0.03	
1975-2017	2	80	46	34	0.22	
1975-2017	3	82	43	39	0.74	
1975-2017	4	78	42	36	0.57	
1975-2017	5	80	41	39	0.91	
1975-2017	6	80	47	33	0.15	
1975-2017	7	80	46	34	0.22	
1975-2017	**8**	**78**	**53**	**25**	**0.002**	*
1975-2017	9	80	36	44	0.43	
1975-2017	**10**	**78**	**25**	**53**	**0.002**	*
1975-2017	11	77	39	38	1	
1975-2017	12	79	45	34	0.26	

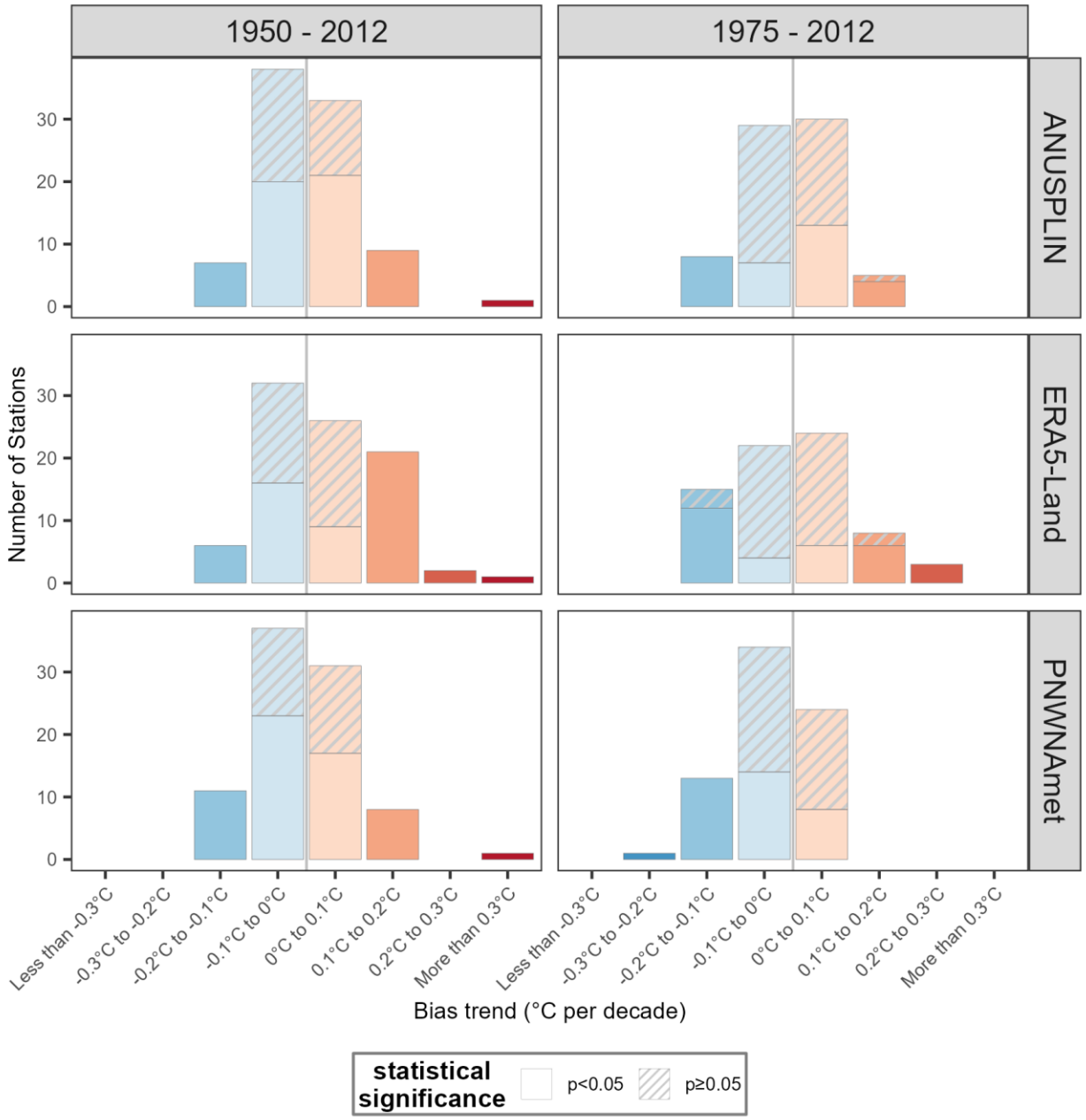

Figure G9: Comparison of bias trends for ANUSPLIN, ERA5-Land, and PNWNAmet mean annual temperature. ANUSPLIN and PNWNAmet have similar performance, while bias trends in the ERA5-Land data are slightly stronger.

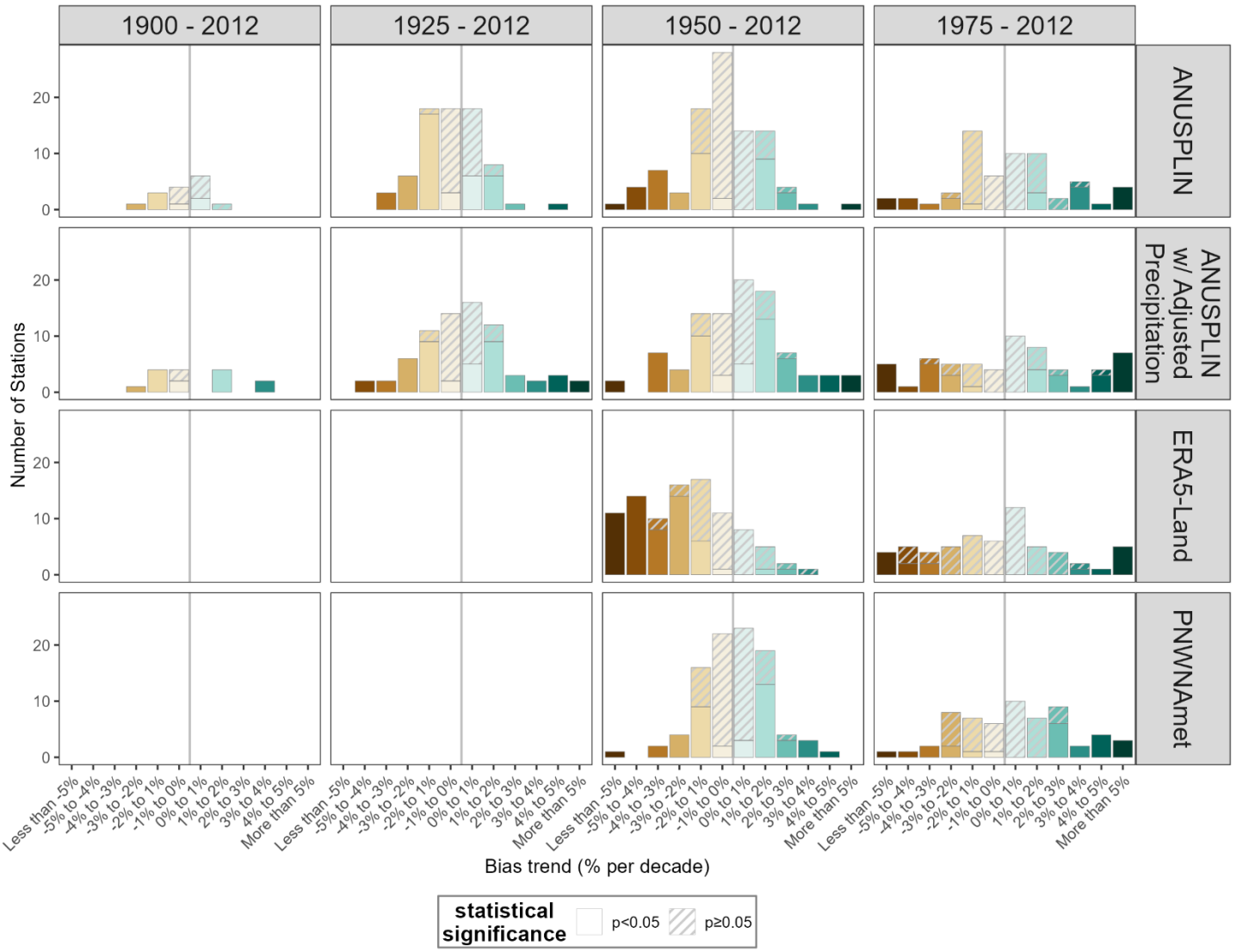

Figure G10: Comparison of bias trends in annual precipitation for ANUSPLIN, ANUSPLIN-adjusted, ERA5-Land, and PNWNAmet data. The ERA5-land data show the strongest bias trends, with mostly negative trends (indicating earlier data are overpredicted or more recent data are underpredicted). The ANUSPLIN and PNWNAmet datasets both show comparatively small bias trends, and positive/negative trends are roughly balanced. The ANUSPLIN-adjusted data show slightly more positive than negative trends, and generally stronger trends than the ANUSPLIN or PNWNAmet datasets.

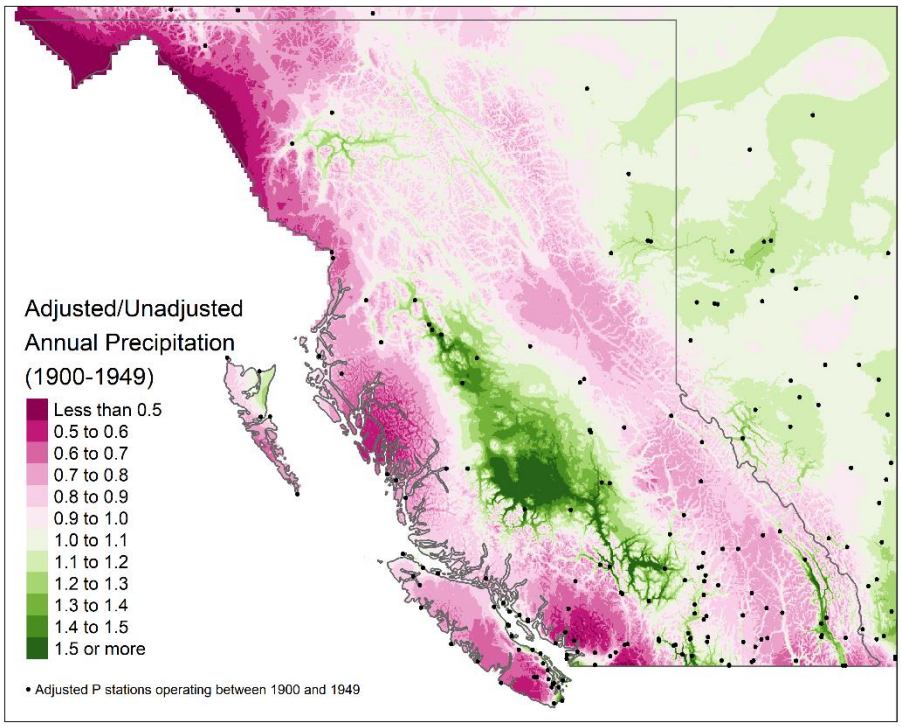

Figure G11: Ratio of adjusted to unadjusted ANUSPLIN precipitation from 1900-1949 across BC. The adjusted precipitation is up to 50% drier than the unadjusted for parts of the coast and more than 50% wetter for parts of the interior plateau. The largest differences occur far away from the climate stations used for the interpolation.

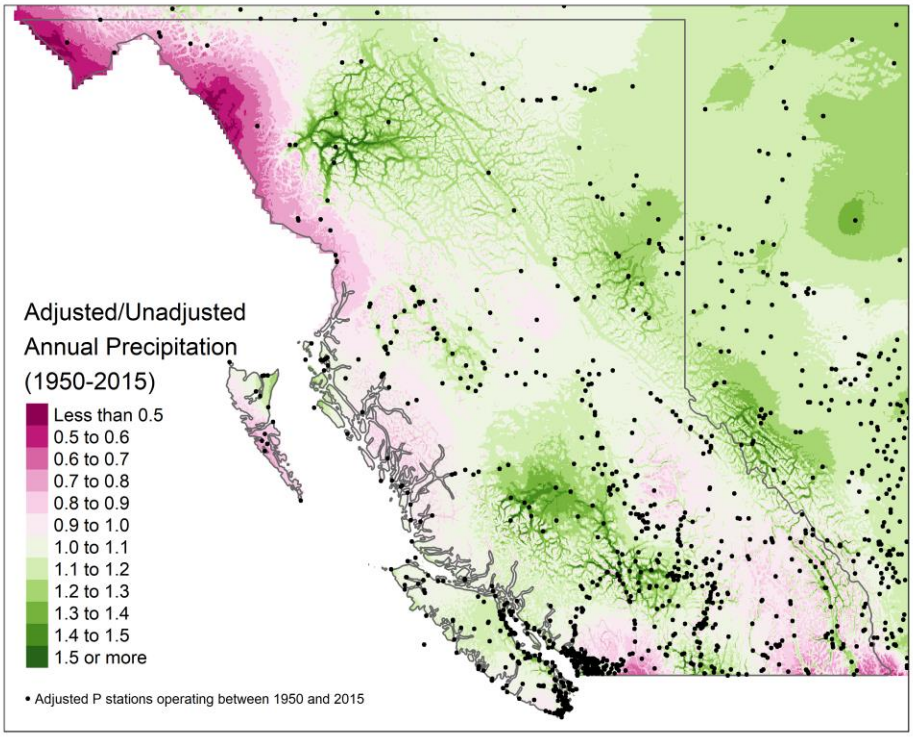

Figure G12: Ratio of adjusted to unadjusted ANUSPLIN precipitation from 1950-2015 across BC. The differences between the two datasets are much smaller than for the 1900-1949 period. Many of the differences are plausibly related to the adjustments made to precipitation measurements, rather than the interpolation algorithm.

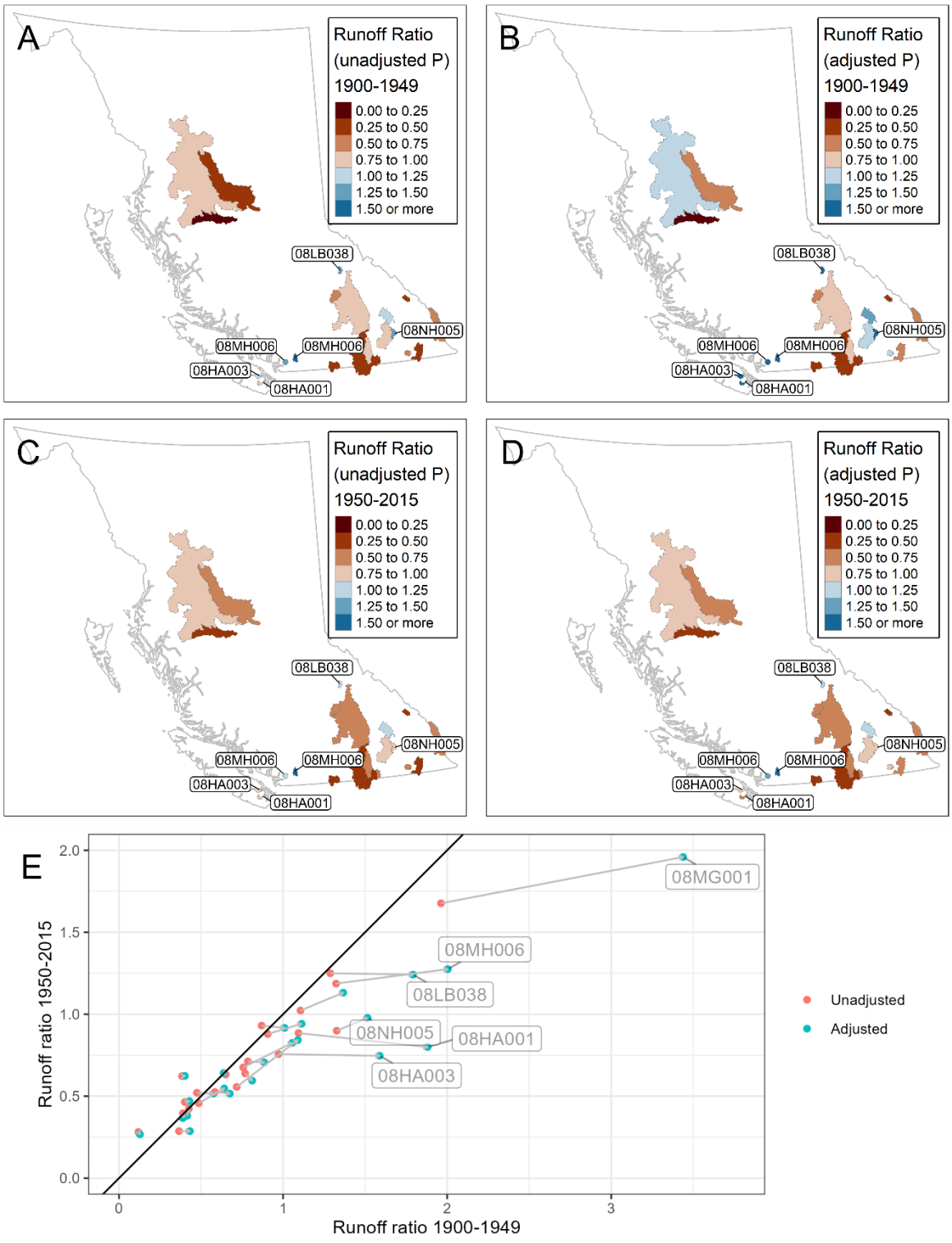

Figure G13: Runoff ratios for 23 unglaciated, unregulated catchments, for 2 periods and 2 datasets (A-D). A: unadjusted ANUSPLIN precipitation for 1900-1949; B: adjusted ANUSPLIN precipitation, 1900-1949; C: unadjusted ANUSPLIN precipitation for 1950-2015; D: adjusted ANUSPLIN precipitation, 1950-2015. E: Comparison of runoff ratios for the two periods. The six catchments with runoff ratios greater than 1.5 are labelled. The adjusted precipitation data have generally higher runoff ratios in the 1900-1949 period, and the runoff ratios are less temporally consistent than the unadjusted data.

APPENDIX H: PREDICTIVE MODELS CONSTRUCTED WITH OTHER CLIMATE DATASETS

We compared predictive regression models using four different climate datasets: (1) ANUSPLIN, as presented in the main text (MacDonald et al., 2020), (2) ANUSPLIN with adjusted precipitation (MacDonald et al., 2021), (3) ERA5-Land (Muñoz Sabater, 2019), and (4) PNWNAmet (Werner et al., 2019).

First, we trained and evaluated models using each dataset on a common observation period of 1951-2012. 198 of our catchments had at least 20 years of data within this window. However, we removed from the evaluation of the adjusted precipitation ANUSPLIN data 9 catchments which have more than 20% of their area in the United States, because the adjusted precipitation data are only available for Canada.

Figure H1 shows the KGE values for the models trained on each dataset. The skill scores are very similar across the four datasets; in order from best to worst, the median KGE is 0.703 for ERA5-Land, for 0.681 for PNWNAmet, 0.677 for ANUSPLIN, and 0.645 for ANUSPLIN with adjusted precipitation.

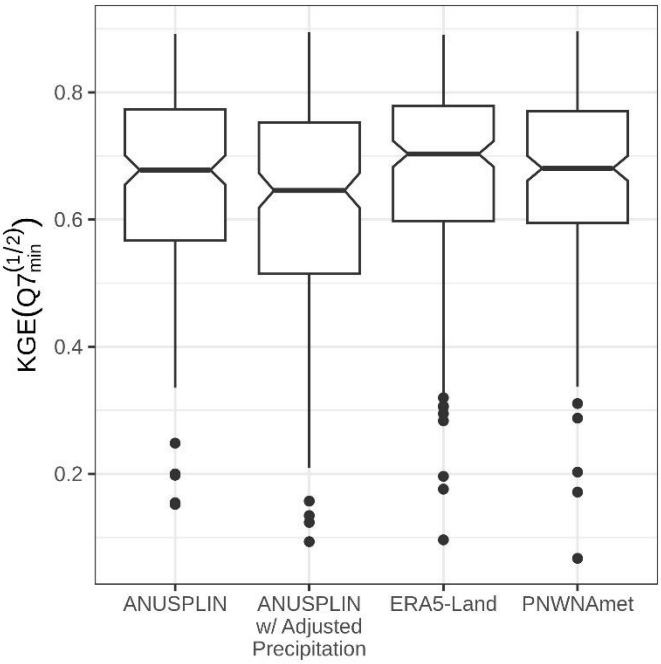

Figure H1: KGE for regression models using four different climate datasets

Figure H2 shows the Sen's slope of the error as a percentage of the mean $Q7_{min}$ per decade. The distribution of error trends in similar across the four datasets. In order from best to worst, the percentage of catchments with an error trend greater than 5% per decade is 54.5% for ANUSPLIN with adjusted precipitation, 55.1% for PNWNAmet and 58.1% for both ERA5-Land and ANUSPLIN.

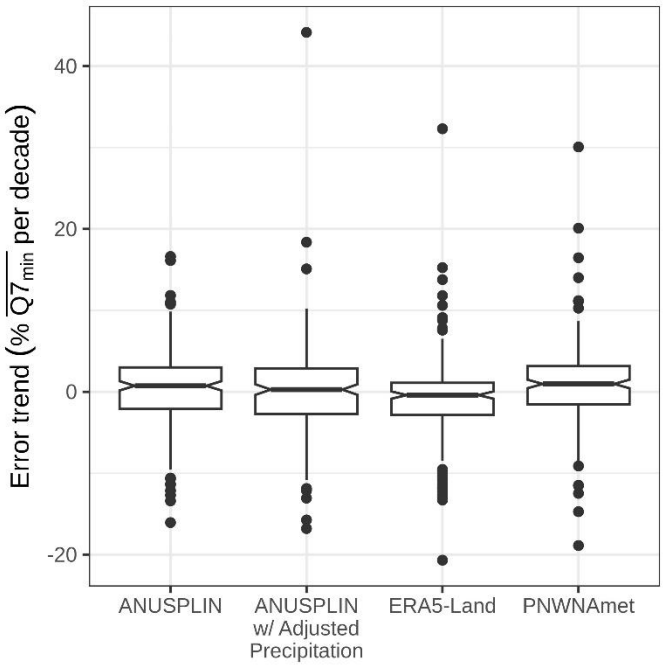

Figure H2: The Sen's slope of the error, expressed as a percentage of the mean $Q7_{min}$ per decade.

Next, we conducted the low-flow anomaly analysis using each dataset (same as Figure 6 in the main text). The models were trained and applied to each climate dataset separately, for all available years in each dataset. 188 catchments could be trained for all datasets. However, one catchment (Honna River Near The Mouth, 08OA004) had a spurious and very large negative coefficient with abstraction when using the ERA5-Land data, so we removed this catchment from the analysis.

Figure G3 shows $Q7_{min}$ anomalies from 1901-2022 for each dataset. The patterns through time match reasonably well for the four datasets, but there are some notable differences.

First, the estimates for the effect of abstraction are notably different across the different datasets. This suggests that these results are not very robust. This makes sense given that the estimates for water use are very rough, and the water use data are highly autocorrelated, increasing the risk of spurious correlations.

Second, negative anomalies associated with precipitation prior to 1950 are much larger when using the adjusted precipitation data with ANUSPLIN. This suggests that low flows in this period may have been lower than we predict in the main text. However, given the temporal inconsistencies observed (Appendix G), we consider the conditions depicted in the ANUSPLIN-adjusted data for the beginning of the 20th century to be somewhat suspect.

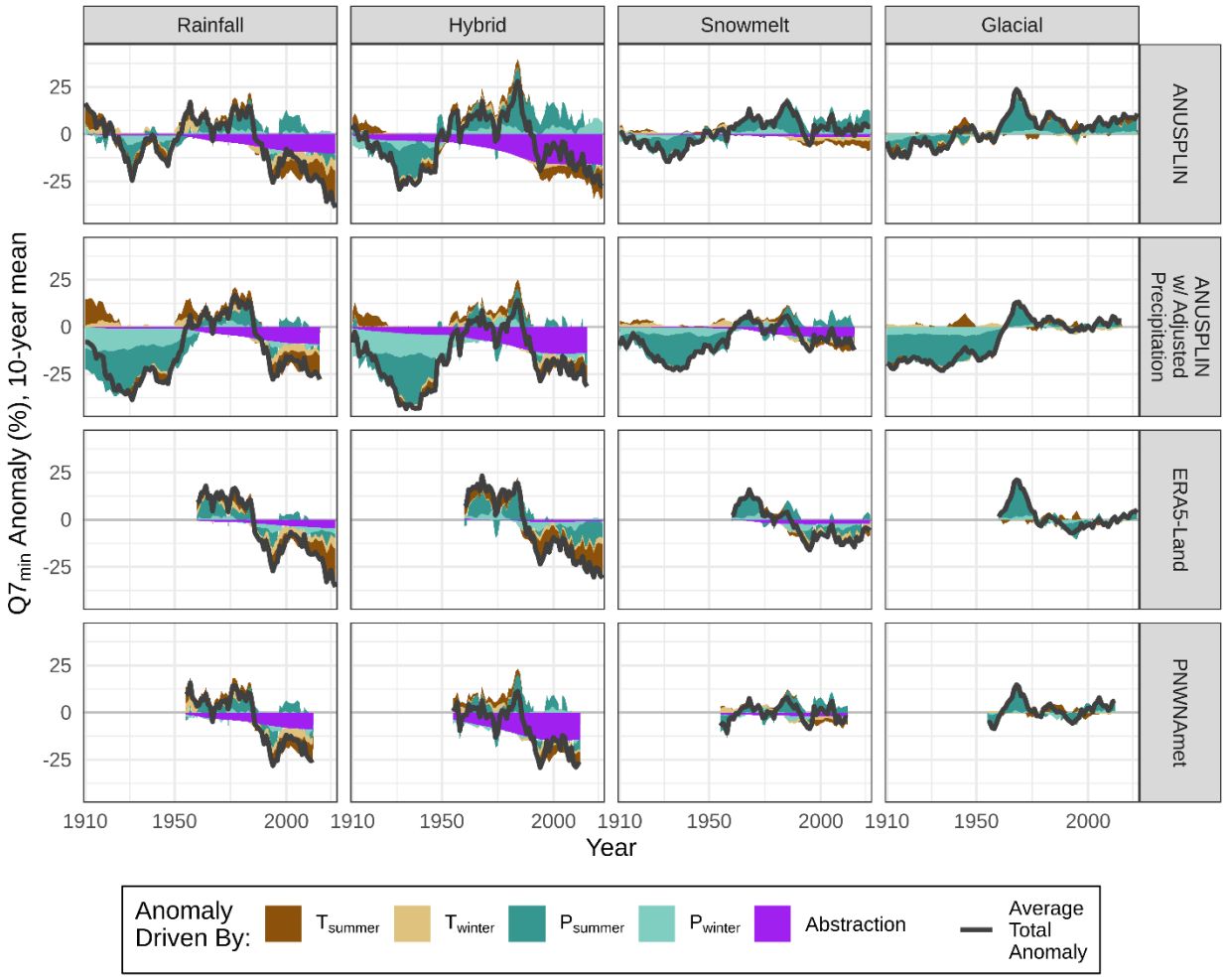

Figure H3: $Q7_{min}$ anomalies for model trained on and applied to four climate datasets. The data represent 187 catchments for which models could be trained on each dataset (18 rainfall, 57 hybrid, 82 snowmelt, and 30 glacial catchments).